



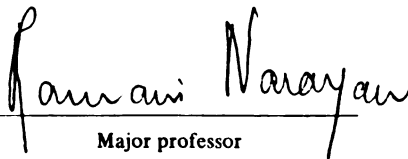
This is to certify that the
thesis entitled
**Biodegradability of Polyactide Film in
Simulated Composting Environments**

presented by

Joseph Brenton Snook

has been accepted towards fulfillment
of the requirements for

M.S. degree in Chemical Engr.


Major professor

Date 8/5/94

**LIBRARY
Michigan State
University**

**PLACE IN RETURN BOX to remove this checkout from your record.
TO AVOID FINES return on or before date due.**

DATE DUE	DATE DUE	DATE DUE
MAR 30 1999 01 06 04	MAY 23 2005	
JUN 01 2001 05 08 07 06 26 2007		

**BIODEGRADABILITY OF POLYLACTIDE FILM IN
SIMULATED COMPOSTING ENVIRONMENTS**

By

Joseph Brenton Snook

A THESIS

Submitted to
Michigan State University
in partial fulfillment of the requirements
for the degree of

MASTER OF SCIENCE

Department of Chemical Engineering

1994

ABSTRACT

BIODEGRADABILITY OF POLYLACTIDE FILM IN SIMULATED COMPOSTING ENVIRONMENTS

By

Joseph Brenton Snook

Poly lactide is one of many new biodegradable materials being designed for compatibility with the developing composting infrastructure. Before using any new material as a part of a compostable waste stream, it is essential to understand its behavior during composting. Experiments were performed to determine the rate, extent, and mechanism of poly lactide film biodegradation in simulated composting environments. The effect of poly lactide film on the physical, chemical, and biochemical processes of composting was also addressed. Poly lactide biodegrades in compost by undergoing random non-enzymatic hydrolysis until the molecular weight average is reduced to approximately M_n 10,000. At this molecular weight average, poly lactide oligomers diffuse out of the polymer bulk and are utilized by microorganisms. Poly lactide film rapidly disintegrated and mineralized in a bench-scale respirometric biodegradability test and a semi-controlled compost exposure, however, a feedback-controlled pilot-scale experiment with a lower average temperature resulted in a slower rate of molecular weight reduction. A temperature dependent model of poly lactide molecular weight reduction was used to accurately predict the extent of poly lactide degradation in the three simulated composting environments.

To my parents, sisters, and brother.

ACKNOWLEDGMENTS

I wish to first thank my advisor, Dr. Ramani Narayan, for providing his uniquely styled guidance and support. I would also like to express my appreciation to everyone at the Michigan Biotechnology Institute (particularly the Biomaterials Group) and the Department of Chemical Engineering for providing an enjoyable working and learning environment. I am grateful to the Biodegradable Polymers advisory committee of the American Society of Testing and Materials Institute of Standards Research for their support of this research and especially Mr. Mike Chanen of Cargill for his assistance and many helpful discussions. Finally, I thank my friends in the Department of Agricultural Engineering for their own special contributions.

TABLE OF CONTENTS

Chapter	Page
LIST OF TABLES.....	viii
LIST OF FIGURES	x
1. INTRODUCTION.....	1
1.1 Objectives.....	1
1.2 Organization of the Thesis	2
2. BIODEGRADABLE MATERIALS.....	3
2.1 Designing Materials for Recycling and Disposal.....	3
2.2 Biodegradable Materials in Composting	4
2.3 Status of the U.S. Biodegradable Materials Industry	11
3. POLYLACTIDE	15
3.1 Polylactide Synthesis	15
3.2 Biodegradation Mechanism and Kinetics	16
3.2.1 Hydrolytic Degradation.....	17
3.2.2 Enzymatic Degradation	22
3.3 Life Cycle Assessment.....	23
3.4 Applications.....	23
3.5 Polylactide Film Properties	25

Chapter	Page
4. ANALYTICAL METHODS	27
5. BIODEGRADATION UNDER EXTERNALLY CONTROLLED COMPOSTING CONDITIONS	31
5.1 Overview	31
5.2 Test method	31
5.3 Preliminary Experiment 1	35
5.3.1 Method.....	35
5.3.2 Results	37
5.4 Preliminary Experiment 2	39
5.4.1 Method.....	39
5.4.2 Results	43
5.5 Preliminary Experiment 3	47
5.5.1 Method.....	47
5.5.2 Results	51
5.6 Biodegradability of Polylactide Film.....	55
5.6.1 Method.....	55
5.6.2 Respirometric Biodegradability.....	56
5.6.3 Polylactide Degradation	60
6. BIODEGRADATION UNDER FEEDBACK CONTROLLED COMPOSTING CONDITIONS	64
6.1 Overview	64
6.2 Pilot-scale Composting System	64
6.2.1 Process Control.....	66
6.2.2 Controller Tuning by the Continuous Cycling Method	70
6.2.3 Controller Tuning by a Process Model-Based Method	72
6.3 Evaluation of Test Matrices	79

Chapter	Page
6.3.1 Mixed MSW Compost	79
6.3.2 Sludge Compost	84
6.3.3 Yard Debris Compost.....	88
6.4 Biodegradation of Polylactide Film.....	97
6.4.1 Experimental Method.....	98
6.4.2 Effect of Polylactide on Process Dynamics	99
6.4.3 Effect of Polylactide on Product Quality	106
6.4.4 Pilot-Scale Polylactide Degradation	110
7. BIODEGRADATION UNDER SEMI-CONTROLLED COMPOSTING CONDITIONS	115
7.1 Overview	115
7.2 Test Apparatus and Conditions	116
7.3 Polylactide Degradation.....	119
8. CONCLUSIONS AND RECOMMENDATIONS	121
8.1 Conclusions	121
8.2 Recommendations for Further Work	124
LIST OF REFERENCES.....	127

LIST OF TABLES

Table	Page
2-1. Growth in number of composting facilities, U.S.	8
2-2. Life cycle requirements for compostable items.	9
2-3. Major biodegradable materials producers	14
3-1. Rate data used in Arrhenius plot.....	21
3-2. Characteristics of polylactide film.....	26
5-1. Results of experiment 1.....	38
5-2. Results of aqueous biodegradability testing.....	39
5-3. Test materials for experiment 2.	40
5-4. Results of experiment 2.....	46
5-5. Results of biodegradability experiment.....	60
5-6. GPC analysis of films from controlled composting.....	62
6-1. Controller settings from the continuous cycling method.	72
6-2. Process characteristics for oxygen concentration	76

Table	Page
6-3. Cohen-Coon settings for oxygen concentration gradient.....	76
6-4. Cohen-Coon process characteristics for temperature	77
6-5. Settings for temperature control.....	77
6-6. Analysis of MSW compost feedstock.	80
6-7. Analysis of sludge compost feedstock.	85
6-8. Elemental analysis of Fairfield compost product.	86
6-9. Analysis of yard debris materials.....	88
6-10. Analysis of Kraft paper/yard waste mixture.....	93
6-11. Carbon balance for Kraft paper/yard waste mixture.....	94
6-12. Change in C/N during Kraft/yard waste composting.....	94
6-13. Distribution of carbon in humic fractions.	97
6-14. Mixtures for pilot-scale composting experiments.....	98
6-15. Compost feedstock characteristics	99
6-16. Carbon balances for pilot-scale composting.....	106
6-17. GPC analysis of films from pilot-scale composting	111
7-1. Synthetic compost mixture for semi-controlled composting.....	117
7-2. GPC analysis of films from semi-controlled composting	119

LIST OF FIGURES

Figure	Page
2-1. Elements of the composting process	5
2-2. Steps in compost processing	6
3-1. Synthesis of polylactide.....	15
3-2. The polylactide cycle	16
3-3. Proposed degradation mechanism for polylactide	19
3-4. Example of rate constant calculation	20
3-5. Arrhenius plot for polylactide degradation rate constant.....	20
5-1. Setup for externally controlled composting experiment 1	36
5-2. Biodegradability of acrylic-coated and uncoated paperboard under the conditions of experiment 1.....	38
5-3. Setup for externally controlled composting experiment 2	41
5-4. Biodegradability of materials tested in experiment 2	44
5-5. Rates of control material biodegradation measured in experiment 2	45
5-6. Setup for externally controlled composting experiment 3	48

Figure	Page
5-7. Predicted effect of air flow rate on time required to achieve 97% purge of gas analysis loop.....	50
5-8. Replacement of gas in analytical loop at 60 ml/min.....	50
5-9. Carbon dioxide concentration of the gas exiting each test vessel	52
5-10. Rate of biodegradation of Kraft paper	53
5-11. Biodegradability of Kraft paper in experiment 3.....	54
5-12. Carbon dioxide concentrations in exhaust gas from blank and polylactide test vessels.....	57
5-13. Carbon dioxide concentrations in exhaust gas from Kraft paper and polyethylene test vessels.....	58
5-14. Rates and cumulative biodegradabilities of polylactide film and Kraft paper	59
5-15. Comparison of predicted and measured decreases in M_n with rate of mineralization during controlled composting	61
5-16. Photographs of the mixture of polylactide film and compost inoculum before and after externally controlled composting.....	63
6-1. Schematic of pilot-scale composting apparatus.....	65
6-2. Typical temperature profile during forced aeration composting (Stentiford et al., 1985)	67
6-3. Primary control algorithm for dual control of temperature and oxygen concentration	69
6-4. Characteristics of the process reaction curve	74

Figure	Page
6-5. Response of oxygen concentration to a step decrease and increase in the air flow rate	75
6-6. Response of temperature to a step increase and decrease in the air flow rate	78
6-7. Process dynamics of MSW compost over the first 32 hours of operation with no mixing.....	81
6-8. Process dynamics for pilot-scale composting of MSW over the first nine days	83
6-9. Process dynamics for pilot-scale composting of sludge-wood chips mixture	87
6-10. Typical process dynamics for pilot-scale yard debris composting trials	89
6-11. Process dynamics for pilot-scale composting of Kraft paper in yard debris mixture.....	91
6-12. Chemical parameters during pilot- scale composting of Kraft paper mixture	92
6-13. Contribution of each extracted fraction to the total extractable carbon.....	96
6-14. Process dynamics for compost mixture containing polylactide film	100
6-15. Average temperatures in the vessels during pilot-scale composting	101
6-16. Respirometric data for compost mixture containing polylactide film	103
6-17. Percent mineralization of initial carbon to carbon dioxide during pilot-scale composting	104
6-18. Pilot-scale composting product quality parameters	108

Figure	Page
6-19. Results of germination and root elongation bioassay for fresh and finished pilot-scale composts	110
6-20. Comparison of predicted and measured decrease in M_n during pilot-scale composting	112
6-21(a). Photograph of polylactide film prior to pilot-scale composting.....	113
6-21(b) Photographs of polylactide film after composting two weeks and four weeks	114
7-1. Apparatus for semi-controlled composting experiment	116
7-2. Processing conditions for semi-controlled composting exposure of polylactide film.....	118
7-3. Comparison of predicted and measured decrease in M_n during semi-controlled composting	120

CHAPTER 1

INTRODUCTION

The development of inexpensive synthetic plastics has had a dramatic impact on modern society. Single-use disposable plastic packaging provides both convenience and public health benefits. However, the proliferation of disposable products has also resulted in tremendous volumes of solid waste. Although landfilling is currently the most common method of solid waste management, its long term economic and environmental costs are becoming apparent. Public objection to landfilling has impeded the siting and construction of new facilities. This has resulted in a shortage of landfill space and a need for alternative solid waste management practices. The use of biodegradable plastics in conjunction with composting can divert a significant portion of the solid waste stream from landfills to be reused as a soil amendment.

1.1 OBJECTIVES

The primary objective of the thesis is to evaluate the potential of one material, polylactide, as a biodegradable replacement for current plastic packaging materials. This objective is attained by:

- Describing how polylactide can be used in conjunction with composting to provide a cost-effective and environmentally sound option for solid waste management.

- Determining the rate and extent of polylactide biodegradation in simulated composting environments.
- Studying the physical, chemical, and biochemical interactions in the composting process that may be affected by the inclusion of polylactide as a substrate.
- Modeling polylactide biodegradation in compost.

1.2 ORGANIZATION OF THE THESIS

The thesis is divided into two parts. The first part is a development of the general and technical background for the work. Chapter 2 reviews the role of biodegradable materials in solid waste management and presents the status of the biodegradable material manufacturing industry. Aspects of polylactide production, use, and biodegradation are reviewed in Chapter 3. The discussion of polylactide includes a model of polylactide molecular weight reduction and its generalization to temperatures occurring in compost. Chapter 4 details the experimental methods used in the research.

The second part of the thesis, Chapter 5 through Chapter 7, describe the experiments performed to evaluate polylactide biodegradability in compost. The experiments in each of these chapters use a different apparatus to simulate the composting environment. Chapters 5, 6, and 7 each begin by relating the rationale of the test method and describing preliminary experiments used to evaluate and validate the apparatus and methods. Polylactide molecular weight reduction and biodegradation using each test method are then compared to the predictions of the model. Chapter 8 summarizes the findings of the experiments and presents recommendations for further work.

CHAPTER 2

BIODEGRADABLE MATERIALS

2.1 DESIGNING MATERIALS FOR RECYCLING AND DISPOSAL

The importance of redesigning single-use packaging for recycling and ultimate disposal has been discussed extensively (Narayan, 1989; 1991; 1992, 1993a, 1993b; Snook and Narayan 1994). Today's polymeric materials were designed with little consideration for their ultimate disposability or recyclability. This has resulted in new environmental regulations and societal concerns regarding the environmental consequences of such materials when they enter the waste stream after their intended uses. Of particular concern are polymers used in single use, disposable plastic applications. Plastics are strong, light-weight, inexpensive, easily processable and energy efficient. They have excellent barrier properties and are very durable. However, it is these very attributes of strength and indestructibility that cause problems when these materials enter the waste stream. They are resistant to biological degradation because microorganisms do not have enzymes capable of degrading and utilizing most man-made polymers. In addition, the hydrophobic character of plastics inhibits enzyme activity, and the low surface area of plastics with their inherent high molecular weight further compounds the problem.

Therefore, there is an urgent need to redesign and engineer new polymeric materials that have the needed performance characteristics of the plastics, but can be transformed in appropriate waste disposal infrastructures to products that are

compatible with the environment or are recyclable to the same or other products. In addition, after the material's intended use, it must end up in appropriate disposal infrastructures that use these recyclability or biodegradability attributes. The use of biodegradable polymeric materials in single use disposable packaging, nonwovens, and paperboard coatings, in concert with composting infrastructures, is an ecologically sound approach to managing the resultant waste and diverting it from landfills.

2.2 BIODEGRADABLE MATERIALS IN COMPOSTING

2.2.1 Composting

As shown in Figure 2-1, composting is a process involving interdependent biodegradation and polymerization reactions. Composting is defined as "accelerated degradation of heterogeneous organic matter by a mixed microbial population in a moist, warm, aerobic environment under controlled conditions" (Narayan, 1993a). Microorganisms break down cellulose and other carbohydrate-based substrates. The breakdown products are used for cellular metabolism with the formation of biomass, new microorganisms, and the evolution of carbon dioxide. Lignolic species are broken down into phenolic components. Some phenolic components are formed during cellular metabolism and released during lysis of dead microorganisms. It has been suggested that the phenolics react with nitrogenous compounds resulting in the formation of humic substances or humic precursors (Flaig, 1975, 1988; Hayes, et al. 1989). The beneficial effect of compost as a horticultural material is in part attributed to these humic substances.

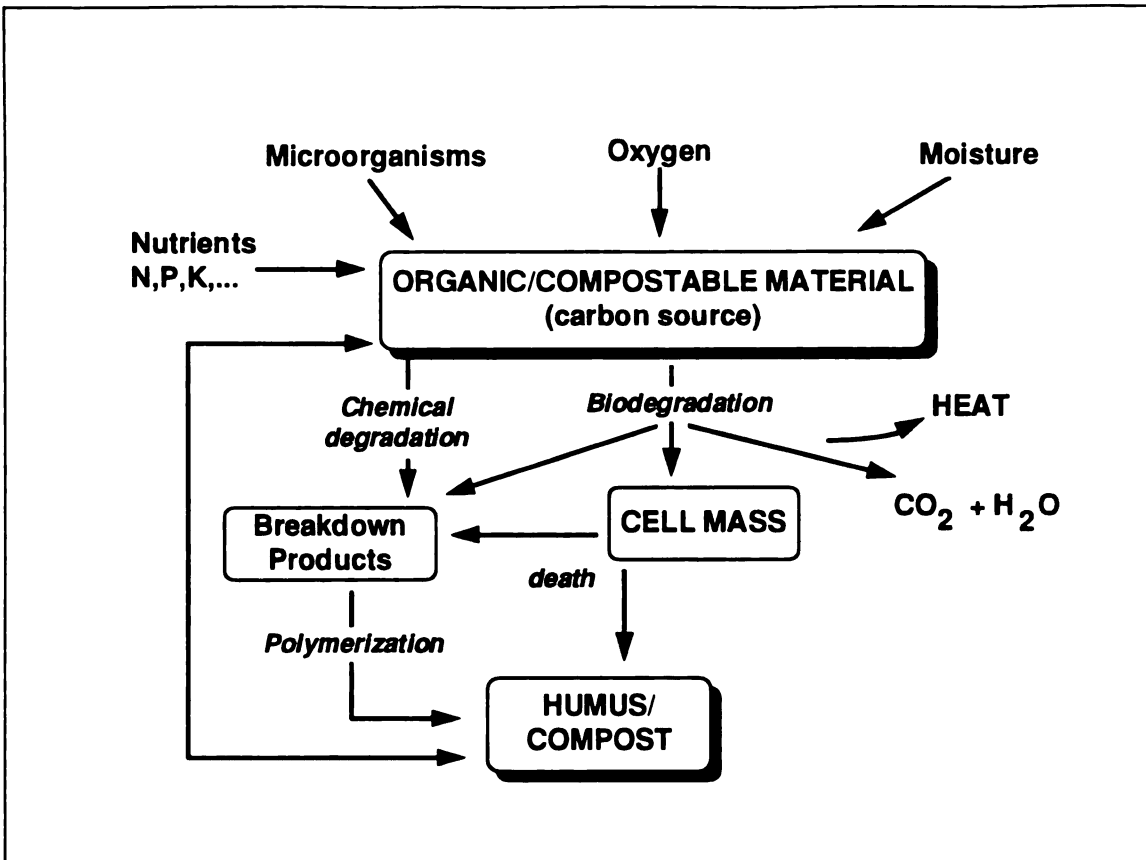


Figure 2-1. Elements of the composting process.

Composting is typically a multi-step process that can be categorized by the configuration and control techniques employed in the early stages. Composting operations can be divided into four types: turned windrow, static pile, in-vessel, and hybrid processes. Turned windrow processing involves the formation of piles (windrows) of the material to be composted, typically 2 m high, 3 to 4 m wide, and 30 to 100 m long. Temperature control, oxygenation, and mixing are provided by periodically turning the windrow using a front-end loader or specialized windrow turning equipment. In the static pile approach, proper conditions are maintained by using forced aeration in place of windrow turning. In-vessel systems are designed to provide optimal conditions by combining forced aeration, intensive

mixing, and complete enclosure of the compost. A variety of hybrid composting schemes are used that combine elements of turned windrow, static pile, and in-vessel composting.

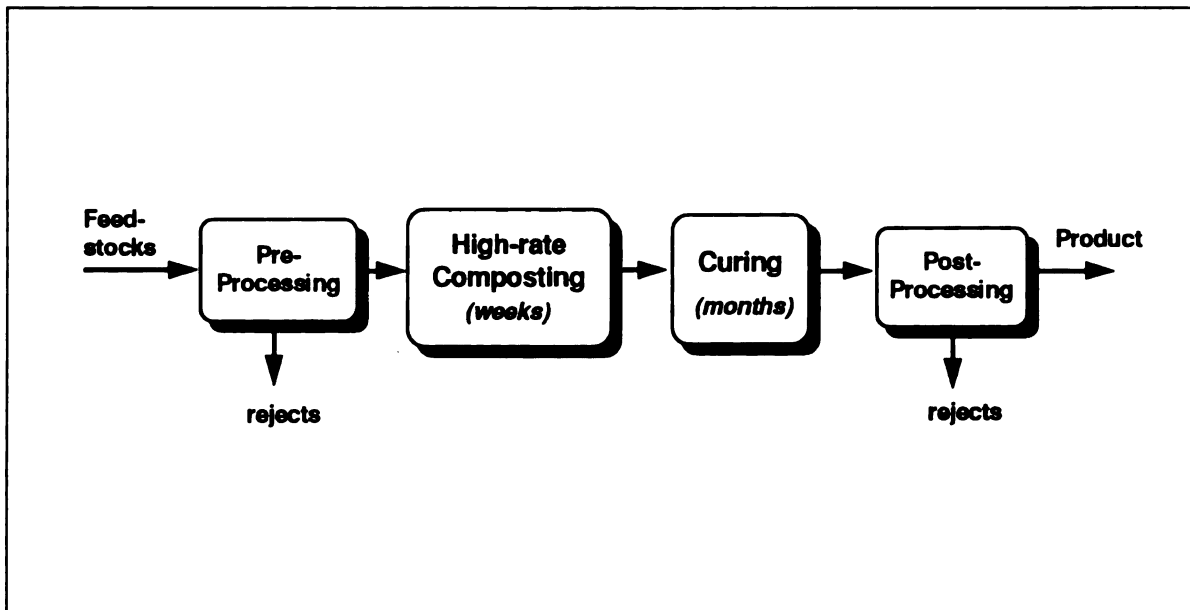


Figure 2-2. Steps in compost processing.

Figure 2-2 shows the four steps that are common to many composting operations. Pre-processing involves the collection and preparation of the compost feedstock materials, which typically includes some type of shredding or other size reduction. The high-rate composting phase is characterized by high oxygen demand and thermophilic temperatures. Frequent windrow turning, forced aeration, or in-vessel operation are required to control the process and to prevent odors during this stage, which typically lasts several weeks. The curing stage is normally performed by storage in a windrow or non-aerated pile over several months with minimal processing. Temperature and oxygen demand decrease during this phase,

which continues until a fully-stabilized product is obtained. Post-processing usually consists of passing the mature compost through a 1/4- or 1/2- inch screen to remove any non-degraded items and ensure a fine and uniform product.

A major logistical advantage of composting over other types of recycling is that of it requires a only a semi-segregated waste stream. Conventional recycling requires the separate collection, transportation, and processing of each component of the waste stream. Processing a mixture of materials is not only possible by composting, it is often essential to the production of quality compost product. Composting can simultaneously handle any mix of materials that are compatible with the composting infrastructure. When operated properly using suitable feedstocks, low-technology composting offers an economically efficient and environmentally sound alternative for managing certain waste streams.

2.2.2 Growth of composting infrastructures

After many years in obscurity, composting has returned as an important approach to managing waste, especially the biodegradable component of our waste stream. Over 3,000 facilities compost yard waste, about 180 compost sludge, 30 compost food and food processing waste, and 25 compost mixed municipal solid waste (MSW). Table 2-1 shows the dramatic growth in the number of facilities, especially for yard waste composting. Since 1988, an average of nearly 500 new yard waste composting facilities have opened each year due to state laws forbidding landfilling, incineration, and open burning of yard wastes.

A number of factors have contributed to the growth of composting infrastructures:

1. Nearly every state has either established or raised recycling goals within the past five years. Based on the composition of MSW, the only way to

reach goals of 30, 40, or 50% recycling is to have a substantial composting element. The U.S. EPA and many states identify composting as a form of recycling.

2. Relative costs for disposal are much higher. The unpopularity of landfills and incinerators and the strict regulations governing them have pushed disposal costs sharply upward. In many parts of the country composting is becoming competitive with other waste management approaches.

3. Separation technologies have improved and contaminants can be effectively separated. Also, community separation programs have had excellent participation.

4. Legislative mandates have been the biggest factor. Twenty six states plus the District of Columbia now have some kind of provision to separate and/or ban yard waste from landfills. Some are outright bans, others are incentives and endorsements.

TABLE 2-1. Growth in number of composting facilities, U.S.

YEAR	Operating composting facilities at year end		
	YARD WASTE	SLUDGE	MIXED MSW
1988	651	79	--
1989	986	119	7
1990	1,407	133	13
1991	2,201	149	18
1992	2,980	159	21
1993	3,014	182	25

Sources: Biocycle, U.S. Composting Council

Another major incentive driving composting is that many states have instituted compost procurement policies. Thus, markets for the finished compost have been created by government fiat. In many states, the state agencies and local governments are required to procure compost product for land maintenance activities including highway construction, landscaping, re-cultivation, and soil erosion control.

2.2.3 Designing materials for compostability

Life Cycle Assessment (LCA) has been used since the 1960's to analyze the environmental impacts associated with a specific product (Curran, 1993). The Society of Environmental Toxicology and Chemistry has defined LCA as "looking holistically at the environmental consequences associated with the cradle-to-grave life cycle of a process or product (Fava et al., 1990). For a compostable item to be properly designed using a biodegradable material, each aspect of the product's life cycle needs to be addressed as shown in Table 2-2. This table lists the necessary attributes in the order that each is required. Issues related to composting and biodegradability (items 5 through 7) are discussed in detail below.

TABLE 2-2. Life cycle requirements for compostable items.

1. Environmentally sound raw materials and production.
2. Processability.
3. Price acceptable to markets or legislation requiring use.
4. Functionality acceptable to end-users.
- 5. Post-use routing to compost infrastructure.**
- 6. Compostability .**
- 7. Complete biodegradability.**

For a waste stream to be useful as a feedstock for composting, all of its constituents must be biodegradable, have no negative impact on compost processing, and contribute to formation of a quality compost product. To meet these requirements, biodegradable plastic items must be made of materials that are both inherently biodegradable and compostable. A material that is inherently biodegradable can, under the proper conditions, be metabolized by microorganisms within a reasonable time frame so that the material does not accumulate in the environment. Compostability requires that the material can be processed in a composting system without ending up in the reject fractions.

Polymeric materials, when designed for compostability using renewable resources (agricultural products) as the major raw material, can be inherently biodegradable and be incorporated into the compost product. Biodegradation of such natural materials will produce high quality compost, along with water and carbon dioxide as by-products. Compost amended soil can have beneficial effects by increasing soil organic carbon, increasing water and nutrient retention, reducing the need for additional chemical inputs, and suppressing plant disease. By using the compost product in agriculture, the carbon in the polymeric materials, compost, and carbon dioxide become a part of the biological carbon cycle. The problem of waste disposal could become the solution for low-input sustainable agriculture.

Studies by the Michigan Biotechnology Institute have demonstrated that conventional plastics are inherently recalcitrant to biodegradation and interfere with the composting process (Snook and Narayan, 1994). For composting to play an ecologically sound role in the biological carbon cycle, the compost product must be of high quality. The presence of inert contaminants such as fragments of

glass and plastic have a negative affect on compost appearance and marketability. Because of the volume and mass reductions that occur during composting, a few percentages of recalcitrant, inert synthetics in the feed material results in a substantial concentration in the compost product. When a compost containing a small amount of inert material is applied to soil repeatedly, a build up of the inert material will occur as compost organic carbon is utilized. In the end, the processability and product quality of compost depends on the quality of every feedstock stream.

2.3 STATUS OF THE U.S. BIODEGRADABLE MATERIALS INDUSTRY

The U.S. biodegradable materials industry made a false start by introducing starch-filled polyethylene and photodegradable plastic bags as biodegradable materials in the 1980's. Films produced from polyethylene with 6-15% starch were designed to disintegrate as the starch component was biodegraded. However, only the starch particles at the surface of the film biodegraded, leaving the embedded starch particles and the polyethylene matrix intact. Photodegradable films were also designed for disintegration by incorporating photosensitive groups or additives into the plastics. Unfortunately, when bags made of photodegradable plastics ended up in landfills or compost piles, they were not exposed to the ultraviolet radiation (sunlight) necessary to initiate radical induced degradation. These initial failures made the public suspicious of biodegradable plastics.

Biodegradable products being introduced today are fully biodegradable or compostable. U.S. Federal Trade Commission guidelines state that:

“Unqualified degradability claims should be substantiated by evidence that the product will completely break down and return to nature, that is, decompose into elements found in nature within a reasonably short period of time after the customer disposes of it in the customary way.”

(U.S. Federal Trade Commission, 1992)

Because of this requirement, the industry is active in the development of standard methods for determining biodegradability to substantiate biodegradability claims. ASTM standards have been developed for determining intrinsic biodegradability, biodegradability under composting conditions, and biodegradability under other environmental conditions. Biodegradable material producers also recognize the need for simultaneous development of appropriate waste management infrastructure, such as composting, so that the material's biodegradability attributes are used when customers dispose of the products in the customary way. The biodegradable plastic industry's attention to scientific substantiation of degradability claims and the public's appreciation of the role for biodegradable materials in solid waste management is leading to greater acceptance of biodegradable materials.

A broad range of biodegradable materials are being produced today or are planned for production, as shown in Table 2-3. Several of these fall under the category of natural biopolymer based materials, such as cellophane, cellulose and starch esters, and starch blends. A second set of technologies are based on polyesters produced from fermentation products. These include the polylactide polymers and poly-(hydroxybutyrate-co-hydroxyvalerate) polymers. The remaining biodegradable

polymers (polyvinyl alcohols, polyethylene oxides, polycaprolactones) are chemically synthesized from petrochemical feedstocks.

The major target markets for biodegradable polymeric materials are single-use disposable packaging, disposable serviceware (cutlery, plates, cups), disposable nonwovens (diapers, personal care products), and paper and film coatings. More than 50 billion pounds of material are used and disposed of annually in these markets (Narayan, 1993b). The planned capacities of the existing biodegradable plastics from Table 2-3 is less than 1 billion pounds, leaving a large potential market share yet to be claimed by biodegradable materials.

TABLE 2-3. Major biodegradable materials producers (Narayan, 1993).

COMPANY	BASE POLYMER	FEEDSTOCK	COST, \$/lb	CAPACITY, MM LB/YR
Cargill, Minneapolis, MN	Poly lactide (EcoPLA)	Renewable Resources, Com	1.00 - 3.00	10 ('94 scaleup); 250 (mid-1996)
Ecochem, Wilmington, DE	Poly lactide copolymers	Renewable Resources, Cheese whey, Com	< 2.00 proj'd	0.15 ('94 scaleup)
Flexel, Atlanta GA	Cellophane, (Regenerated cellulose)	Renewable resources	2.15	100
Zeneca, (business unit of ICI Americas)	Poly(hydroxybutyrate-co-hydroxyvalerate), (PHBV)	Renewable resources -- carbohydrates (glucose), organic acids	8.00 - 10.00; 4.00 proj'd	0.66, additional capacity slated for '96 is 11 - 22
Novamont, Montedison, Italy	Starch-synthetic polymer blend containing approx. 60% starch	Renewable resources + petrochemical	1.60 - 2.50	50, in Tumi, Italy
Novon Products (Warner-Lambert), Morris Plains, NJ*	Thermoplastic starch polymer compounded with 5-25% additives	Renewable resources, Starch	2.00 - 3.00	100
Union Carbide, Danbury, CT	Polycaprolactone (TONE polymer)	Petrochemical	2.7	< 10
Air Products & Chemicals, Allentown, PA	Polyvinyl alcohol (PVOH) & Thermoplastic PVOH alloys (VINEX)	Petrochemical	1.0 - 1.25 (PVOH); 2.50-3.00 (VINEX)	150 - 200 (water sol. PVOH); 5 (VINEX)
National Starch & Chemical, Bridgewater, NJ	Low ds starch ester	Renewable resources, Starch	2.00 - 3.00	Not available
MBI/Japan Corn Starch Co., Lansing, MI	Water repellent, thermoplastic modified starches (AMYPOL)	Renewable Resources, Starch	1.0 - 1.50	0.1(pilot scale); 150 slated for early '96
Planet Packaging Technologies, San Diego, CA	Polyethylene oxide blends (Enviroplastic)	Petrochemical	3.00	10
Showa Highpolymer Co., Ltd.	condensation polymer of glycols with aliphatic dicarboxylic acids (BIONELLE)	Petrochemical	approx. 3.00	0.2 (pilot); 7(semi-commercial, end '94)

CHAPTER 3

POLYLACTIDE

3.1 POLYLACTIDE SYNTHESIS

Lactic acid polymers prepared by ring-opening polymerization of the lactide dimer are known as polylactides (see Figure 3-1). The six-membered cyclic diester L-lactide is prepared by dehydrating the naturally occurring form, L-lactic acid. High molecular weight poly-L-lactides can be synthesized in a controlled manner using a variety of metal catalyst initiators, preferably tin catalysts (Dijkstra et al., 1990). The poly-L-lactide polymer (PLLA) is an optically active, isotactic, semicrystalline polymer, with a glass transition temperature (T_g) around 58°C and

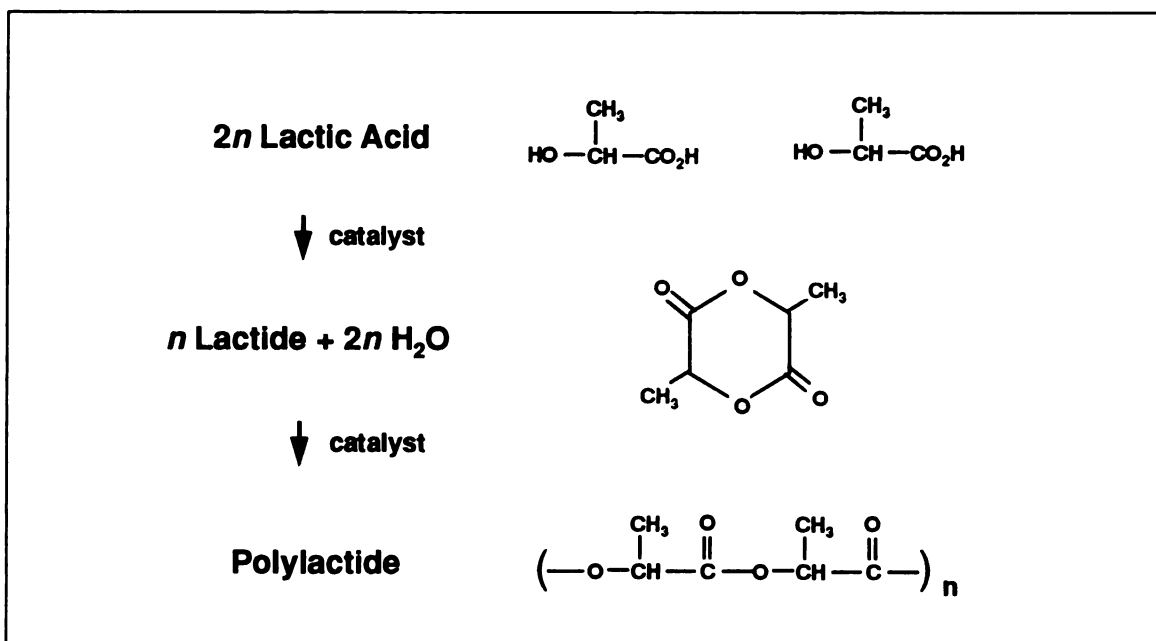


Figure 3-1. Synthesis of polylactide.

melting temperature (T_m) around 178°C . This material has a very narrow window of processibility, since molecular weight degradation occurs at around 180°C . Polymerization with a small amount of lactide containing D-lactic chiral centers disrupts the crystallinity and produces an amorphous polylactide. This decreases the melting point from 178°C to 124°C as the composition is changed from pure L-lactide to 8% of the D-lactide (Spinu, 1993) and improves processability.

3.2 BIODEGRADATION MECHANISM AND KINETICS

Polylactide degradation occurs in two distinct stages. First, random non-enzymatic chain scission of the ester groups leads to a loss in molecular weight. The molecular weight of the polymer eventually decreases to the point where the oligamers can diffuse out of the polymer bulk and be utilized by microorganisms. The pathways for chemical and biological cycling of polylactide are shown in Figure 3-2.

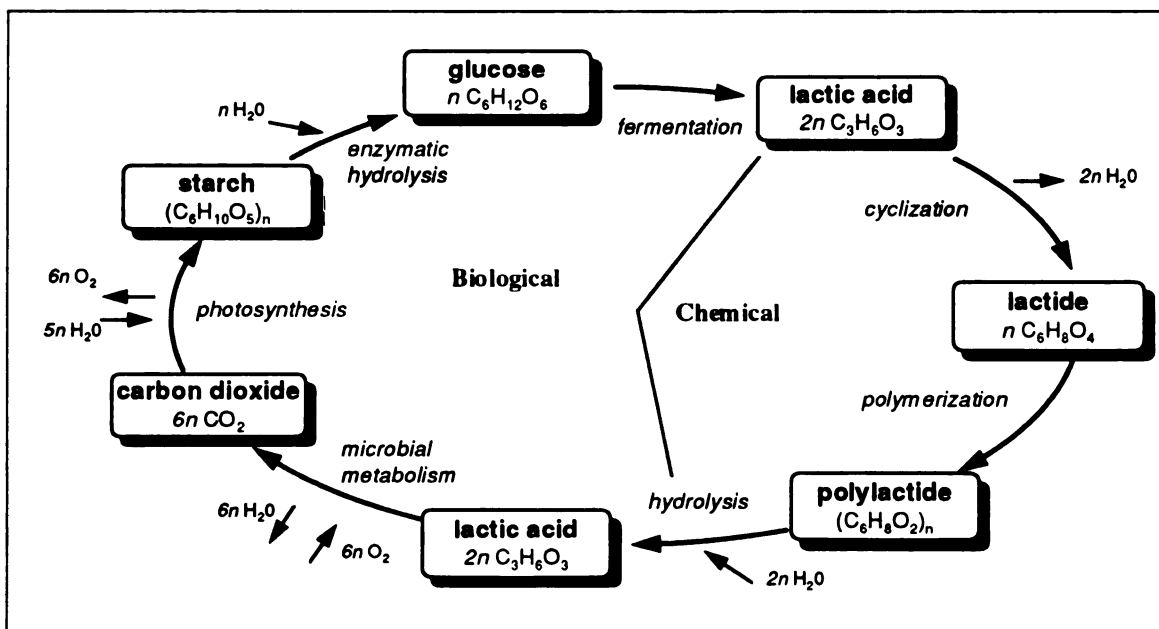


Figure 3-2. The polylactide cycle (adapted from Ozeki and Ohara, 1993).

3.2.1 Hydrolytic degradation

Poly lactide chain scission is autocatalyzed by the carboxy endgroups as described by the following rate equation (Schindler et al., 1977; Pitt et al., 1981; Zhu et al., 1991):

$$\frac{d [\text{COOH}]}{dt} = k [\text{COOH}] [\text{H}_2\text{O}] [\text{ester}] \quad (3-1)$$

where $[\text{COOH}]$ is the concentration of carboxy end groups in the polymer, $[\text{H}_2\text{O}]$ is the concentration of water in the polymer, and $[\text{ester}]$ is the concentration of the ester groups in the polymer. The carboxy group concentration can be related to ester concentration, degree of polymerization (DP), weight, volume, and density of the polymer sample (W, V, ρ), and the number average molecular weight (M_n):

$$[\text{COOH}] = \frac{[\text{ester}]}{\text{DP} - 1} \quad (3-2)$$

$$[\text{COOH}] = \frac{W}{M_n V} = \frac{\rho}{M_n} \quad (3-3)$$

Using a lumped rate constant, k' :

$$k' = \frac{k [\text{H}_2\text{O}] \rho}{M_n} \quad (3-4)$$

the rate equation for the change in degree of polymerization is:

$$\frac{d (1 / \text{DP})}{dt} = k' \frac{\text{DP} - 1}{\text{DP}^2} \quad (3-5)$$

Integrating this equation gives:

$$\ln \frac{1 - \text{DP}}{1 - \text{DP}_0} = -k' t \quad (3-6)$$

with DP and DP_0 being the degree of polymerization at time t and $t = 0$. For $\text{DP} \gg 1$ this expression becomes:

$$\ln \frac{\text{DP}}{\text{DP}_0} = \ln \frac{M_n}{M_{n,0}} = -k' t \quad (3-7)$$

Equation 3-7 applies until the molecular weight is reduced to around $M_n = 10,000$ when the diffusivity of the oligomer through the polymer matrix is high enough for weight loss to begin.

Figure 3-3 shows a proposed schematic of polylactide degradation via a two-step mechanism. Initially molecular weight reduction occurs by non-enzymatic hydrolysis without significant diffusion of oligomer out of the polymer bulk. As the polylactide molecular weight decreases, oligomers are increasingly able to diffuse out of the polymer bulk and be utilized by microorganisms.

In massive polylactide objects a concentration gradient of carboxy groups develops with the highest concentration at the center. This leads to more rapid weight loss from the center, leaving a hollow core (Li et al., 1990a). In thin films, weight loss occurs at a nearly constant rate through the film, leaving a porous structure. Crystalline regions are inaccessible to water and oligomer diffusion, so are degraded from the edges. Higher chain mobility in amorphous regions is believed to reduce the energy required to achieve the transition state of the hydrolysis reaction. Since hydrolysis occurs at a higher rate in amorphous regions, the overall crystallinity initially increases as degradation begins (Li et al., 1990b).

The rate of hydrolysis of polylactide and other poly(α -hydroxy acids) increases with temperature and shows an increase in rate at the glass transition temperature (Reed and Gilding, 1980). The sources in Table 3-1 provided data for polylactide molecular weight loss with time at constant temperatures under the conditions listed. Rate constants at the various temperatures were calculated as shown in Figure 3-4 using these data and the rearranged form of Equation 3-7:

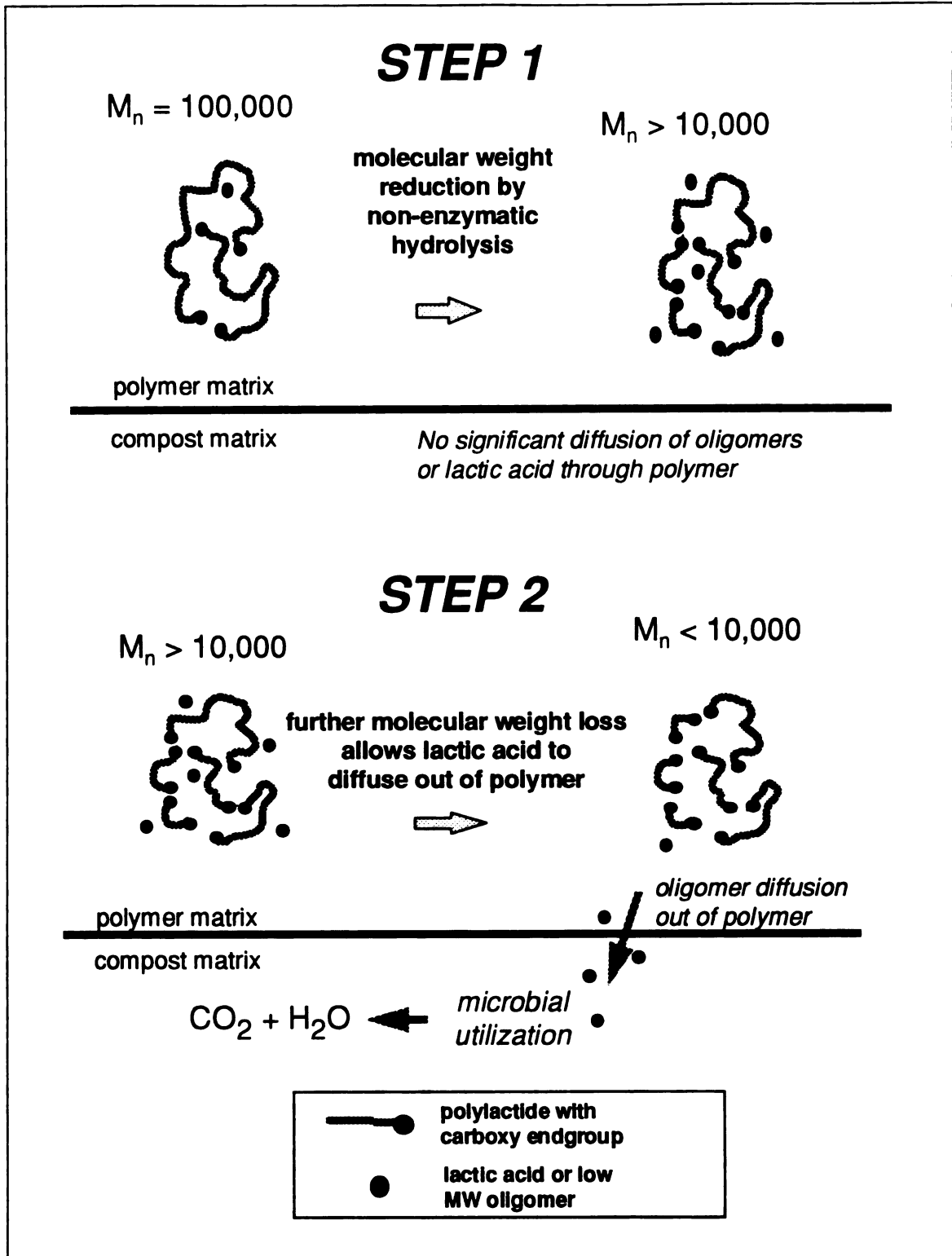


Figure 3-3. Proposed degradation mechanism for polylactide.

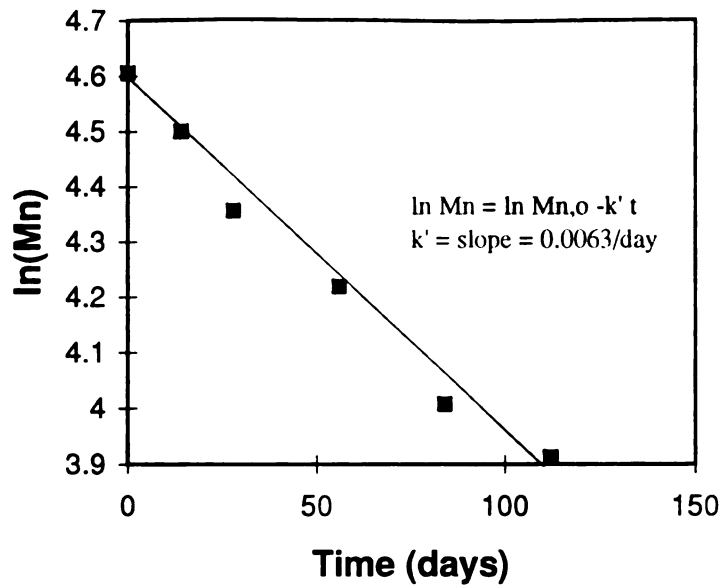


Figure 3-4. Example of rate constant calculation using data from Reed and Gilding, 1980.

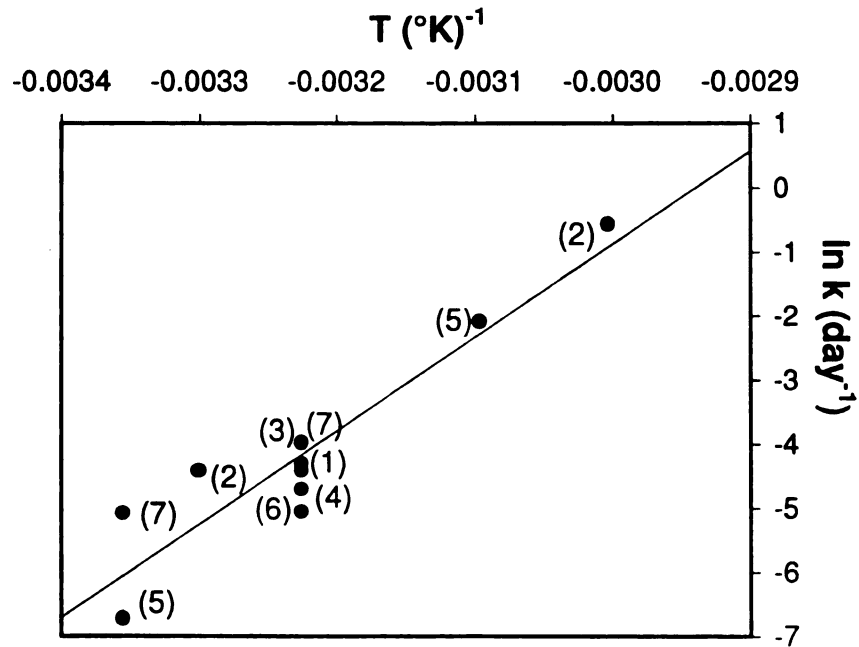


Figure 3-5. Arrhenius plot for polylactide degradation rate constant.

$$\ln M_n = \ln M_{n,o} - k' t \quad (3-8)$$

The resulting rate constants were used to generate an Arrhenius type rate expression for the rate constant k' using a least squares regression to the $\ln(k)$ vs. $(1/T)$ data, as shown in Figure 3-5. The expression for the rate constant:

$$k' = a \cdot \exp\left(\frac{-E_a}{RT}\right) = 3.664 \times 10^{18} \cdot \exp\left(\frac{-14543}{T}\right) \quad (3-9)$$

could then be used in Equation 3-9 to calculate the rate of hydrolysis at temperatures near or below T_g and to predict the rate of decrease in number average molecular weight:

$$\ln M_n = \ln M_{n,o} - 3.664 \times 10^{18} \cdot \exp\left(\frac{-14543}{T}\right) \cdot t \quad (3-10)$$

The activation energy for hydrolytic molecular weight reduction, E_a , was calculated at 29.8 kcal/mol. Fitting a logarithmic curve to k vs. T data yielded an expression equivalent to that found using the Arrhenius plot.

Table 3-1. Rate data used in the Arrhenius plot.

Label	Source	PLA Type	Conditions of Experiment
(1)	Li et al, 1980	semi-crystalline PLLA	37°C in buffered saline, pH 7.4
(2)	Schindler et al., 1977	amorphous P-D,L-LA	30°C and 60°C in water
(3)	Nakamura et al., 1989	crystalline PLLA	<i>in vivo</i> (rabbit, 37°C)
(4)	Reed and Guilding, 1980	37% crystalline PLLA	37°C in buffer, pH 7.0
(5)	Mason et al., 1980	amorphous P-D,L-LA	25°C and 50°C in deionized water
(6)	Mason et al., 1980	amorphous P-D,L-LA	37°C in pH 7 buffer
(7)	Mason et al., 1980	amorphous P-D,L-LA	25°C and 37°C in porcine plasma

The ratio M_w/M_n gives a measure of the polydispersity of the polylactide. A wider distribution of molecular weights gives a larger polydispersity since the contribution of each molecule to the number average molecular weight, M_n , is proportional to its mass, and its contribution to the weight average molecular weight, M_w , is proportional to the square of its mass as shown in Equations 3-11 and 3-12.

$$M_n = \frac{\sum_{i=1}^{\infty} N_i M_i}{\sum_{i=1}^{\infty} N_i} \quad (3-11)$$

$$M_w = \frac{\sum_{i=1}^{\infty} N_i M_i^2}{\sum_{i=1}^{\infty} N_i M_i} \quad (3-12)$$

where N_i is the number of molecules of type i and M_i is the molecular weight of molecule type i . Since the hydrolysis of polylactide occurs randomly, longer polymer chains are more susceptible to cleavage than short chains. This will result in a narrowing of the distribution of molecular weights as degradation proceeds.

3.2.2 Enzymatic degradation

Several enzymes, including proteinase K, pronase, and bromelain, have been shown to bring about hydrolysis of polylactide *in vitro* (Williams, 1981). However, enzymes are large molecules and are unable to diffuse through crystalline regions. Little enzymatic degradation occurs during the early stages of degradation when the polymer crystallinity is high (Holland et al., 1986). In the later stages enzymatic involvement can become more pronounced as pores develop, fragmentation occurs, and more polymer regions are accessible to enzymes.

3.3 LIFE CYCLE ASSESSMENT

The raw materials for lactic acid production are annually renewable agricultural products that are produced in surplus. The lactic acid fermentation itself makes especially efficient use of the feedstock (glucose) carbon. Unlike the fermentations used to produce other agriculturally-derived products, such as ethanol, the lactic acid fermentation does not result in a loss of carbon as carbon dioxide. This results in a larger yield of product per unit of feedstock consumed.

Poly lactide is a thermoplastic polyester that can be processed by melt flow or by solution processing. The price of poly lactide is decreasing as production scales increase and processing technologies improve. Resin mechanical properties and shelf life under moderate temperature storage make it applicable for a number of single-use disposable products.

The mechanism of poly lactide biodegradation makes it especially suited to disposal in composting infrastructures. High compost temperatures and moisture aid in rapid hydrolysis, and compost microorganisms use the lactic acid as an energy source. The heat generated accelerates decomposition of other compost substrates, and biomass sustained by the lactic acid eventually becomes a part of the compost product.

3.4 APPLICATIONS

Implantable Prosthetic Devices

The potential of lactic acid polymers as a material for resorbable prosthetic devices was first investigated by the U.S. Army (Kulkarni et al., 1966). Massive implantable devices of poly(lactic acid) provide temporary structural support or

fixation until natural healing occurs and do not require a second surgical procedure for device removal. Extensive *in vivo* testing in laboratory animals has been necessary to precisely balance the rate of erosion with the rate of tissue regeneration, and such devices are only now entering clinical trials.

Resorbable Sutures

Lactic acid polymers found their first commercial success as a replacement for collagen fiber in resorbable sutures (Cutright et al., 1971). Polymers of lactic acid and glycolic acid are now widely used to produce bioresorbable sutures that are sold under the trade names Dexon, Medifit, and Vicryl. These sutures have a predictable rate of mechanical property reduction and are resorbed by the body within 2 or 3 months (Craig et al., 1975).

Controlled-Release Matrices

Polymers of lactic acid were among the first to be applied in the pharmaceutical industry as matrices for the controlled-release of drug products (Yolles, 1971). Microspheres, capsules, and pellets are designed so that zero-order drug release is achieved by balancing the rate of diffusive release with the rate of release by polymer erosion. Similarly, pesticides and other agricultural chemicals could be incorporated into poly(lactic acid) matrices for slow release action (Sinclair, 1973). Incorporation into a polymer matrix has been proposed as a way to provide safer handling of pesticides and reduce chemical runoff.

Biodegradable Packaging

Surgical and pharmaceutical applications for poly(lactic acid) are low volume markets able to tolerate high resin costs. In contrast, penetration of the 50 billion pound per year markets for single-use disposable packaging depends on low resin

price. Considerable research and development effort is currently aimed at commercial production of lactic acid polymers (Narayan, 1993b). Argonne National Laboratories is developing a technology for polymerizing lactic acid produced by fermentation of potato waste. Low molecular weight poly(lactic acids) are synthesized by condensation polymerization and spliced together using coupling agents. Batelle and Golden Technologies are jointly developing lactic acid polymer technology for packaging applications. Cargill and Ecochem (a joint venture of DuPont and ConAgra) are producing lactic acid from corn and cheese whey. This is followed by dimerization to the lactide and ring-opening polymerization to high molecular weight polylactide polymers suitable for packaging, as described below. Cargill brought a 10 million pound per year pilot lactic acid production facility on-line in early spring of 1994.

3.5 POLYLACTIDE FILM PROPERTIES

The polylactide film used in this work was produced by Cargill Inc., Minneapolis, MN (Gruber et al., 1993). Table 3-2 gives some physical and chemical characteristics of this film.

TABLE 3-2. Characteristics of polylactide film.

Film Thickness	2.91 mil
Appearance	transparent
Elemental Analysis:	
Carbon	49.8%
Hydrogen	5.8%
Nitrogen	0.004%
Oxygen	44.8%
Phosphorus	0.016%
Sulfur	< 10 ppm
Mn	95,971
Mw	215,034
Mw/Mn	2.24
Degree of crystallinity	43%
Tg	57°C
Tm	138°C

CHAPTER 4

ANALYTICAL METHODS

Methods that were used in the studies of polylactide biodegradability are outlined in this chapter. The weights and volumes used for characterization of test materials and feedstock materials that were more homogeneous were sometimes lower than those listed for compost analysis.

Weight Determination

Three balances were used to measure sample mass. Large samples were weighed using an Ohaus I-10 platform balance, which had a range from 0.00 to 50.00 kg. The weight of medium size samples, 0.000 to 2000.00 g, were measured using a Fisher Scientific XD-2KD balance. A Perkin-Elmer AD-4 Autobalance was used to measure the mass of samples in the 0.000 to 20.000 mg range.

Measurement of pH

A slurry of 10 g wet weight compost was made by mixing with 50 ml dH₂O for 30 seconds. Slurries were prepared in triplicate and pH was measured using an Omega PHB-70X water analyzer.

Moisture Content

Triplicate samples of approx. 150 g w.w. compost were dried to constant weight in a vacuum oven at 105°C and 15 in. Hg. Weights of samples are referred to on the

basis of their wet weight (w.w.) or dry weight (d.w.), and the moisture content is calculated as the percent of the wet weight removed by drying.

Milling

Dried composts were milled in a Fitzpatrick Model JT-6 homoloid mill to pass through a 25 mesh (0.7 mm) screen. This material was used for determining ash content, for elemental analyses, and for humic substance fractionation.

Ash Content

Approximately 2 g d.w. of dried, milled compost was ignited at 550°C for 2 h to determine the ash content of the composts. Ash content was reported as percent of dry weight remaining after ignition.

Carbon and Nitrogen Contents (CHN)

Samples of 5-10 mg of dried, milled compost were analyzed for carbon and nitrogen content using a Perkin-Elmer 2400 CHN Elemental Analyzer.

Humic Substances Analysis

The degree of humification of compost samples was determined using the method of Ciavatta et al. (1990). Dried, milled compost samples (0.8 g) were mixed with 40 ml of a solution of 0.1 M $\text{Na}_2\text{P}_2\text{O}_7$ and 0.1 M NaOH and shaken at room temperature for 2-3 hours. After centrifuging 20 min. at 13,000 x g the supernatant was removed and filtered through a 0.45 μm syringe filter and referred to as total extract (TE). Humic acids (HA) were then precipitated by adding 6N H_2SO_4 to 20 ml of TE to acidify it to pH 2.0, and humic acids were collected by centrifuging 20 min. at 13,000 x g and redissolving the pellet in 0.1 N NaOH. The 20 ml of supernatant from this centrifugation was loaded onto 2 g of solid polyvinylpyrrolidone (PVP) equilibrated with 0.005 N H_2SO_4 . The PVP was

washed with an additional 20 ml of 0.005 N H₂SO₄, and the two non-retained fraction were combined and referred to as the non-humified (NH) fraction. The retained fulvic acids (FA) were eluted from the PVP using 40 ml of 0.1 N NaOH. The carbon contents of the TE, HA, FA, and NH fractions were determined by dichromate oxidation using 0-150 ppm Hach COD vials.

Cress Germination Bioassay

Compost maturity and phytotoxicity were determined using the cress germination bioassay based on the method of Zucconi et al. (1981). Compost extracts were prepared by adding 100 g D.W. of moist compost to distilled water to a final moisture content of 1000 g and mixing in a blender on lowest speed for 30 seconds. The slurry was then strained through a 1 mm mesh and centrifuged for 30 min. at 1000 x g to remove solids. The compost extract was used as a germination medium for curly cress (*L. sativum*). Eight replicate 15 x 95 mm petri dishes were prepared with 2 ml of compost extract and 10 cress seeds on a 9.0 cm Whatman #1 filter paper. The dishes were incubated at 28°C in the dark for 48 hours when the seeds were removed and the number of seeds germinated and their weight were determined and compared to the germination of seeds in a control of water only.

Gas Chromatography (GC)

Samples of compost vessel gases were collected in a syringe, and composition was determined using a Gow-Mac 580 Gas Chromatograph. Separation of 200 µl sample was performed on a CarboSphere column at 100°C and detected at 150°C with helium as the carrier gas at 30 ml/min.

Gas Analyzer Calibration

The Ultramat 22P and Ultramat 21P carbon dioxide analyzers and the Model 755A oxygen analyzer were calibrated using four cylinder gases from AGA Industries. Medical air and nitrogen were used to span and zero the oxygen analyzer. The carbon dioxide analyzers were zeroed using nitrogen and spanned using certified 3.85% carbon dioxide/balance nitrogen for the 0-4% range channels, or using 100% carbon dioxide for the 0-100% range channels.

Differential Scanning Calorimetry (DSC)

Poly lactide glass transition temperature and melting temperature were measured using a Perkin-Elmer DSC7 differential scanning calorimeter at a temperature ramp of 10°C/min.

Gel Permeation Chromatography (GPC)

A solution of 0.5% polylactide in chloroform was separated at 1 ml/min on a Waters K-800 Ultrastyrigel column at 35°C. A Waters model 410 differential refractometer was used to detect polylactide and results were reported based on calibration with polystyrene standards.

CHAPTER 5

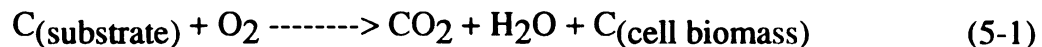
BIODEGRADATION UNDER EXTERNALLY CONTROLLED COMPOSTING CONDITIONS

5.1 OVERVIEW

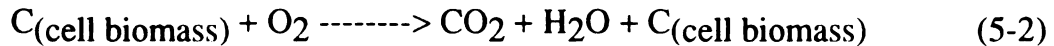
As discussed in Section 2.2, the inherent biodegradability of new materials must be established if they are destined for disposal in composting infrastructures. This chapter presents the development of an apparatus for measuring the biodegradability of materials under controlled composting conditions and its application in measuring the biodegradability of polylactide film.

5.2 TEST METHOD

Evaluating the biodegradability of any material requires some parameter or set of parameters that can be measured and related to the rate and extent of biodegradation of the material being tested. Under aerobic conditions, biodegradation of an organic substrate can be expressed as:



If the experiment to measure biodegradability continues over many cell generations, biomass is metabolized by predator species:



and as the substrate is depleted and predation continues, the carbon originally present as substrate will be largely mineralized to carbon dioxide.

This view of the microbial processes occurring during biodegradation has been used to develop test methods which use the amount of carbon released as carbon dioxide to approximate the amount of carbon consumed from the material being tested. One of many such methods, American Society for Testing and Materials (ASTM) method D 5338-92, has been designed specifically to be used for laboratory measurement of the degree and rate of aerobic biodegradation of plastic materials on exposure to a controlled composting environment. This method involves exposing the test material to an inoculum of mature compost in a two-liter vessel and either measuring the carbon dioxide evolved directly or by trapping evolved carbon dioxide in an alkaline scrubbing solution and quantifying by titration.

The conditions of the experiment mimic the physical and biochemical environment present during composting. By housing the two-liter vessels containing the test material and compost matrix in a controlled temperature room, temperatures characteristic of optimal composting can be maintained. During the 45 day experiment the temperature is set at 35°C for the first day, 58°C for four days, 50°C until day 28, and at 35°C for the remaining 17 days. Although high temperatures improve the kinetics of decomposition, excessive composting temperatures kill or inactivate many microbial species and result in a less diverse

microbial population. At temperatures in excess of 55-60°C, fungi are strongly inhibited, and bacteria and actinomycetes are reduced to a few thermotolerant species (McKinley and Vestal, 1984; Strohm, 1985). High temperatures also result in conditions which favor the formation of ammonia and the volatilization of other malodorous compounds. The temperature regimen enforced on the composting mixture is representative of the temperatures occurring in full-scale processes tuned for maximum decomposition and minimum odor generation (MacGregor et al., 1981; Sikora and Sowers, 1985; Stentiford et al., 1985).

Aerobic decomposition results in less odor production and proceeds at a higher rate than anaerobic metabolism. Since aerobic metabolism requires oxygen for oxidative phosphorylation, maintaining a healthy population of aerobes depends on providing adequate aeration. A higher concentration of oxygen in the interstices of the compost matrix leads to a greater depth of oxygen penetration into the biofilm layer on the surface of a compost particle. Increasing the layer of non-oxygen limited conditions maximizes substrate utilization (Suler and Finstein, 1977; Hamelers, 1993). The air flow rates through the test vessels are set so that the oxygen content in the effluent gas remains above 6% by volume while the carbon dioxide concentration stays at a concentration high enough to be accurately detected or efficiently trapped in solution.

Moisture content is another parameter that is set to maximize microbial activity. The optimum depends on the moisture holding capacity of the compost, which is a function of the particle size distribution, porosity, water solubility, and structural integrity of the compost particles. Excessively dry conditions limit microbial growth and motility, but a water content higher than the moisture holding capacity

will cause clumping or will block interparticle spaces and hinder oxygen transfer. Moisture levels below 30% and above 70% by weight severely limit aerobic activity in composts. For most composts the optimal moisture content lies between 50% and 60% (Jeris and Regan, 1973). The initial moisture content of the test material and compost matrix is set in this range. Drying is prevented by humidifying the air before it enters the test vessels.

Other chemical parameters are set within the optimal ranges for composting. The initial hydrogen ion concentration of the test mixture is checked to make sure that it falls between a pH of 7 and 8. The ratio of carbon to nitrogen in the initial mixture is set between 25 and 40.

In addition to the sample mixtures containing the test material, three sets of vessels provide control data during the experiment. These include a set of "blank" vessels containing the compost matrix alone, a set containing polyethylene as a negative control, and another using cellulose as a positive control. The amount of carbon dioxide which can be attributed to the test material is calculated as the difference between the amount of carbon dioxide evolved from the test material/compost mixture and the amount of carbon dioxide evolved from the blank vessels containing compost only. Biodegradability is expressed as the cumulative percentage of the carbon from the test material which has been mineralized to carbon dioxide. Experimental error is calculated as the standard deviation of the biodegradability.

5.3 PRELIMINARY EXPERIMENT 1

The first controlled composting experiment evaluated the biodegradability of paperboard used in frozen food packaging. An acrylic copolymer coating on this paperboard provides the moisture resistance necessary in frozen food packaging applications. If the acrylic coating is sufficiently biodegradable it will be consumed during composting and will allow normal biodegradation of the paperboard component.

5.3.1 Method

The experimental set-up was based on the ASTM D 5338 procedure described above. Each two-liter test vessel contained 180 g dry weight of compost and 30 g dry weight of the test material, adjusted to an overall water content of 50% by weight. Polyethylene and cellophane films 25 μm (1 mil) thick were cut into 6 cm x 6 cm squares, and paperboards 300 μm (12 mil) thick were cut into 3 cm x 3 cm squares. Compost used in the experiment resulted from a mixture of restaurant waste (55%), leaves (10%), turkey manure (10%), pine chips (3%), and onion tops (22%) windrowed for 10 weeks. The finished product had the following characteristics: carbon content, 22.6%; nitrogen content, 1.92%; pH of 7.5; and volatile solids, 63%. This compost formulation provided an appropriate nutrient balance for test material exposure and did not result in a background carbon dioxide evolution rate which would obscure that from the test material.

An incubator room, maintained at 37° C, housed the test apparatus (Figure 5-1). Air from an aquarium pump bubbled through two 20-liter preconditioning vessels in series for carbon dioxide removal and humidification before passing to the 15 sample vessels. The first preconditioner contained 10 N NaOH solution and the

second contained water so that carbon dioxide-free, humidified air entered the sample vessels. A manually adjusted needle valve at the exit of the sample vessel controlled the air flow rate. After passing through the compost and test material mixture, the air bubbled through two 50 ml trapping tubes containing 30 ml each of 5 N NaOH hydroxide. Periodic titration of the trapping solutions provided data for calculating the rates of carbon dioxide evolution.

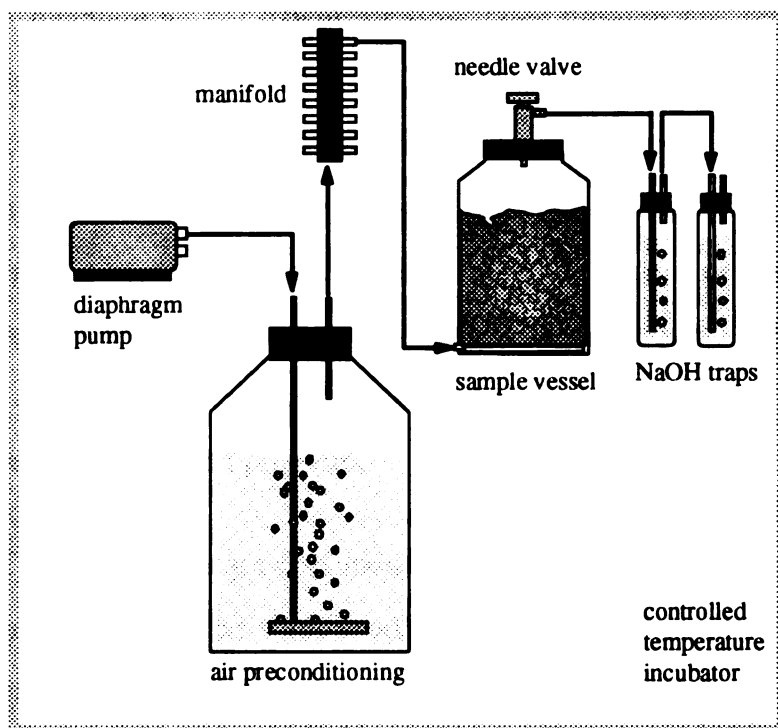
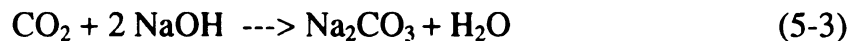


Figure 5-1. Setup for externally controlled composting experiment 1.

At high pH, carbon dioxide reacts with sodium hydroxide to form sodium carbonate:



Addition of barium chloride to this mixture precipitates the carbonate as barium carbonate. Titration of the initial and precipitated sodium hydroxide trapping solutions with standardized 0.05 N HCl provides the concentrations of sodium hydroxide in the trapping solution before and after carbon dioxide absorption. This titration allows the calculation of the amount of carbon dioxide evolved from each vessel and from the test materials individually.

5.3.2 Results

Difficulties in maintaining consistent air flow rates through the apparatus led to excessive variation within triplicates and disruptions in the data collection. The pump delivered low pressure air to the 15 vessels, and a small adjustment to one vessel's valve affected the air flow rates in all of the vessels. The long time required to regain system pressure after any valve adjustment or loss of pressure made flow rate adjustment a painstakingly slow procedure. However, the tendency for a leak in any vessel to stop air flow through all of the trapping solutions presented the largest problem.

The results of this preliminary experiment (Figure 5-2) show that cellophane and both paperboards biodegraded significantly in one month, but the high variation within triplicates indicates the limitations of the data (Table 5-1). Sample vessels containing polyethylene film consistently produced less carbon dioxide than the blanks. The flexible squares of polyethylene film tended to envelope portions of the compost matrix, which may have created anaerobic pockets and reduced microbial activity, while the rigidity of the cellophane and paperboards did not cause this behavior.

The constant temperature of 37°C provided less than optimal conditions for biodegradation. Exposure to the typical pattern of temperatures found in composting gives rise to periods in which different sets of microorganisms dominate. Furthermore, higher temperatures increase the rates of hydrolysis and other chemical and enzymatic reactions occurring.

TABLE 5-1. Results of Experiment 1.

TEST MATERIAL	%C in sample mineralized to carbon dioxide	
	MEAN	Standard deviation
Cellophane	44.2	11.9
Uncoated paperboard	36.3	17.7
Acrylic coated paperboard	33.0	11.4
Polyethylene	-2.5	3.9

A separate study investigated the biodegradability of the acrylic copolymer coating material in its liquid form (David, 1994). This experiment, based on the method ASTM D 5209-91, determined the aerobic biodegradation of plastic materials in the presence of municipal sewage sludge. Instead of using compost as a test matrix and inoculum source, this method uses the return activated sludge from a municipal wastewater treatment plant.

The ASTM D 5209-91 apparatus was nearly identical to the composting apparatus described previously, using a higher pressure air source and needle valves placed at the inlet to the sample vessels. This alleviated the air flow problems and resulted in much smoother rate data. Results from the polymer and cellulose after

38 days of exposure in duplicate are included in Table 5-2. Biodegradation of the acrylic coating material reached only 18% while cellulose achieved 85%, indicating that the acrylic polymer is either only partially biodegradable or biodegrades slowly under these conditions.

TABLE 5-2. Results of Aqueous Biodegradability Testing (David, 1994).

TEST MATERIAL	%C mineralized to CO ₂
Cellulose powder	85
Acrylic coating (liquid)	18

5.4 PRELIMINARY EXPERIMENT 2

5.4.1 Method

The second controlled composting experiment used an improved apparatus to measure the biodegradability of six test materials and five control materials. These included an MBI modified starch formulation (Amypol), polycaprolactone (PCL), polyhydroxybutyrate-co-hydroxyvalerate (PHB/V), two polyvinyl alcohols (PVOH), and a degradable film (Material A). Cellulose and starch powders were the positive controls, and Kraft paper provided an additional positive control that would give bulking effects similar to rigid films. Polyethylene film was used as the negative control material along with an additional negative control polypropylene film (Material B) that was used because it had the same geometry as Material A. As in the previous experiment, 180 g dry weight of compost provided the exposure matrix for 30 g dry weight of each test material.

Table 5-3 gives descriptions, sources, and geometries of the six test materials and five control materials.

Several modifications to the test method and apparatus improved the quality of the resulting data (Figure 5-3). A change from using an aquarium pump to using a pressure-vacuum air handling system allowed much easier control of air flow rates. The needle valve at the sample vessel outlet regulated the air flow rate as a

TABLE 5-3. Test Materials for Experiment 2.

MATERIAL	DESCRIPTION	SOURCE	GEOMETRY
Amypol	thermoplastic starch	MBI	180-710 μM
Cellulose	analytical grade	Sigma	20 μM powder
Kraft paper	40# Kraft paper	Tape, Inc.	5.6 mil sheet
PE	transparent film	Webster Industries	1.3 mil film
PCL	Tone 767	Union Carbide	180-710 μM
PHB/V	12%HV	Zeneca	<425 μM
PVOH	hot water soluble	Air Products & Chemicals	2.2 mil film
PVOH c.w.	cold water soluble	Air Products & Chemicals	1.7 mil film
Starch	hylon VII	National Starch & Chemical	180-710 μM
Material A	degradable film	-	0.67 mil film
Material B	polypropylene film	-	0.67 mil film

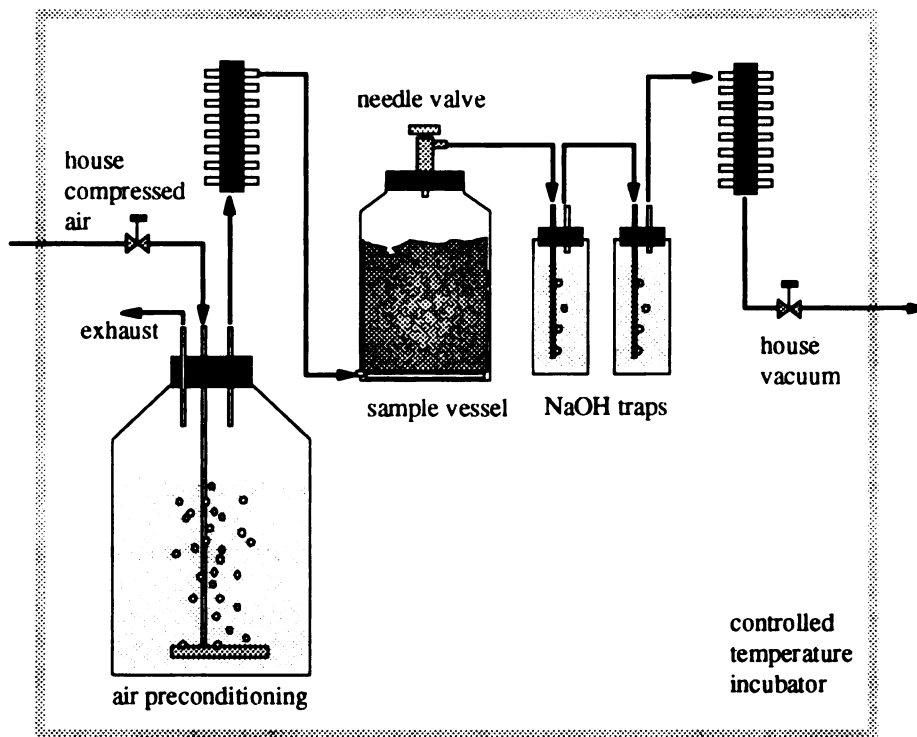
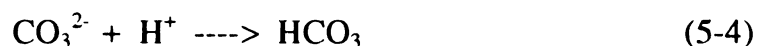


Figure 5-3. Setup for externally controlled composting experiment 2.

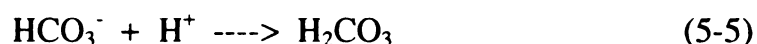
vacuum pulled air through the trapping solutions. Air supplied to the sample vessels sparged through two 20 liter bottles containing sodium hydroxide solution and distilled water. An exhaust port in the second preconditioner ensured that air was being delivered to the sample vessels at a low pressure and at a rate not exceeding the vacuum take-off rate.

A method for automatic titration of the trapping solutions reduced the time required for analysis and increased the accuracy of the titrations. Instead of measuring the depletion of sodium hydroxide during the trapping, the new titration measured the amount of carbon dioxide trapped. An Orion 960 Autochemistry System was programmed to add 0.5 N H_2SO_4 to a sample of the trapping solution

until the pH reached 8.3, which takes the carbonate system to the endpoint of the reaction:



Further addition of titrant until reaching the pH 4.5 endpoint of the reaction:



is used to calculate the amount of carbon dioxide trapped based on the volume of titrant required to convert bicarbonate ion to carbonic acid.

Problems with liquid slugging up the narrow diameter trapping tubes at higher air flow rates were resolved by switching from 50 ml tubes to 500 ml bottles. Investigations into the efficiency of the new traps using 300 ml of 1 N NaOH solution per bottle at an air flow rate of 30 ml/min showed that over 90% of the carbon dioxide was trapped by a single bottle. The remainder of the detectable carbon dioxide could be trapped using a second bottle in series. This trapping method proved to be more reliable than the previous method and was adopted for the new set-up. The air flow rate of 30 ml/min resulted in a maximum carbon dioxide concentration of around 12% in the sample vessels.

A controlled composting temperature succession of 35-58-50-35°C, as described earlier, was used in this experiment instead of the constant 37°C used for Experiment 1. Although this succession gave a better approximation of the temperatures in practical composting, the higher temperatures caused the tubing in the trapping solutions to plug and also caused the compost mixtures to dry out.

After each bubble pushed out of the stainless steel tubing into the trapping solution a small amount of the solution backed into the tubing. This continual rewetting of the tubing wall formed a deposit of sodium hydroxide that eventually restricted or even blocked air flow. At the higher temperatures this plugging occurred more frequently than at the lower temperatures.

Evaporative cooling in the preconditioning bottles presented another temperature related problem. The water temperature in the final humidification bottle remained 5 to 10°C below the temperature of the air entering and leaving this bottle, which was at the temperature of the incubator room. Drying of the composting samples resulted, since the air passed to the sample vessels was saturated with water at the lower temperature. Water added to the samples on days 23 and 27 of the experiment made up for moisture lost by this drying.

5.4.2 Results

Biodegradabilities of the eleven test materials tested fell into two groups as shown in Figure 5-4 and Table 5-4. Starch, cellulose, PCL, PHB/V, Kraft paper, and Amypol gave 55-80% conversion to carbon dioxide while PVOH, Material A, and the negative controls remained below 20%. The cold water soluble PVOH triplicates were aborted after the first day because the film dissolved and filled the air spaces in the compost matrix. Standard deviation from the mean of the triplicates was less than 8% for all test materials, an improvement over the results of Experiment 1. Additionally, the improved control of air flow rates through the vessels resulted in the generation of meaningful carbon dioxide rate data as shown in Figure 5-5.

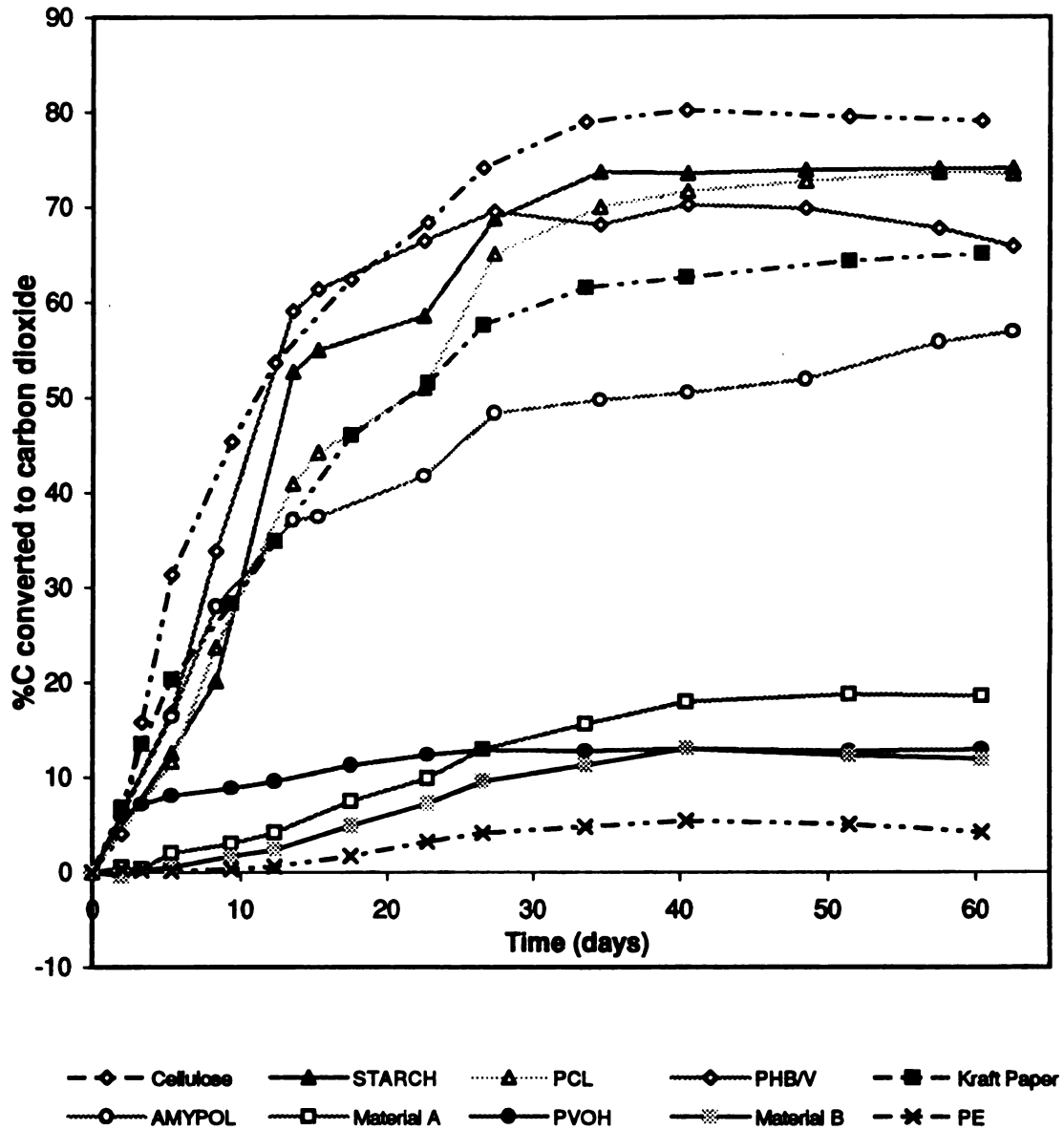


Figure 5-4. Biodegradability of materials tested in experiment 2.

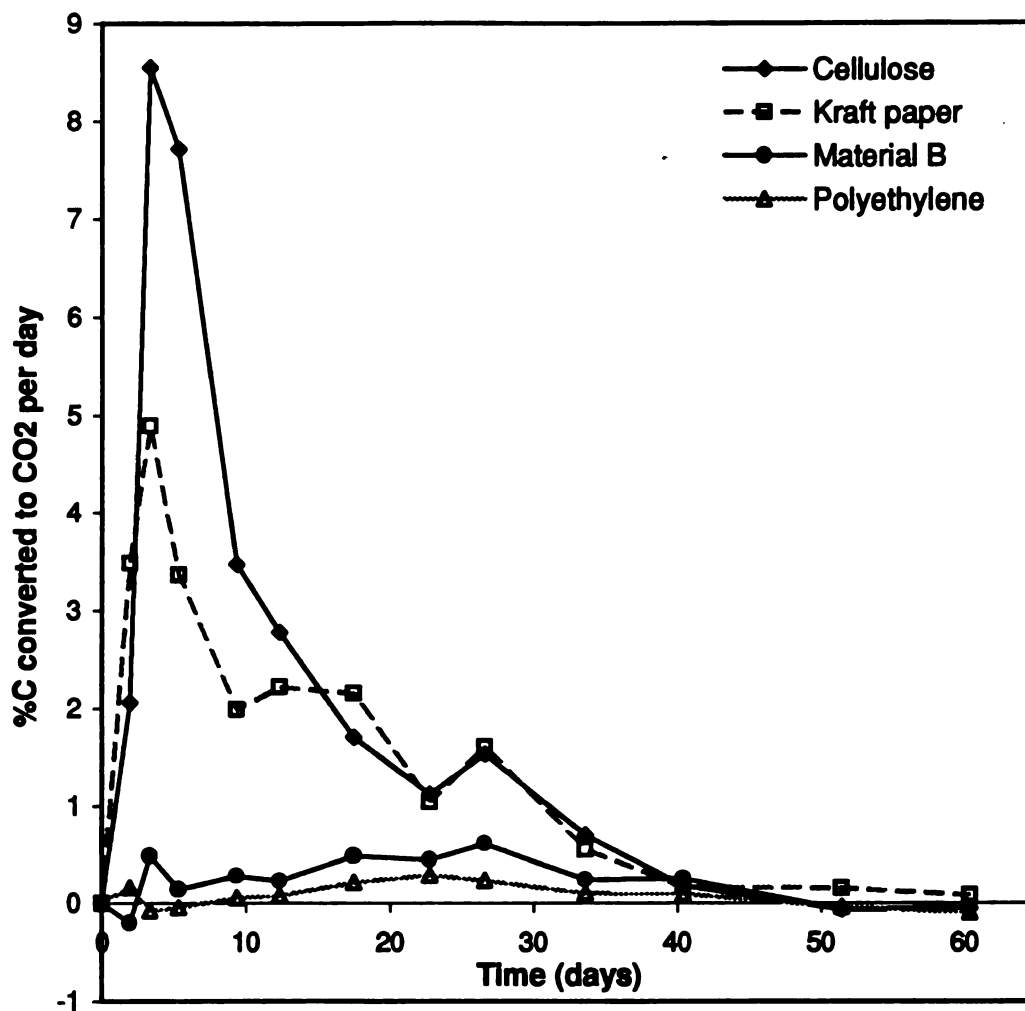


Figure 5-5. Rates of control material biodegradation measured in experiment 2.

TABLE 5-4. Results of Experiment 2.

	%C in sample mineralized to carbon dioxide	
TEST MATERIAL	MEAN	Standard deviation
Cellulose	79.0	7.4
Starch	74.0	6.1
PCL	73.4	5.7
PHB/V	65.8	4.2
Kraft Paper	65.0	4.3
Amypol	56.8	6.5
Material A	18.5	4.9
Material B	11.9	6.7
PVOH	12.8	7.8
PE	4.2	2.2

The low conversion to carbon dioxide measured for PVOH and the data from the negative control Material B highlight some of the physical effects of test materials that either influence actual biodegradation or affect experimental results by altering the rate of background carbon dioxide generation from the compost matrix. During the initial four days at 58°C, the hot water soluble PVOH film became gummy and formed aggregates with compost particles when the temperature was lowered to 50°C. This may have lowered the overall rate of microbial activity in the compost matrix, decreased the difference between the blank triplicates and the PVOH sample triplicates, and resulted in an erroneously low calculation of the extent of mineralization of PVOH.

Conversely, Material A and its negative control, Material B, were very thin films that had a high bulk volume as used. When mixed with these materials the

compost matrix spread into thin layers on the film surface, which improved aeration. This resulted in carbon dioxide evolution greater than the blank for both Material A and its negative control. The calculation of test material mineralization attributed the consequential increase in microbial activity in the compost matrix to the test material itself. A similar effect was seen for polyethylene film, but this was less dramatic since the thicker polyethylene film did not increase the bulk volume to the same extent as the thinner films.

5.5 PRELIMINARY EXPERIMENT 3

5.5.1 Method

A final overhaul of the controlled composting system design (Figure 5-6) addressed the problems encountered with the previous set-ups and raised the experiment's reliability another level. The use of constant flow rate restrictors (Mott Metallurgical Model 25) provided the major improvement by setting a stable rate of air delivery of through the system. Instead of using one set of air preconditioning vessels for the entire system, one small humidification bottle treated the air entering each sample vessel. Due to the increased surface area per volume, the smaller bottles remained within 0.5°C of the room temperature and minimized drying in the sample vessels. A manifold of Clippard ES Series miniature three-way solenoid valves directed the air flow from one vessel at a time through a carbon dioxide analyzer. The exhaust gas purged the sample loop and Siemens Ultramat 22P infrared carbon dioxide analyzer for 15 minutes; after this purge the carbon dioxide concentration was measured 30 times at one second intervals and averaged. The Ultramat 22P has two channels for detecting low (0.000 to 4.000%) and high (0.00 to 100.00%) carbon dioxide concentrations. A Microsoft Quickbasic program running on an IBM personal computer was

interfaced with DuTec I/Oplexer input-output boards and facilitated data acquisition and valve switching.

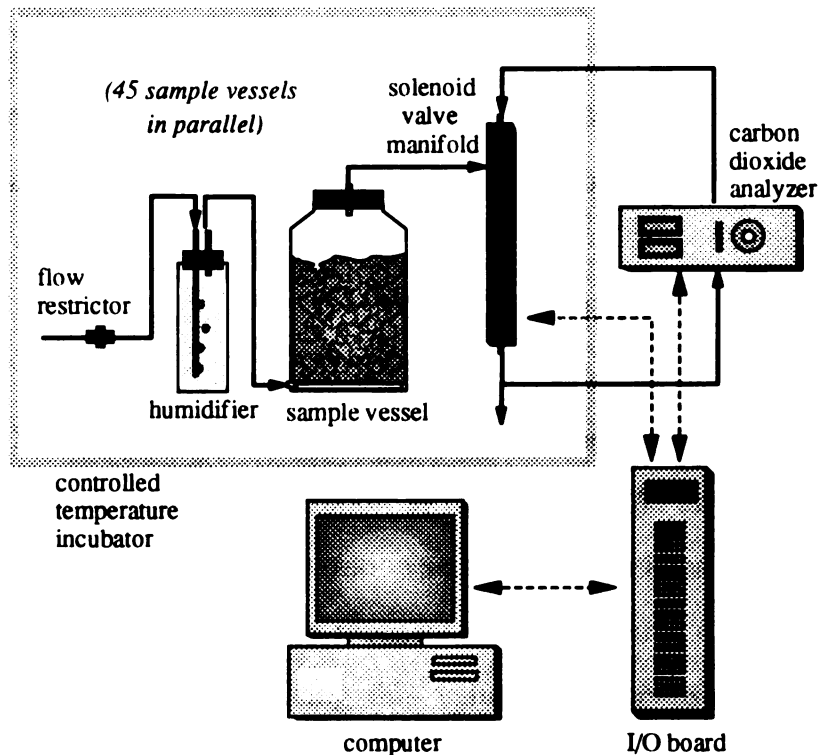


Figure 5-6. Setup for externally controlled composting experiment 3.

The gas sampling loop was designed to allow accurate and frequent measurement of gas composition. A mathematical model of the analytical loop as a mixed unit was used to predict the time required to replace the gas from one sampling with the exhaust gas from the next sample vessel after switching. Sampling the effluent air composition from each of the 45 sample vessels twice per day required that each purge and measurement could be completed in 16 minutes. Setting the purge completion criterion at 97% replacement after a step change resulted in accuracy within 1% for a sample reading because of the small difference in carbon dioxide

con

limi

con

the

Th

in

ap

lr

C

m

fr

w

c

w

ti

F

pr

flc

A

cap

concentration between samples. The pressure of the in-house compressed air limited the air flow rate to a maximum of 70 ml/min. The need to maintain a concentration of carbon dioxide sufficient for accurate measurement also limited the air flow rate through the vessels.

The response of the carbon dioxide concentration at the detector to a step change in the input air composition was used to determine the volume of the loop, V , by applying the equation

$$V = F(C_o - C)/(dC/dt) \quad (5-6)$$

In Equation 5-6 F is the air flow rate, C is the carbon dioxide concentration, and C_o is the carbon dioxide concentration at time $t = 0$. At an air flow rate of 20 ml/min the carbon dioxide concentration required 50 minutes to reach 97% of its final concentration. This response revealed that the volume of the analytical loop was approximately 300 ml. Using this value, the response of carbon dioxide concentration at different air flow rates was predicted using the equation

$$C(t_{n+1}) = C(t_n) + F(C_o - C(t_n))/V \quad (5-7)$$

with $C(t_n)$ and $C(t_{n+1})$ being the carbon dioxide concentrations during successive time intervals. Figure 5-7 shows the time required for purge versus air flow rate. From these results it was anticipated that an air flow rate of 60 ml/min would provide a purge within 15 minutes; measurement of the system response at this air flow rate verified the model's prediction (Figure 5-8).

A short controlled composting experiment using 40# Kraft paper revealed the capabilities of the new apparatus. Strips of paper approximately 0.5 cm x 4 cm

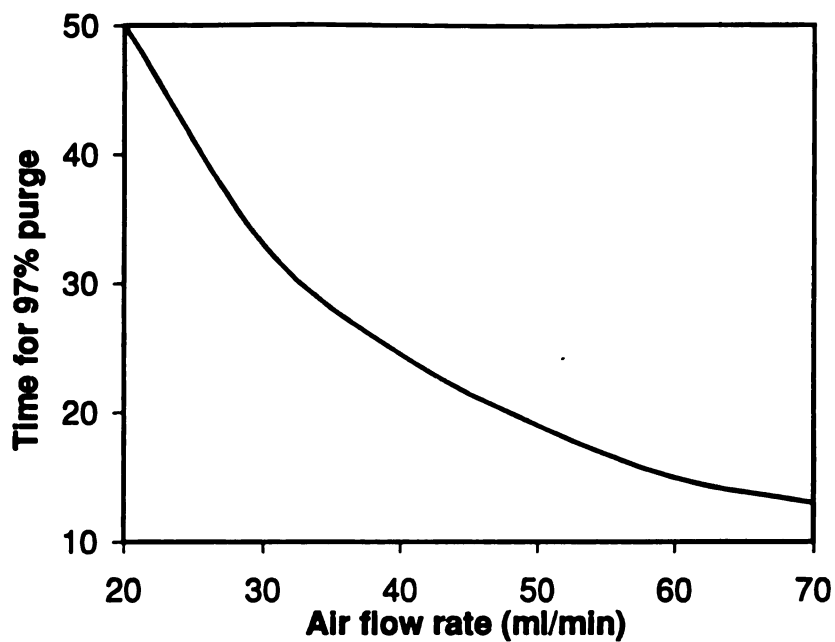


Figure 5-7. Predicted effect of air flow rate on time required to achieve 97% purge of gas analysis loop.

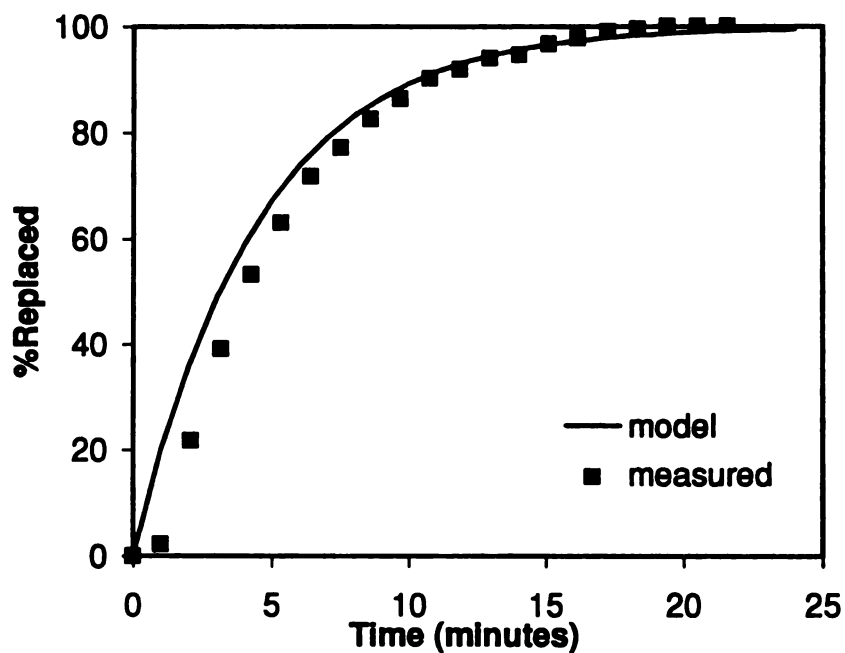


Figure 5-8. Replacement of gas in analytical loop at 60 ml/min.

were prepared using an office paper shredder. The customary mixture of 30 g dry weight test material and 180 g dry weight compost matrix was adjusted to the moisture holding capacity (MHC) of the mixture. MHC was calculated as a weighted average of the compost matrix MHC of 43% and the Kraft paper MHC of 49%, each determined by application of ASTM D 425. The mixture was exposed to a temperature succession of 2 days at 35°C, 4 days at 58°C, and 11 days at 50°C at an air flow rate of 60 ml/min.

5.5.2 Results

Figure 5-9 compares the carbon dioxide concentrations from the vessels containing Kraft paper in compost to the concentrations from the blank vessels containing only the compost. Rate data observed over shorter time intervals provided insight into the biodegradation process not available using the previous method. The small peak in carbon dioxide generation for the Kraft paper mixtures during the first day, when the paper still possessed some structural integrity, was most likely the result of the bulking effect seen in previous experiments. A short burst of carbon dioxide production occurred in both the test and blank vessels when the temperature was raised to 58°C. This apparently resulted from the mesophilic populations which built up during the 35°C phase. Before they were inactivated by the increased temperature, the improved chemical and enzymatic kinetics caused a brief burst of activity. Approximately one day later carbon dioxide evolution from the Kraft paper peaked dramatically (Figure 5-10). Increased activity of thermophilic cellulose-degrading species was seen before the temperature was reduced to 50°C on the sixth day. Microbial activity decreased in all of the vessels when the temperature was lowered.

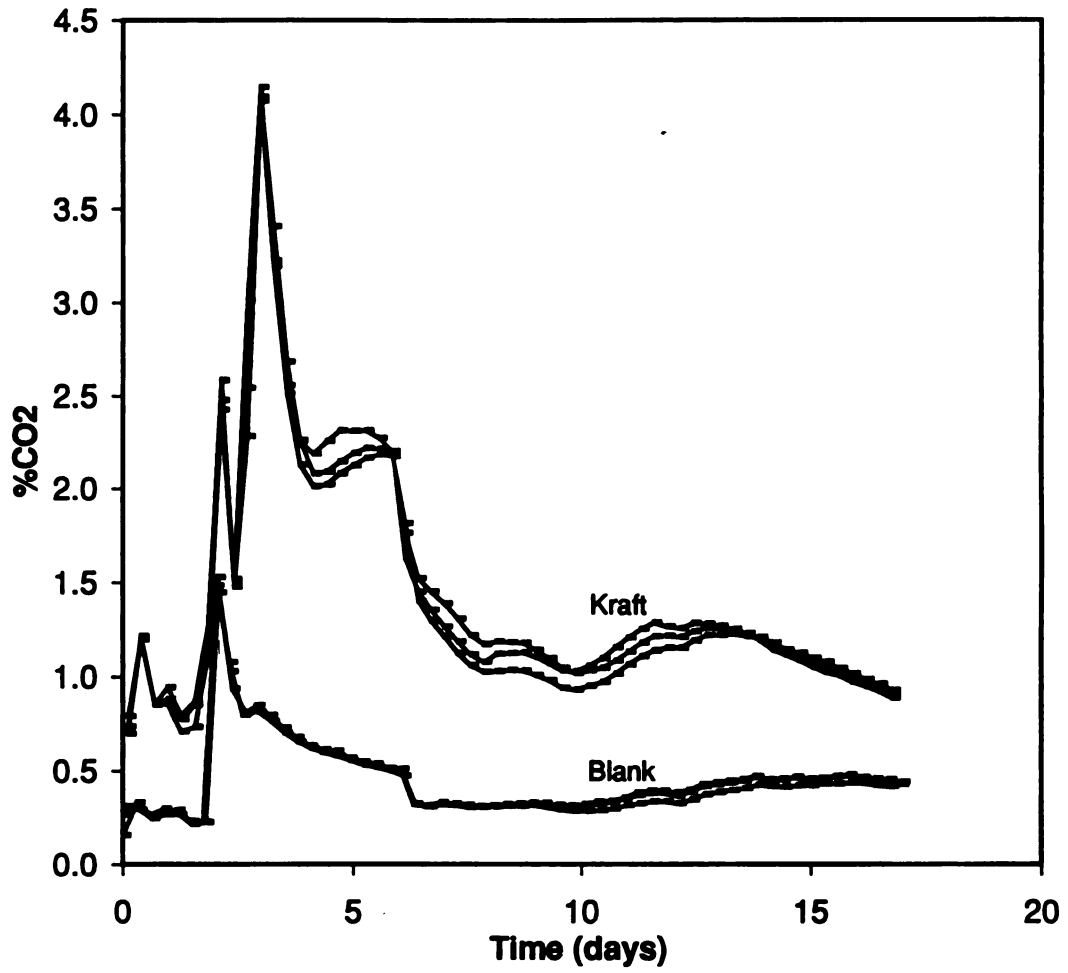


Figure 5-9. Carbon dioxide concentration of the gas exiting each test vessel.

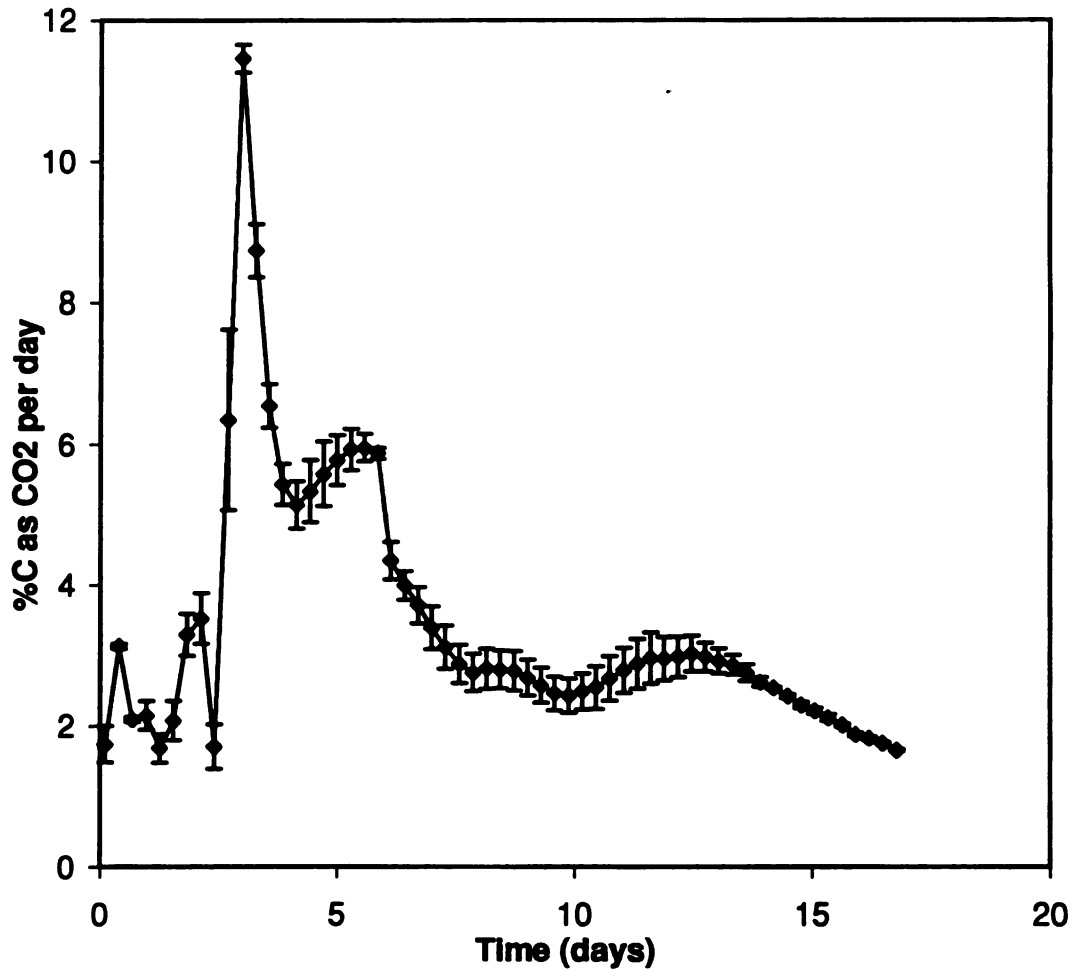


Figure 5-10. Rate of biodegradation of Kraft paper. (Error bars show the standard deviation from the mean of triplicates)

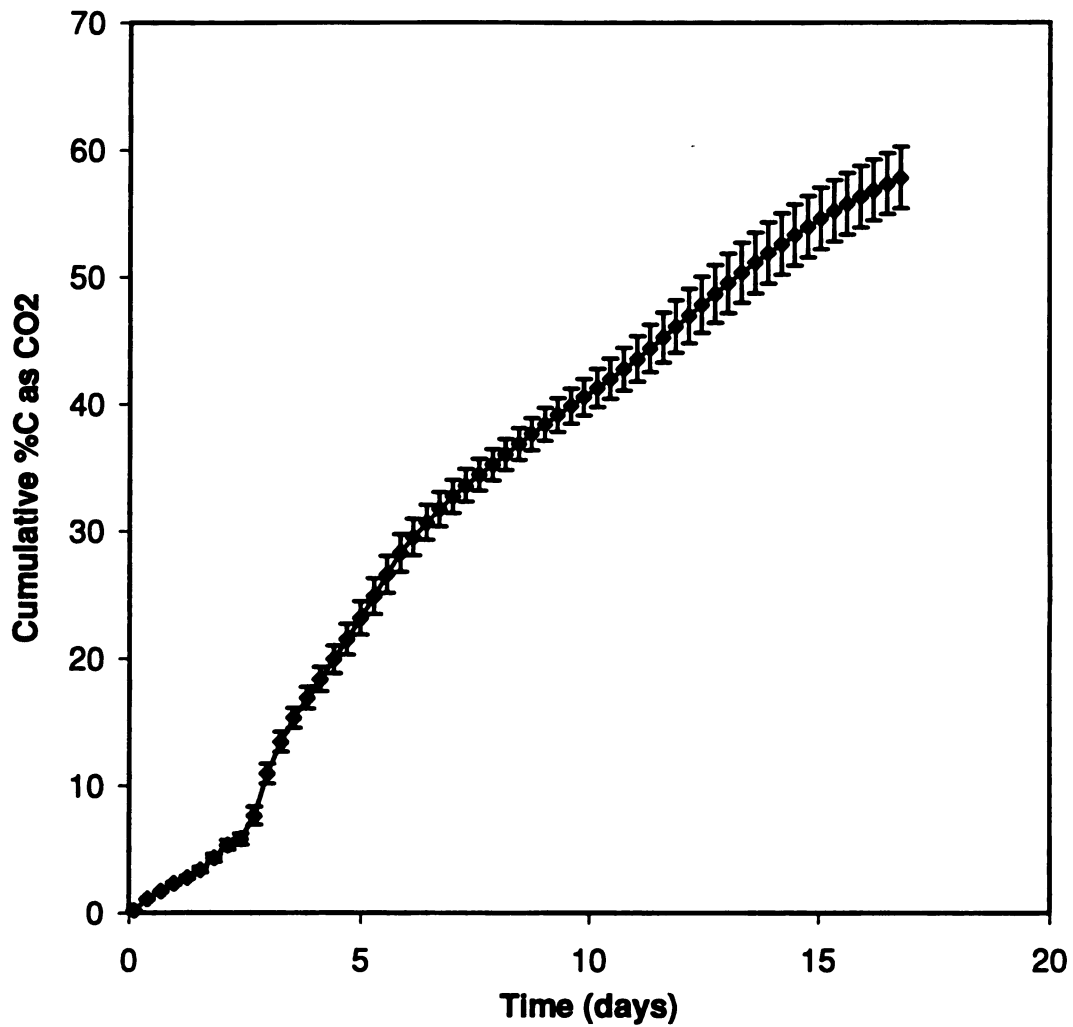


Figure 5-11. Biodegradability of Kraft paper in Experiment 3.
(Error bars show the standard deviation from the mean of triplicates)

The percent of the carbon in the Kraft paper mineralized to carbon dioxide accrued to nearly 60% over 17 days as shown in Figure 5-11. In the previous experiment, Kraft paper achieved less than 45% cumulative conversion in the same period. The increased rate of biodegradation was attributed to a combination of several factors including the smaller size of the shredded paper pieces, the decrease in the moisture content of the mixture to its MHC, and the higher oxygen concentration in the compost interstices due to the higher air flow rate. Less information was available from the cumulative conversion data than the rate data, so few conclusions could be drawn from these data alone. This underscored the importance of rate data as a source of insight into the behavior of test materials under controlled composting conditions. If collected on a sufficiently frequent basis, rate data also provide a quality control check and monitor of system performance.

5.6 BIODEGRADABILITY OF POLYLACTIDE FILM

5.6.1 Method

The controlled composting apparatus developed and validated in the three preliminary experiments was used to measure the biodegradability of polylactide film. Unbleached virgin softwood Kraft paper 165 μm (6.5 mil) thick was the positive control and transparent polyethylene film 100 μm (4 mil) thick was the negative control. All of the test materials were cut into 2 cm x 2 cm inch squares, a mixture was prepared using the standard 30 g d.w. test material and 180 g d.w. compost inoculum, and the mixtures were adjusted to their moisture holding capacities. The 70 day experiment used the 35-58-50-35°C temperature succession with an air flow rate of 60 ml/min to each test vessel. Purging of the sample loop for 17 minutes after switching effluent gas samples allowed each

bottle's effluent to be measured twice per day. The vessels were mixed by shaking three times per week.

5.6.2 Respirometric Biodegradability

Carbon dioxide concentrations in the test vessel effluents over the first 45 days are shown in Figures 5-12 and 5-13. These figures show the carbon dioxide concentrations measured from the triplicates for each test material, in the sequence that they were measured. Except for three gas samples resulting from the Kraft paper test vessels, all carbon dioxide concentrations were measured in the low range (0.000 to 4.000%) cell of the carbon dioxide analyzer. The rates of carbon dioxide generation displayed variability between the triplicate samples, but the rate for each bottle remained relatively smooth (see Fig 5-12 inset). This demonstrated that the main source of variability was the actual difference in the rate of carbon dioxide generation between triplicate vessels and did not result from the carbon dioxide measurement technique.

Figure 5-14 shows the rate and cumulative biodegradation of the polylactide film and Kraft paper. Table 5-5 gives their 70 day cumulative biodegradabilities. These values were calculated using the average of the triplicates containing the test materials and the average of the blank triplicates. Carbon dioxide generation from the polyethylene negative control was slightly above that of the blank vessels, as observed in previous experiments. The Kraft paper rate of biodegradation peaked during the 58°C period from days 2 to 5. During the following period at 50°C the carbon dioxide generation rate decreased steadily. By the time of the decrease to 35°C the Kraft paper was asymptotically approaching complete biodegradation, and the rate of mineralization was affected only slightly.

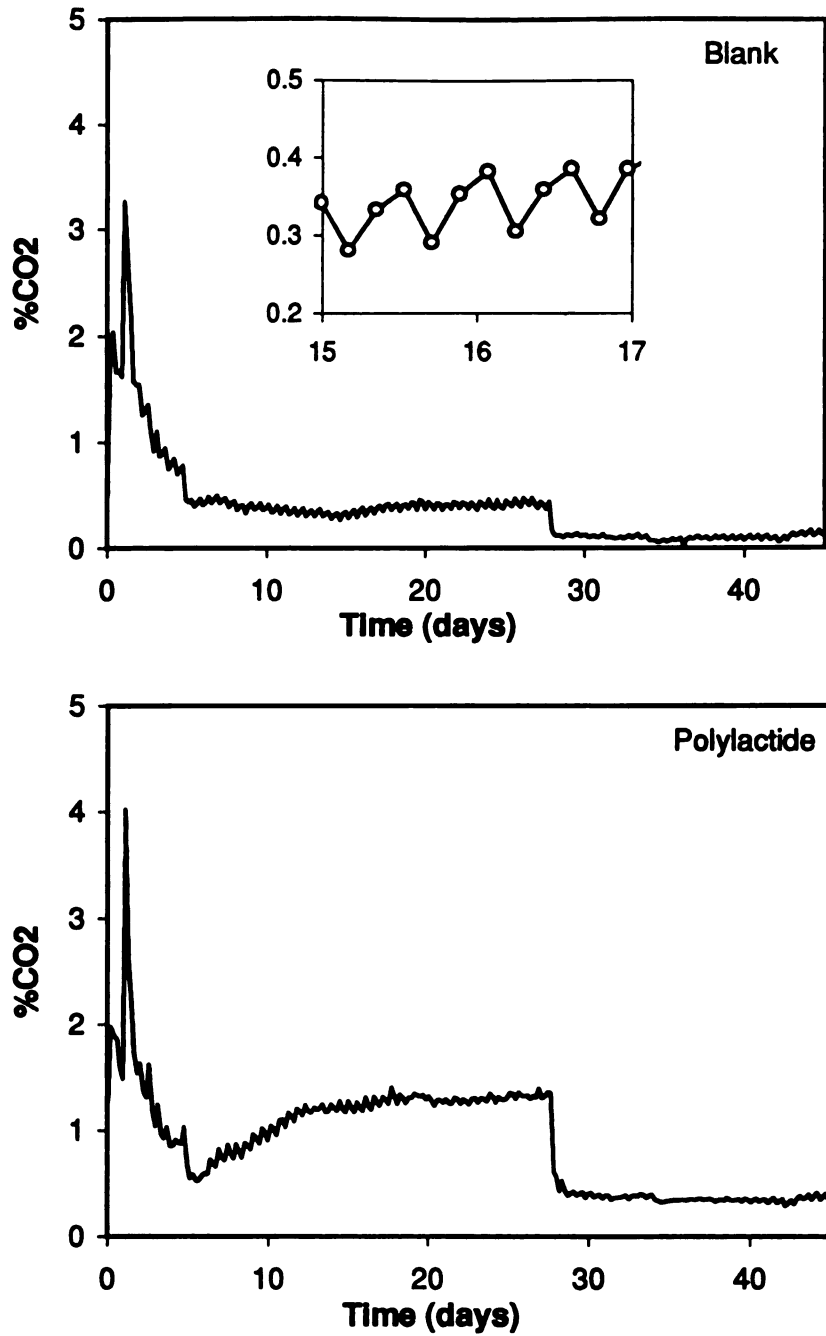


Figure 5-12. Carbon dioxide concentrations in exhaust gas from blank (top) and polylactide (bottom) test vessels. (Inset: detail of the concentrations from the blank vessels)

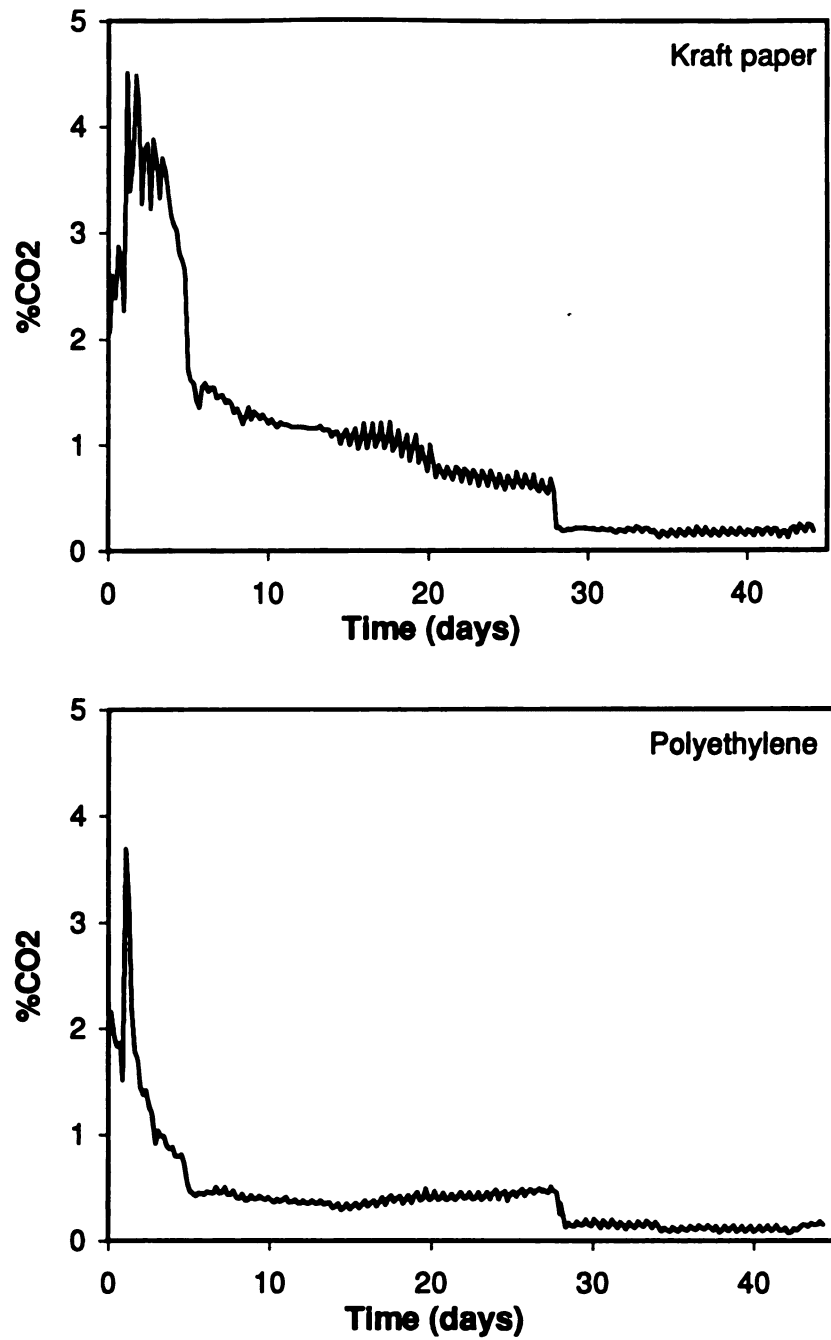


Figure 5-13. Carbon dioxide concentrations in exhaust gas from Kraft paper (top) and polyethylene (bottom) test vessels.

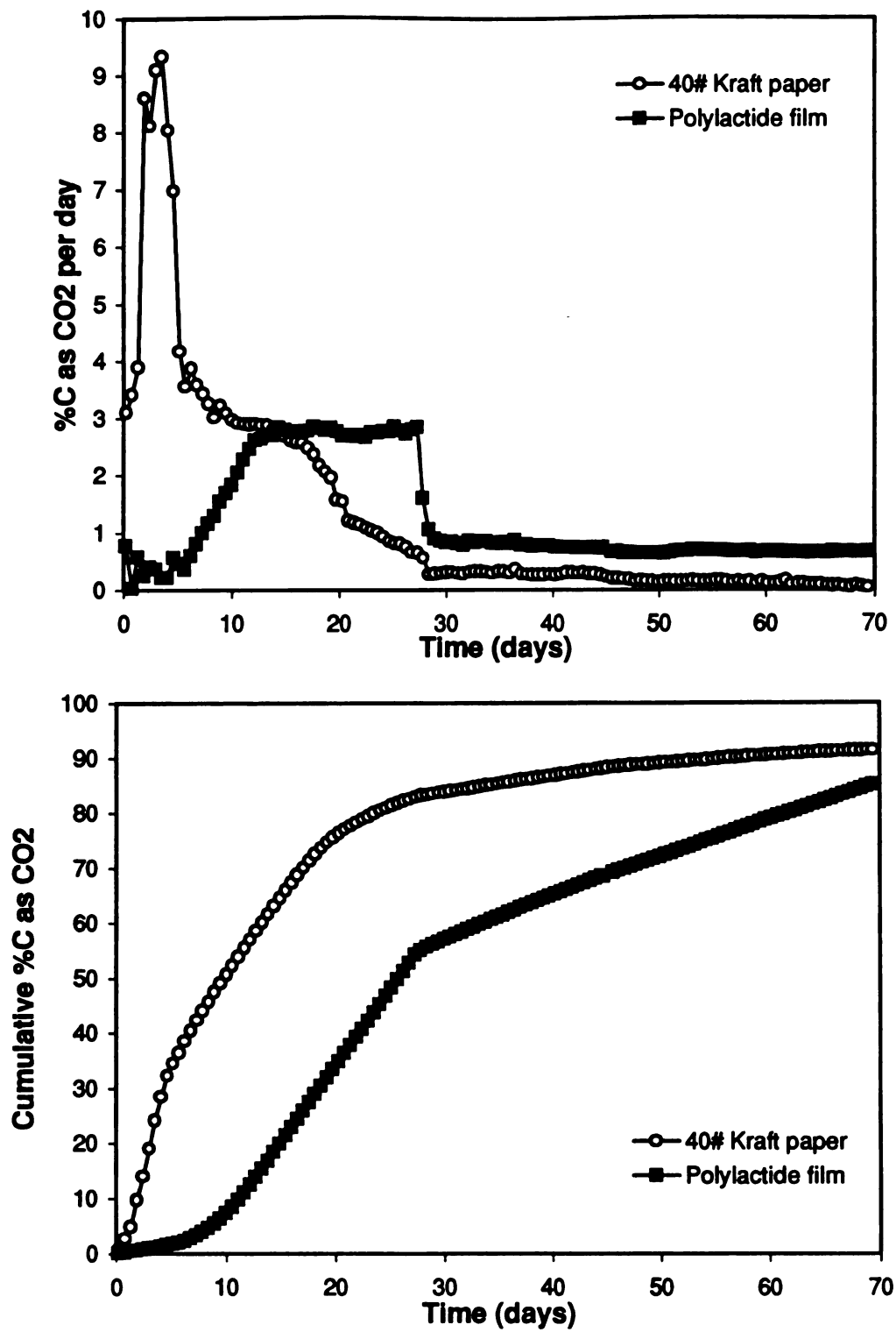


Figure 5-14. Rates and cumulative biodegradabilities of poly lactide film and Kraft paper.

Poly lactide displayed a lag in biodegradation until day five, when the rate of mineralization began to steadily increase to a maximum and steady rate of 2.8% per day. The decrease in temperature on day 28 slowed the rate of mineralization to less than 0.7% per day for the remainder of the experiment.

TABLE 5-5. Results of Biodegradability Experiment.

TEST MATERIAL	%C in sample mineralized to carbon dioxide	
	Mean	Standard deviation
Kraft Paper	91.3	5.0
Poly lactide film	85.2	2.5
Polyethylene film	2.6	0.9

5.6.3 Polylactide degradation

Samples of polylactide film residue were collected on days 10, 25, and 45, and the molecular weight distributions were determined by GPC at Cargill Inc., Minneapolis, MN. Approximately 100 mg of film fragments were collected from the triplicate test vessels at each sampling time and air dried at room temperature. Table 5-6 shows the results of the GPC analysis.

Using Equation 3-10 for molecular weight loss verses time:

$$\ln M_n = \ln M_{n,0} - 3.664 \times 10^{18} \cdot \exp\left(\frac{-14543}{T}\right) \cdot t \quad (3-10)$$

and the temperature profile of the externally controlled composting experiment resulted in a prediction of the molecular weight loss of polylactide. Figure 5-15

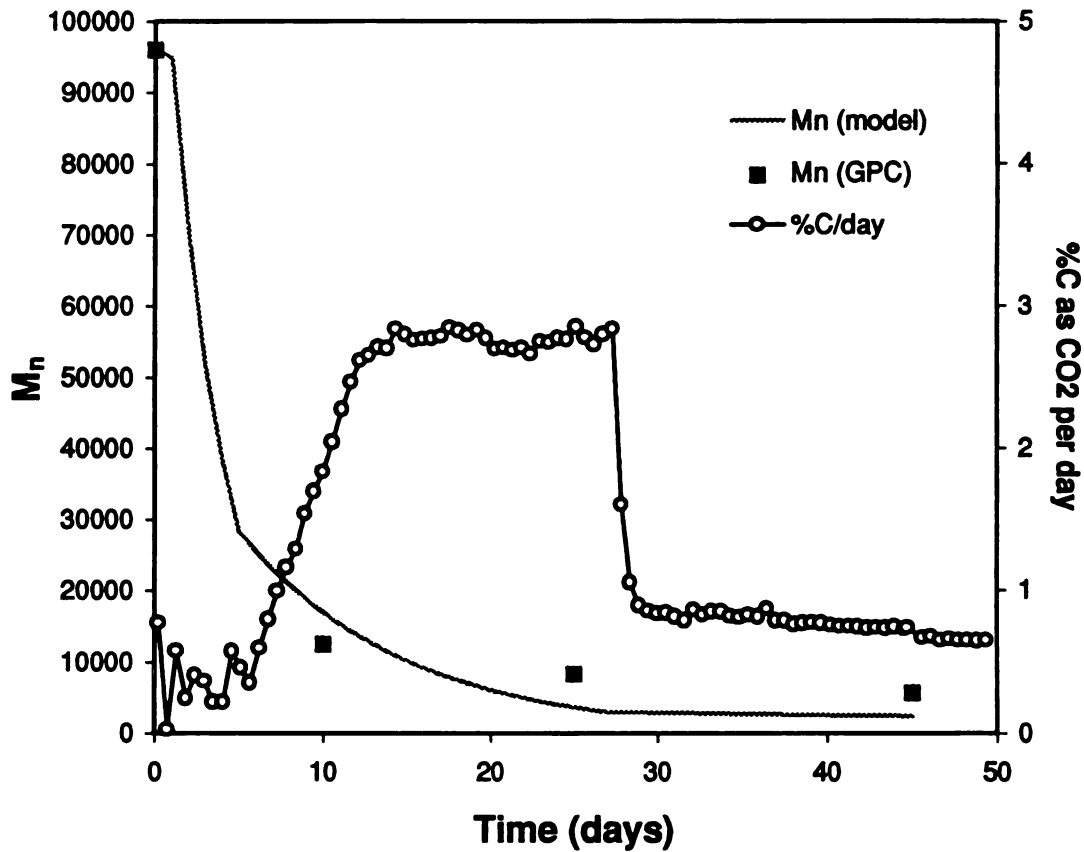


Figure 5-15. Comparison of predicted and measured decreases in M_n with rate of mineralization during controlled composting (ASTM D 5338).

shows the model's predictions for M_n over the course of the experiment compared to the M_n measured by GPC and the rate of mineralization. Most of the molecular weight reduction occurred during the 58°C period between the first and fifth days, bringing the polylactide below M_n 10,000 soon after the tenth day. The polydispersity decreased from 2.24 to 1.57 in the first 45 days, indicating that the hydrolytic cleavage of the polylactide occurred randomly during composting. Between days 5 and 15 the rate of carbon dioxide evolution from the polylactide climbed to its maximum. The behavior in compost was consistent with the biodegradation mechanisms described earlier, with the initial lag time required for hydrolysis of the polymer to diffusible oligamers before the onset of mass loss from the polymer and microbial utilization.

TABLE 5-6. GPC analysis of films from controlled composting.

Time (days)	M_n	M_w	M_w/M_n
0	96,000	215,000	2.24
10	12,500	25,000	2.03
25	8,300	15,600	1.89
45	5,600	8,800	1.57

By the end of the 70-day composting experiment the polylactide film had been reduced to tiny, opaque, brittle fragments of low molecular weight, and biodegradation continued at a steady rate toward completion. The photographs in Figure 5-16 illustrate the disappearance of the polylactide film by hydrolytic degradation and microbial utilization.



Figure 5-16. Photographs of the mixture of polylactide film and compost inoculum before (top) and after (bottom) externally controlled composting.

CHAPTER 6

BIODEGRADATION UNDER FEEDBACK CONTROLLED COMPOSTING CONDITIONS

6.1 OVERVIEW

The experiment in Section 5.6 demonstrated the inherent biodegradability of the polylactide film under externally controlled composting conditions. Although inherent biodegradability is a necessary attribute of a compostable material, it is not sufficient. As explained earlier, the material must not hinder compost processing, reduce product quality, or end up in the reject fractions. This chapter addresses these issues by determining the behavior of the polylactide film in a pilot-scale feedback controlled compost system. Section 6.2 describes the system design and implementation of optimal process control for the pilot-scale units. The process dynamics and compost quality resulting from different compost feedstocks are explored in Section 6.3 to establish normal composting behavior. Finally, in Section 6.4 the fate and effects of the polylactide film in pilot-scale composting are determined.

6.2 PILOT-SCALE COMPOSTING SYSTEM

The pilot-scale composting system (Figure 6-1) consisted of two identical 60-liter vessels, each constructed from a 3 foot long section of 12-inch PVC pipe. Thermal mass flow controllers (MKS Type 1159B) regulated the flow rates of

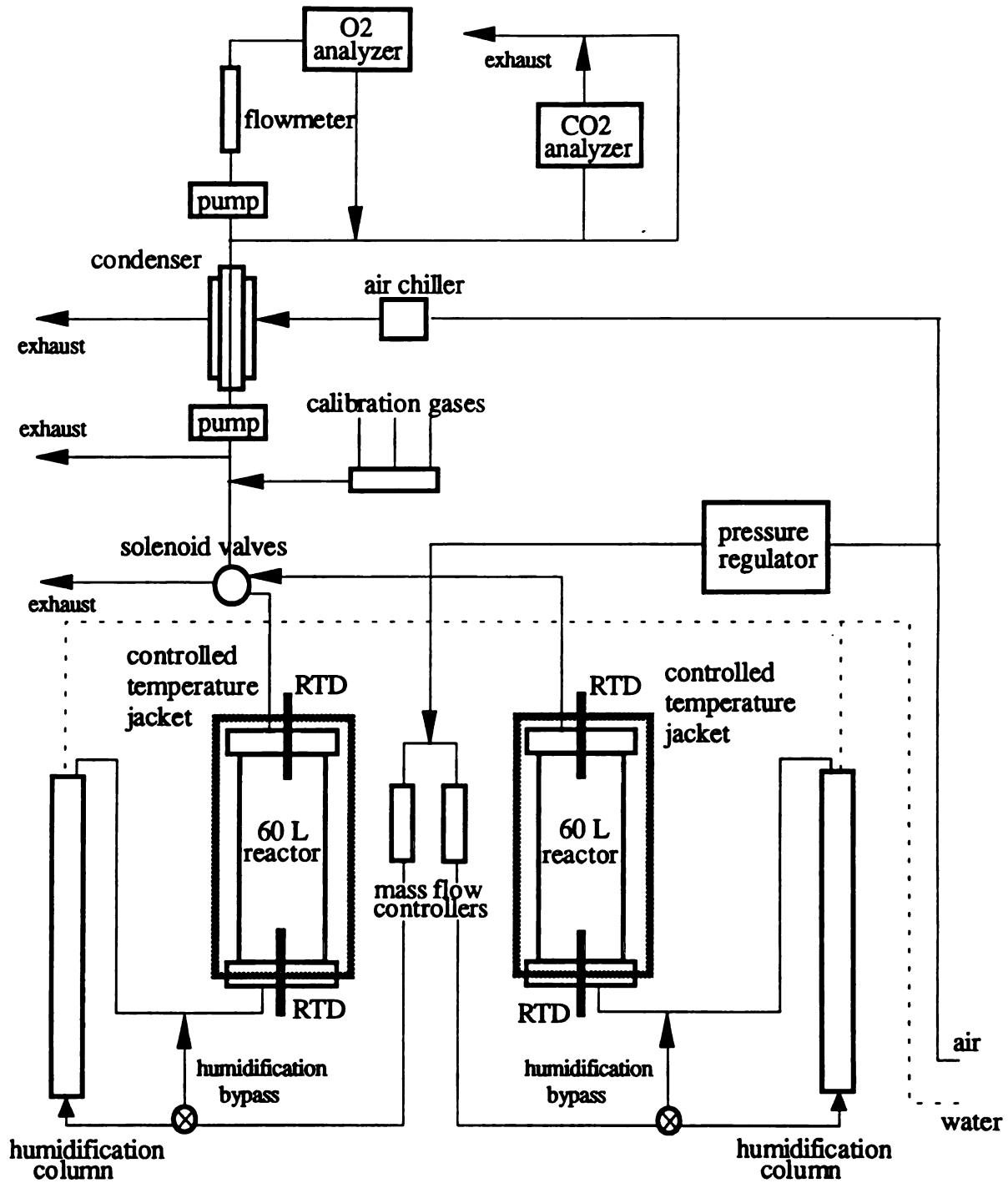


Figure 6-1. Schematic of pilot-scale composting apparatus.

influent air, which bubbled through a humidification column before passing into each composting vessel through its perforated base. After the air flowed upwards through the composting mass, Asco 8320 Series 3-way solenoid valves directed the effluent air either to exhaust or through a condenser and into the gas analysis loop. Effluent gas composition was measured using a Beckman Model 755A paramagnetic oxygen analyzer and Siemens Ultramat 21P infrared carbon dioxide analyzer. Stainless steel RTD probes inserted into the test vessels measured the temperatures approximately 4 inches into the top and bottom of the composting mass. An electrically heated insulating jacket, which was maintained at the lower of the temperatures in the composting mass, minimized conductive heat losses.

Humidification of the cooling air supply and condensation at the outlet prevented drying of the compost during processing. Air entered the vessel saturated with water at 25°C, or approximately 0.02 g water/g air. In reaching saturation at 55°C (0.11 g water/g air), the air removed heat from the compost equivalent to the heat of vaporization of 0.09 g water/g air plus the sensible heat required to raise the temperature of the moist air by 30°C. The 0.09 g water/g air carried out of the compost condensed at the vessel outlet and returned to the compost, and periodic mixing redistributed this moisture.

6.2.1 Process Control

DuTec I/OPlaxer input-output boards facilitated communication between the system instrumentation and FIX D/MACS personal computer-based data acquisition and control software. Control algorithms implemented via this software maintained set oxygen levels and temperatures in the compost by manipulating the aeration rate. A dual-control PID algorithm was used to maintain

a minimum oxygen concentration of 15% in the effluent gas and a maximum compost temperature of 55°C.

Heat and mass transfer limitations quickly result in temperature and oxygen concentration gradients in a composting mass (Finger et al., 1976). Forced aeration results in temperature and oxygen concentration gradients through the compost pile with lower temperature and higher oxygen concentration where the air enters the compost. Figure 6-2 shows how these temperature gradients develop in full-scale aerated static pile composting (Stentiford et al., 1985). Similarly, the pilot-scale composting vessels developed an axial temperature gradient from the inlet to outlet of the composting vessels. The largest effect occurred during periods of peak aeration demand, when temperatures in the vessel were as low as 30°C near the inlet and 55°C at the outlet. Since composting at the optimum

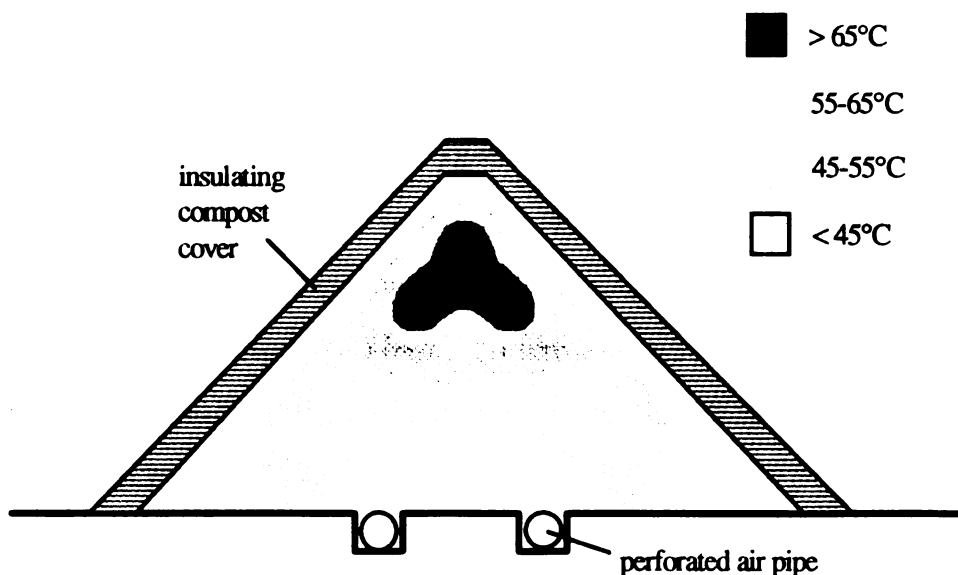


Figure 6-2. Typical temperature profile during forced aeration composting (Stentiford et al., 1985).

con

air

con

no

mi

ef

co

T

s

j

u

conditions used in the pilot-scale apparatus requires as much as nine times more air for heat removal than is necessary for maintaining an adequate oxygen concentration (MacGregor et al., 1981) a steep oxygen concentration gradient was not established. Air entered the vessel at approximately 21% oxygen and left at a minimum of 15% oxygen during the compost warm-up phase. However, the effluent oxygen concentration remained even higher than 15% during most of the composting, since excess air was supplied based on the need for heat removal.

The computer control algorithms collected process data, performed valve switching, manipulated the air flow rates to the vessels, and maintained the vessel jacket temperatures. Every ten minutes the primary control algorithm (Figure 6-3) used process data to calculate a new air flow rate for both vessels as follows:

1. Switch solenoid valves to direct flow from desired vessel through analytical loops.
2. Wait 5 minutes to purge instruments.
3. Record carbon dioxide and oxygen concentrations.
4. Calculate PID output (p_T) based on oxygen concentration setpoint.
5. Record compost temperatures.
6. Calculate PID output (p_O) based on temperature setpoint.
7. Select minimum air flow rate or higher PID output as new air flow rate.
8. Repeat 1-7 for the other vessel.

Preliminary experiments determined that, after switching flows in step 1 above, an analytical loop purge time of 5 minutes was sufficient to accurately measure gas

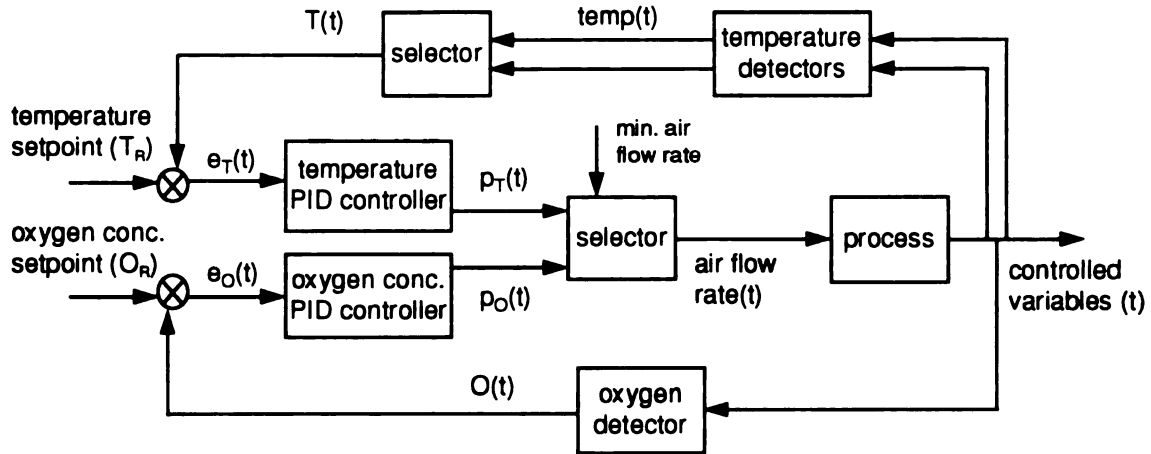


Figure 6-3. Primary control algorithm for dual control of temperature and oxygen concentration.

composition. The data acquisition program collected oxygen and carbon dioxide concentrations every second and used a smoothed value in Step 3 of the primary control algorithm. Temperatures were collected every 10 seconds and smoothed to be used in Step 5 and in controlling the jacket temperatures. On-off control of the heat element in the insulating jackets kept the exterior of the vessels at the lower of the temperatures measured in the compost vessel.

The digital control algorithm shown in Figure 6-3 used proportional, integral, and derivative (PID) feedback control to drive process variables to their setpoints. The deviations e_T and e_O were calculated as the difference between the actual values of temperature and oxygen concentration, T and O , and the setpoints, T_R and O_R . By changing the controlled variable (air flow rate) in response to the deviations from the setpoints, the PID blocks attempted to reduce the deviations to zero and maintain desired process conditions. The PID blocks calculated the appropriate

control output signals, p_T and p_O , for temperature and oxygen concentration control using the discrete form of the PID equation:

$$\Delta p_n = \frac{100}{PB_c} \left[e_n + \frac{\Delta t}{T_I} \sum_{k=0}^n e_k + \frac{T_D}{\Delta t} (e_n - e_{n-1}) \right] \quad (6-1)$$

where:

- Δp_n = change in controller output at time n
- e_n = process variable deviation at time n
- PB_c = proportional band
- T_I = integral time constant
- T_D = derivative time constant
- Δt = scan time of the digital PID block.

Proportional, integral, and derivative control actions are provided by the three terms in brackets on the right hand side of Equation 6-1. The first term imparts a change to the controller output that is proportional to the deviation from the setpoint. The next term provides the integral action by bringing the controlled variable back to the setpoint in the presence of a sustained deviation. The derivative action is supplied by the third term, which uses the rate of change in the error to make a predictive adjustment to the controlled variable. Equation 6-1 shows that, for a given deviation, small values of PB_c and T_I and large values of T_D cause greater changes to the controlled variable.

6.2.2 Controller Tuning by the Continuous Cycling Method

Selecting values of the parameters PB_c , T_I , and T_D to give optimal control of process variables is known as controller tuning. Several methods of controller tuning are available ranging from trial-and-error to model-based controller design.

Controller tuning parameters used in the PID algorithms were selected based on a combination of these methods.

These tuning techniques were developed for processes that are linear and stationary and have dynamics that approximate the simple models these techniques are based on. Biological processes are usually non-linear, that is, the process dynamics change as the process values change. In addition, biological systems are highly non-stationary, meaning that different responses result from the same stimulus depending on the state of the system (Wilson, 1991). The following discussion describes the selection of controller settings that were applied during the various pilot-scale composting experiments.

Tuning parameters used in the preliminary pilot-scale composting experiments of Section 6.3 were selected using the closed loop continuous cycling method (Ziegler and Nichols, 1942). The continuous cycling method was performed by tuning the controller for proportional action only, i.e. setting T_I at its maximum value and T_D at zero. By trial-and-error the lowest value of PB_c was found that resulted in a stable oscillation after a step change to the setpoint. At this ultimate proportional band, PB_{cu} , the time for a single cycle in the oscillation is known as the ultimate period of the controller, P_u . The controller settings were then calculated based on the values of PB_{cu} and P_u as:

$$PB_c = 1.7 \cdot PB_{cu} \quad (6-2)$$

$$T_I = 0.5 \cdot P_u \quad (6-3)$$

$$T_D = 0.125 \cdot P_u \quad (6-4)$$

This tuning method generally provides a good set of starting values that must be further adjusted by trial-and-error. Using the feedstock mixture described in

TABLE 6-1. Controller settings from the continuous cycling tuning method.

		Oxygen Concentration		Temperature	
Parameter	Range	Z-N Setting	Setting used	Z-N Setting	Setting used
PB_c	1-10,000	425	500	20	20
T_I (min)	0-99	50	50	99	90
T_D (min)	0-20	12.5	0	20	0

Section 6.3.1, the continuous cycling tuning method gave PB_{cu} of 250 and P_u of 100 minutes for the oxygen concentration PID controller. Initial tuning of the temperature PID controller led to the use of overly tight control parameters, but subsequent tuning gave better values of PB_{cu} at 10 and P_u at 1200 minutes. Adjustments to these resulting control parameter settings were made based on subsequent trial-and-error tuning trials. Table 6-1 shows the best controller settings found during the preliminary pilot-scale composting experiments in Section 6.3, which were based on these adjusted Ziegler-Nichols settings.

6.2.3 Controller Tuning by a Process Model-Based Method

As described in Section 6.3, compost process dynamics varied depending on the feedstock mixture. A second round of controller tuning was required before proceeding from the preliminary composting trials to the pilot-scale tests of polylactide biodegradation. However, due to the long period of oscillation for the

temperature controller, several days were required for each iteration by the closed loop continuous cycling method. Model-based controller tuning methods, such as the process reaction curve method, can give controller settings after a single trial and are therefore desirable in tuning controllers for slow processes. A method for extracting tuning parameters from the open loop response of the process based on an empirical model (Ziegler and Nichols, 1942; Cohen and Coon, 1953) was applied to find controller settings suited to the pilot-scale composting feedstock mixture for the polylactide biodegradation experiments.

The process reaction curve method uses an empirical model of the process based on the response, Δy , to a step change in the controller output, Δp . For many processes the response of the system has the characteristics of the curve shown in Figure 6-4. This type of response, first-order-plus time delay, can be modeled using the transfer function:

$$G(s) = \frac{K \cdot \exp(-\theta s)}{\tau s + 1} \quad (6-5)$$

where:

- K = the process gain
- τ = dominant time constant
- θ = time delay constant
- θ_d = $\theta + \Delta t/2$ (for digital controller)

The process gain is the ratio of the change in the steady-state value of the controlled variable to the change in controller output, $\Delta y/\Delta p$. The time constants θ and τ can graphically extracted from the process reaction curve as shown in Figure 6-4. A set of correlations developed by Cohen and Coon (1953) can then be used to find the controller settings PB_c , T_I , and T_D :

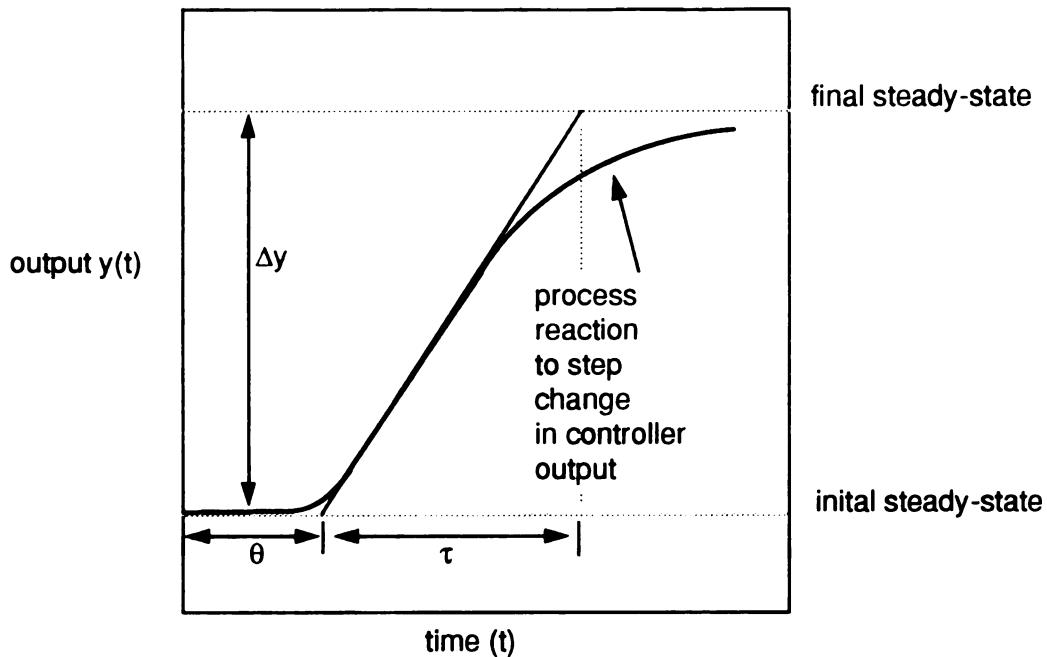


Figure 6-4. Characteristics of the process reaction curve.

$$\frac{PB_c}{100} = \frac{\tau}{K\theta_d} \left(\frac{4}{3} + \frac{\theta_d}{4\tau} \right) \quad (6-6)$$

$$T_I = \theta_d \left(\frac{32 + 60\theta_d/\tau}{13 + 80\theta_d/\tau} \right) \quad (6-7)$$

$$T_D = \theta_d \left(\frac{4}{11 + 20\theta_d/\tau} \right) \quad (6-8)$$

Figure 6-5 shows how oxygen concentration responded to step changes in the air flow rate. Process reaction curves were generated using step changes as both increased and decreased air flow rate. These step changes were made at conditions near the target concentration of 15% oxygen. Process characteristics extracted graphically from the process reaction curves were similar for increased and decreased air flow rates, as shown in Table 6-2.

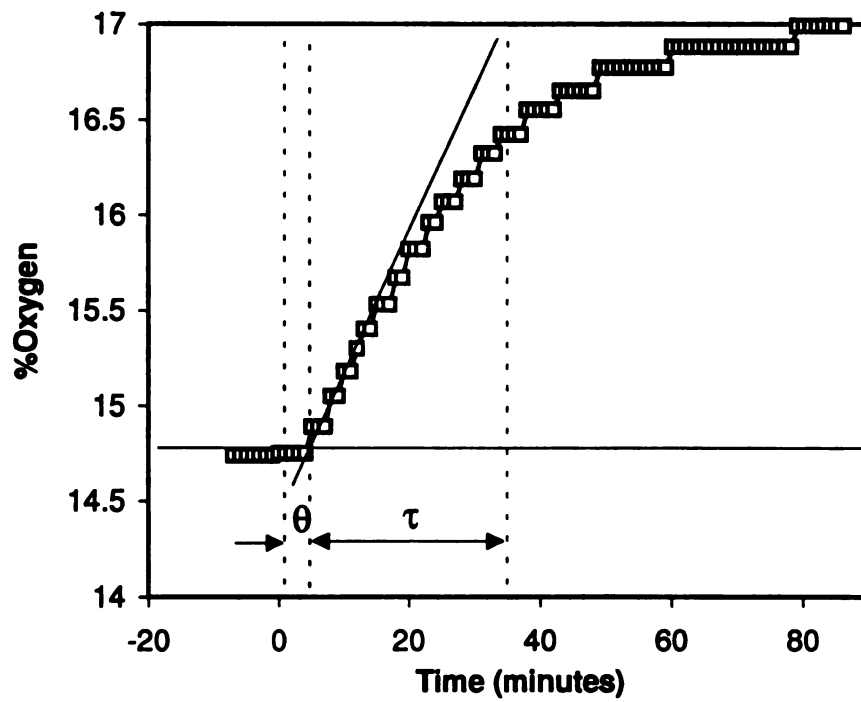
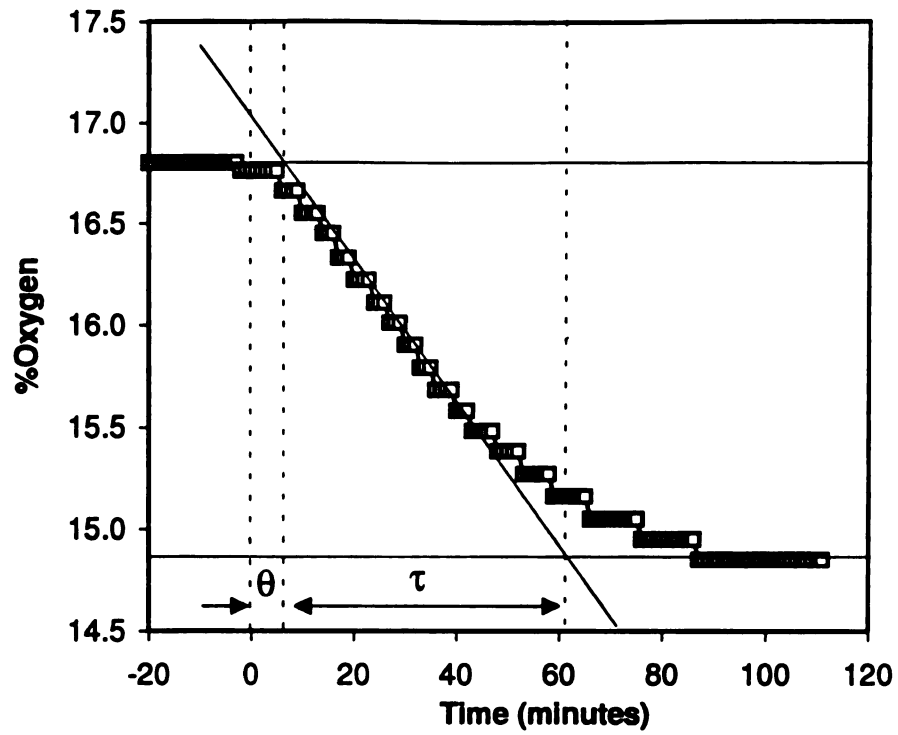


Figure 6-5. Response of oxygen concentration to a step decrease (top) and increase (bottom) in the air flow rate.

TABLE 6-2. Process characteristics for oxygen concentration

Parameter	Decreased air flow rate	Increased air flow rate
K	6.8	7.4
τ (min)	50	30
θ_d (min)	12	8.5

The process characteristics were used to calculate the controller settings based on the Cohen-Coon correlations. These settings were developed to give a setpoint overshoot with a decay ration of 1:4, meaning that the amplitude of the initial setpoint overshoot is four times that of the next oscillation. By relaxing the Cohen-Coon controller settings to the final settings shown in Table 6-3, tight control of oxygen concentration was maintained with less oscillation of the process variables.

TABLE 6-3. Cohen-Coon settings for oxygen concentration control.

Parameter	Range	Decreased air flow	Increasing air flow	Setting
PB_c	1-10,000	117	150	300
T_I (min)	0-99	27	18.8	80
T_D (min)	0-20	4.2	2.9	0.3

Figure 6-6 shows how temperature responded to step changes in the air flow rate. Again, process reaction curves were generated using step changes as both increased and decreased air flow rate. Due to the long settling time of temperature

after a process perturbation, steady-states of temperature were extremely difficult to maintain. Oxygen concentration reached a new steady-state approximately one hour after a change in air flow rate, and in this time the system was relatively unchanged. Temperature, on the other hand, required one to two days to reach a new steady-state. Radical changes to the system could occur in the time for temperature to settle at the new steady-state. Process characteristics extracted graphically from the process reaction curves revealed this non-stationary behavior, as shown in Table 6-4.

TABLE 6-4. Cohen-Coon process characteristics for temperature.

Parameter	Decreased air flow rate	Increased air flow rate
K	0.19	0.54
τ (min)	900	1740
θ_d (min)	600	5

TABLE 6-5. Settings for temperature control.

Parameter	Range	Decreased air flow	Increased air flow	Setting
PB _c	1-10,000	8.41	0.12	30
T _I (min)	0-99	1178	12	99
T _D (min)	0-20	194	1.8	10

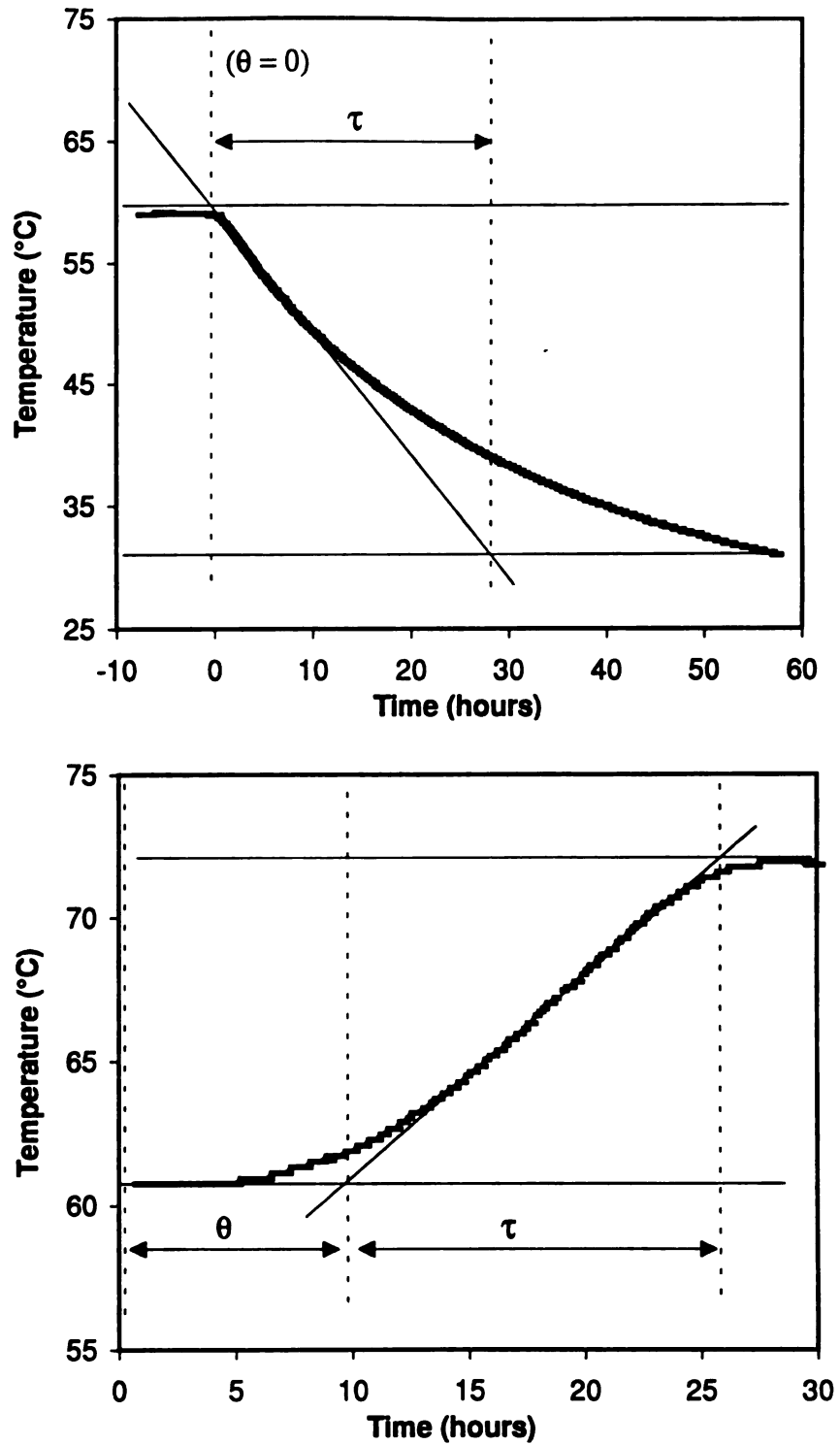


Figure 6-6. Response of temperature to a step increase (top) and decrease (bottom) in the air flow rate.

The process characteristics were then used to calculate the controller settings for temperature control based on the Cohen-Coon correlations. Based on these settings, the final values were selected as shown in Table 6-5. Controller settings were selected primarily on the basis of the results from the response of the system to the decreased air flow rate. The increased air flow rate response was disregarded, since the step change drove the temperature out of the thermophilic range and the process reaction curve did not exhibit a time delay. The settings selected used primarily proportional and derivative (PD) controller action, which is common in temperature control.

6.3 PRELIMINARY EVALUATION OF COMPOST FEEDSTOCKS

Municipal solid waste (MSW), sludge, and yard debris are common feedstocks for composting. Pilot-scale composting of mixtures from each of these three categories provided process data that was used to evaluate the processing requirements, dynamics, and product quality using each of these feedstocks.

6.3.1 MSW Compost

Pretreated MSW from the Recomp of Minnesota composting plant in St. Cloud, MN was selected as a representative MSW feedstock, collected and shipped to Lansing, MI, and stored refrigerated at 2-4°C until used. This material had been homogenized for three days in a rotating drum digester and passed through a 1.5 in screen. At the Recomp facility this pretreatment was followed by 7 weeks of composting in an aerated, agitated trench system. The raw compost was extremely heterogeneous, and had a high level of plastic, glass, and metal contamination. Analysis of this fraction by researchers at the Ohio State University revealed that

these inert materials accounted for 62% of the solids in the raw compost (Ionatti et al., 1993). Other characteristics of the feedstock are shown in Table 6-6.

TABLE 6-6. Analysis of MSW compost feedstock.

Moisture content (%)	47
Ash content (%)	33
pH	6.6
%C	38
%N	0.72
C/N ratio	53

The first batch of MSW compost to be tested performed as shown in Figure 6-7. Within 15 h of loading the oxygen concentration dropped below 15%, and an air flow rate increase followed. A local maximum in microbial activity occurred at 19 h, as evidenced by the carbon dioxide production rate (CPR) and inflection of the compost temperature verses time. This occurred when the average temperature of the compost was 35-40°C, the optimum temperature for many mesophilic species.

As the compost temperature increased, overall activity decreased temporarily until the average temperature exceeded 50°C. At this time a surge of activity attributed to thermophilic species brought about another increase in the air flow rate. During the period of peak air flow rate the temperatures at the top and bottom of the composting vessel began to drift apart. Operation was discontinued after 32 h

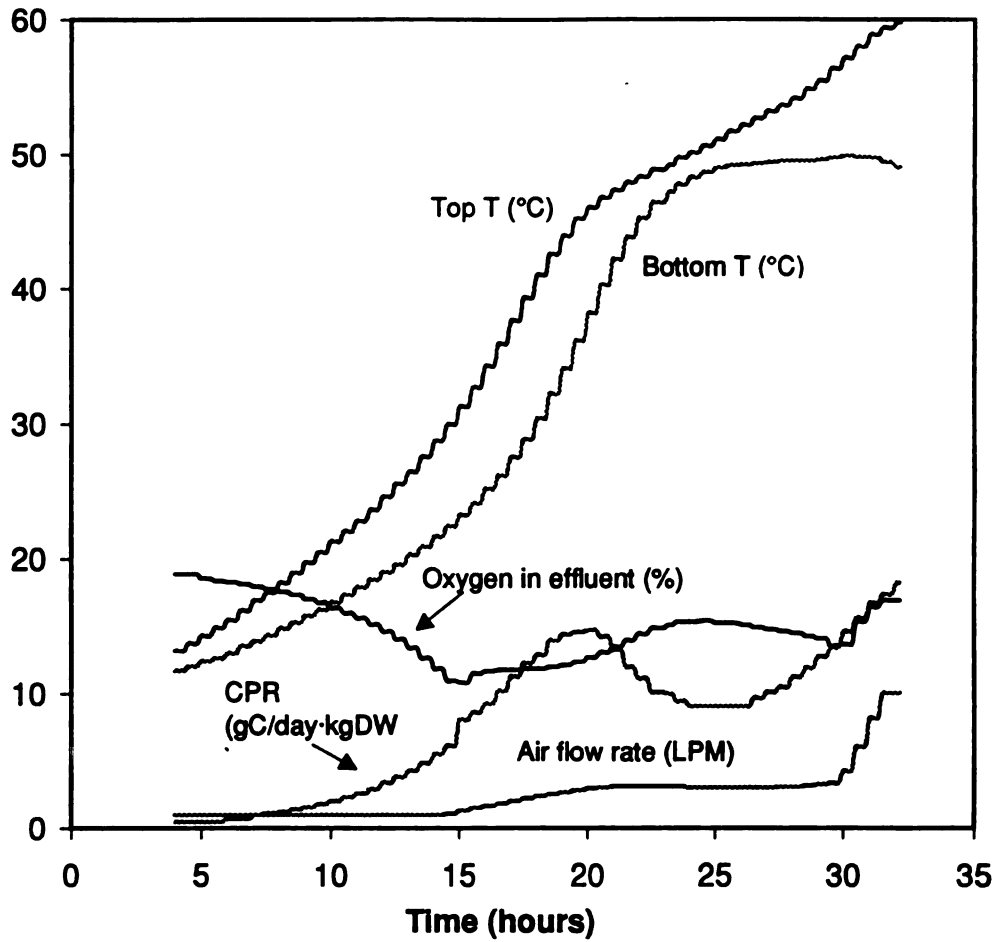


Figure 6-7. Process dynamics of MSW compost over first 32 hours of operation with no mixing.

when the aeration demand exceeded the 10 L/min limit of the mass flow controllers.

A second trial with the MSW compost successfully passed through periods of peak activity after the mass flow controller limits were reset to 30 L/min. Results are shown in Figure 6-8. Mixing after the first day prevented the distinction of mesophilic and thermophilic maximums apparent in the first MSW trial. Tight temperature control was possible because of the high level of inert material in the compost. The energy balance for a compost can be written as:

$$\begin{aligned} (\text{Heat removal}) = & (\text{losses by conduction}) + (\text{losses to cooling air}) + \\ & + (\text{losses to evaporation}) - (\text{heat generation}) \end{aligned} \quad (6-9)$$

Energy removal through the cooling air will make conductive losses negligible if the system is well insulated, and if inert materials do not result in heat generation. Increasing the air flow rate to an inert material results in the classical cooling response that is a function of the heat capacity of the material and heat transfer rate to the cooling air. An increase in air flow rate to an active biomass, however, can have many effects. The rate of heat generation will increase if the air flow rate change relieves an oxygen or temperature limited condition. If an increased air flow rate takes the system away from optimal conditions the heat generation rate will decrease.

Control was effective due to the high level of inerts, but controller settings were extreme and resulted in instability. PB_c and T_1 were set at 10 and 50, respectively for the MSW trials. This resulted in far too much integral action in the temperature controller. Evidence of this instability showed up at around 3 days as

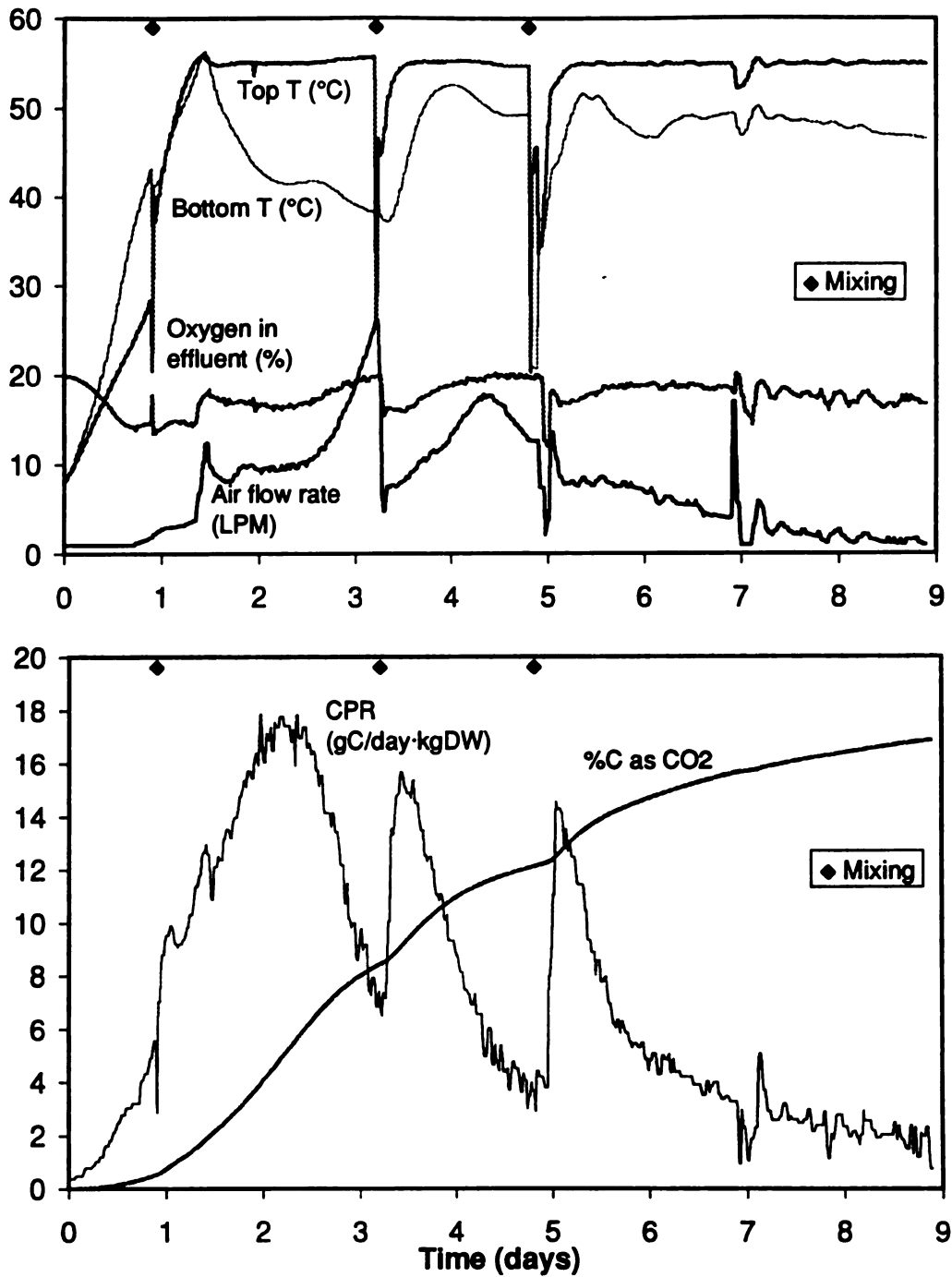


Figure 6-8. Process dynamics for pilot-scale composting of MSW over the first nine days.

integral windup. Further controller tuning led to the application of the more relaxed tuning parameters in Table 6-1 for subsequent trials, giving less rigorous but more robust control.

The loss of activity and subsequent resurrection on mixing at 3.2 days and 5 days was due to failure of the moisture control mechanism described earlier. At high flow rates the air entrained water as it condensed at the vessel outlet and prevented it from returning to the compost. Drying was severe at the air inlet side of the vessels, and water was added before mixing the compost.

6.3.2 Sludge Compost

A mixture of dewatered anaerobic digester sludge and shredded wood from the water pollution control facility (WPCF) of Fairfield, CT was selected as a representative sludge composting feedstock, collected and shipped to Lansing, MI, and stored refrigerated at 2-4°C until used. At the Fairfield facility this sludge was dewatered to 15-20% solids, aided by the addition of 10 lb/ton Percol 763 acrylamide:DMAEA copolymer. The dewatered sludge was then mixed with shredded wood at a 1:4 ratio (sludge:wood, dry weight basis) and composted for 3 weeks in an aerated, agitated trench system. Chemical characteristics of the feedstock are shown in Table 6-7.

Sludge compost is relatively homogeneous and free of plastic film, but there is some concern regarding the possibility of high metal concentrations in municipal sludge. A sample of finished compost product from the Fairfield WPCF was analyzed by the Michigan State University Animal Health Diagnostics Laboratory using Ion Coupled Plasma (ICP) Spectroscopy. The concentrations of 25 metals,

TABLE 6-7. Analysis of sludge compost feedstock.

Moisture content (%)	57.6
Ash content (%)	19.2
pH	7.3
%C	43.3
%N	1.56
C/N ratio	28

shown in Table 6-8, are reported in ppm. ICP spectroscopy did not detect any metal concentrations in excess of the EPA 503 limits for compost.

Pilot-scale composting was operated for 19 days at an oxygen concentration setpoint of 15% and with the temperature setpoint at 55°C from day 0-10, 50°C from day 10-15, and 40°C from day 15-19. Results are shown in Figure 6-9. Oxygen demand determined the air flow rate for the first 5 days until the compost temperature reached 55°C. Temperature control was not as tight for pilot-scale sludge composting as it was for MSW composting, but performed adequately. The cooling air demand and carbon dioxide production rates for the sludge mixture were lower and less variable than for MSW. Even though the MSW compost used had a high level of inerts, the organic fraction consisted mostly of high energy food waste and cellulotics. Fairfield WPCF sludge, on the other hand, had already been through aerobic and anaerobic treatment steps. When composted at the pilot-scale the sludge and shredded wood mixture gave a maximum carbon dioxide production rate half that of the MSW mixture.

TABLE 6-8. Elemental analysis of Fairfield compost product.

Element	Detection Limit (ppm)	Concentration (ppm)	standard deviation	EPA 503 limits
Al		5590	1178	
As	12.5			41
B	25.0	27.6	*	
Ba		282	64	
Ca		13533	1877	
Cd	2.50	2.89	0.17	39
Co		3.79	0.37	
Cr		40.2	5.2	1200
Cu		483	61	1500
Fe		12200	5336	
Hg	50			17
K		4867	316	
Mg		2603	439	
Mn		584	84	
Mo		5.48	0.23	18
Na	250			
Ni		20.1	0.9	420
P		6067	1070	
Pb		121	16	300
S		5687	524	
Sb	25			
Se	100			
Tl	62.5			
V		8.13	2.75	
Zn		1123	162	2800

*only one of the triplicate samples was above the DL for boron

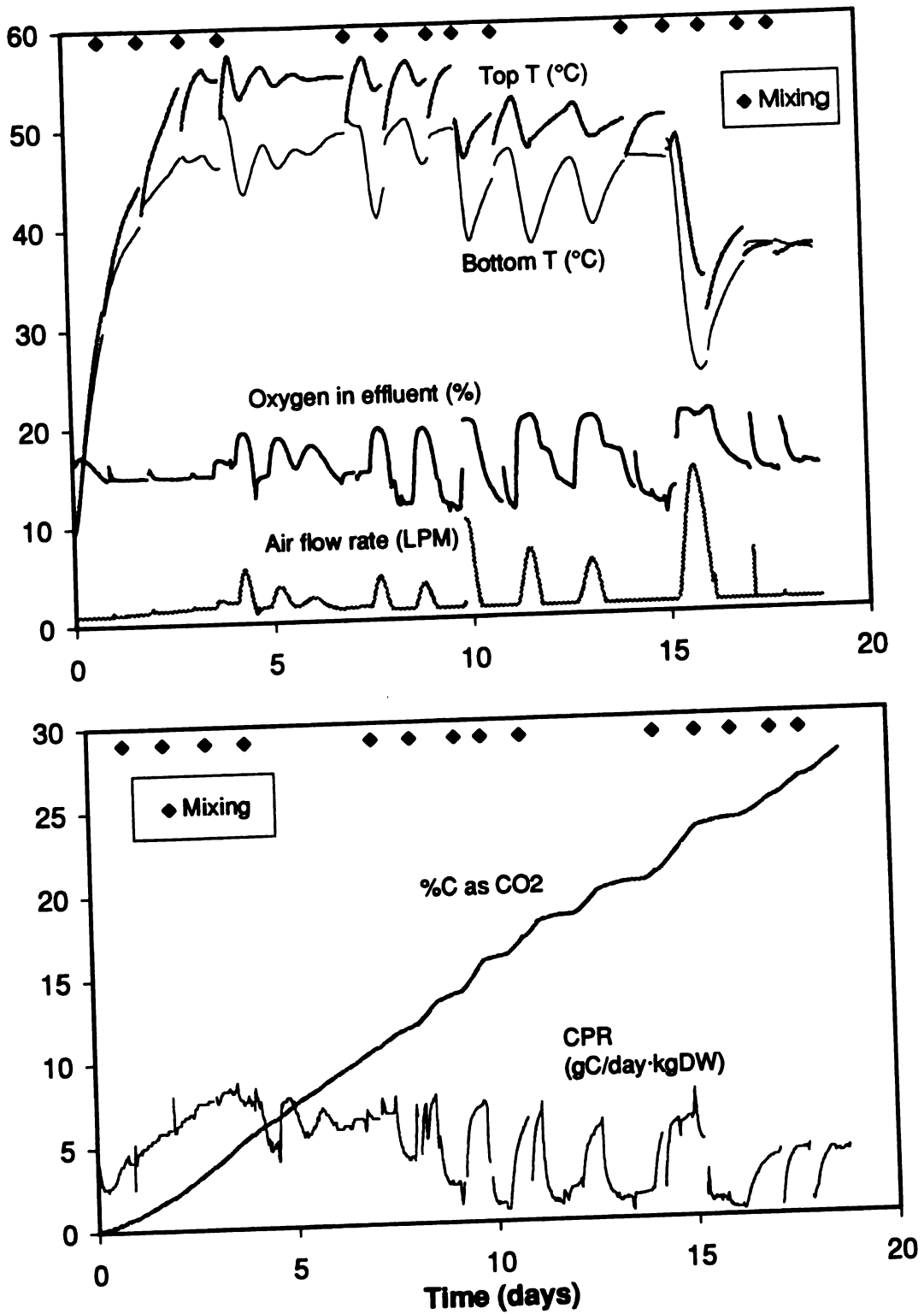


Figure 6-9. Process dynamics for pilot-scale composting of sludge-wood chips mixture.

6.3.3 Yard Debris Compost

A mixture of yard debris, obtained from the Michigan State University grounds department, was selected as a representative yard debris composting feedstock. Leaves, grass, and shredded wood were mixed at a ratio of 3:1:1. Water was added to raise the moisture content of the mixture to 60%. Chemical characteristics of the yard debris components and the mixture are shown in Table 6-9.

TABLE 6-9. Analysis of yard debris materials.

	LEAVES	GRASS	WOOD	MIXTURE
Moisture (%)	52.8	81.1	52.9	65
pH	6.6	8.0	8.3	8.4
%Carbon	43.0	44.4	48.5	44.4
%Nitrogen	1.16	3.92	0.14	1.51
C/N ratio	37.1	11.3	>100	29.4

Several short pilot-scale composting trials were performed using this yard debris formulation. The resulting process data was used in fine tuning PID parameters suitable for pilot-scale composting of this mixture. Typical behavior of yard debris compost is shown in Figure 6-10. As discussed earlier, control of oxygen concentration at the setpoint was easily achieved since the response of oxygen concentration to a change in air flow rate was relatively predictable and occurred rapidly in this system. On the other hand, temperature response was non-stationary and had a natural period on the order of one day, making tight control

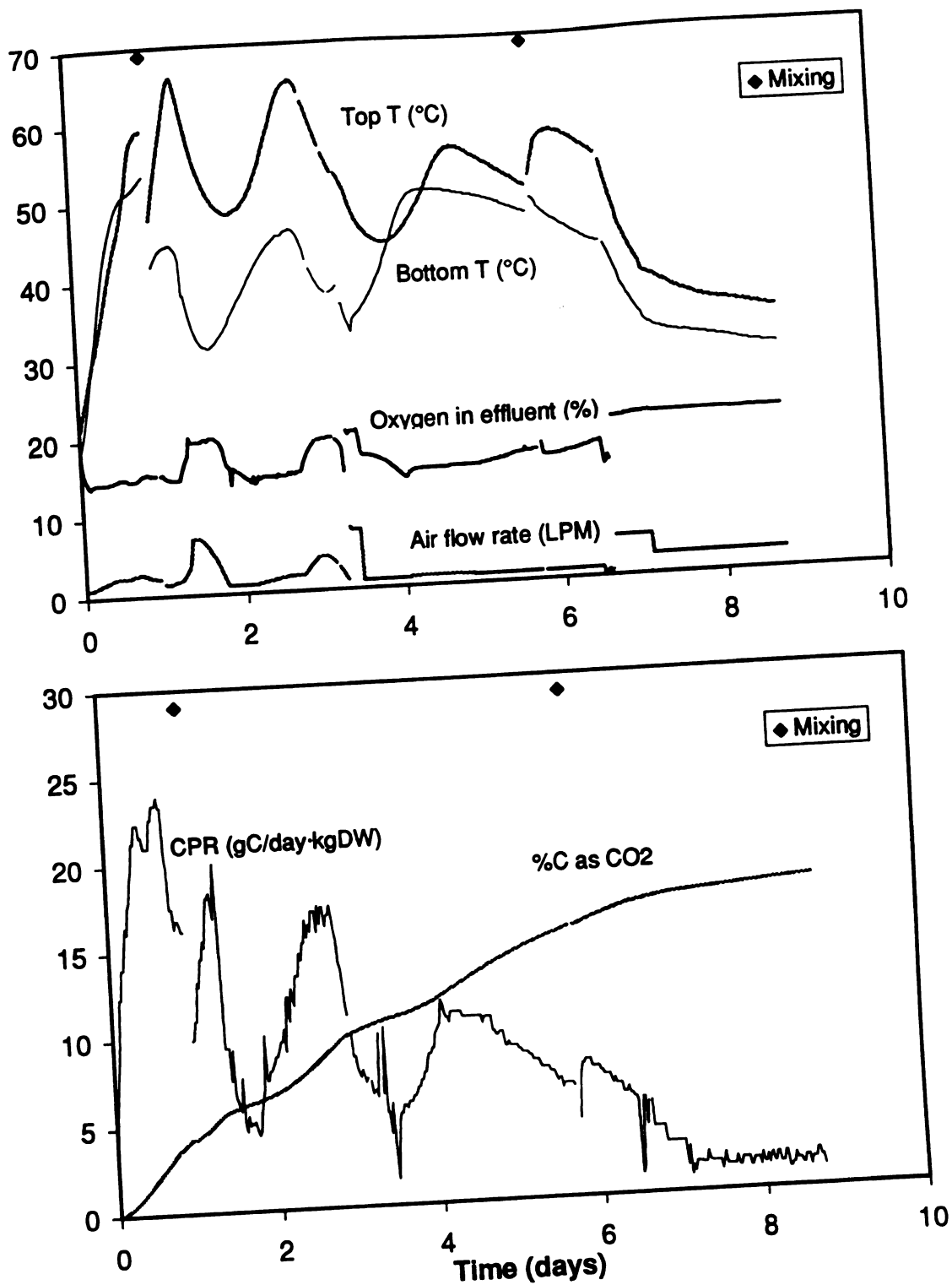


Figure 6-10. Typical process dynamics for pilot-scale yard debris composting trials.

very difficult. These process characteristics require that PID tuning parameters reflect a compromise between the desire to keep the temperature from exceeding the setpoint and the desire to prevent overcooling. Based on the results of several such trials using yard debris, a process control strategy using relaxed temperature control parameters was selected for subsequent pilot-scale composting.

Composting of a mixture of yard debris and 40# Kraft paper was performed in the pilot-scale system using the process control strategy developed for yard debris composting and the PID tuning parameters in Table 6-3 and Table 6-5. The experiment used a mixture of 40% leaves, 30% grass, 20% wood mulch, and 10% Kraft paper adjusted to a moisture content of 60%. Initial characteristics of this mixture are shown in Table 6-10.

Results of the 38-day composting experiment are shown in Figure 6-11. A period of peak activity occurred during the initial week, when carbon dioxide generation rates were high and air flow rate was controlled based on compost temperature. Over the first four days of the experiment the air flow rate exceeded 10 L/min, and a steep temperature gradient developed in the composting vessel. Water was added during mixing on day 4, since the overall moisture content had fallen to 37%. From day 7 to 20 the compost oxygen demand determined the air flow rate. After this period the minimum air flow rate of 1 L/min was sufficient for oxygenation. The compost had an overall moisture content of 75% on day 26. In an attempt to lower the moisture content the humidification column was bypassed and the air flow rate was increased to 2 L/min. However, the compost was at ambient temperature by this time and very little evaporative drying followed.

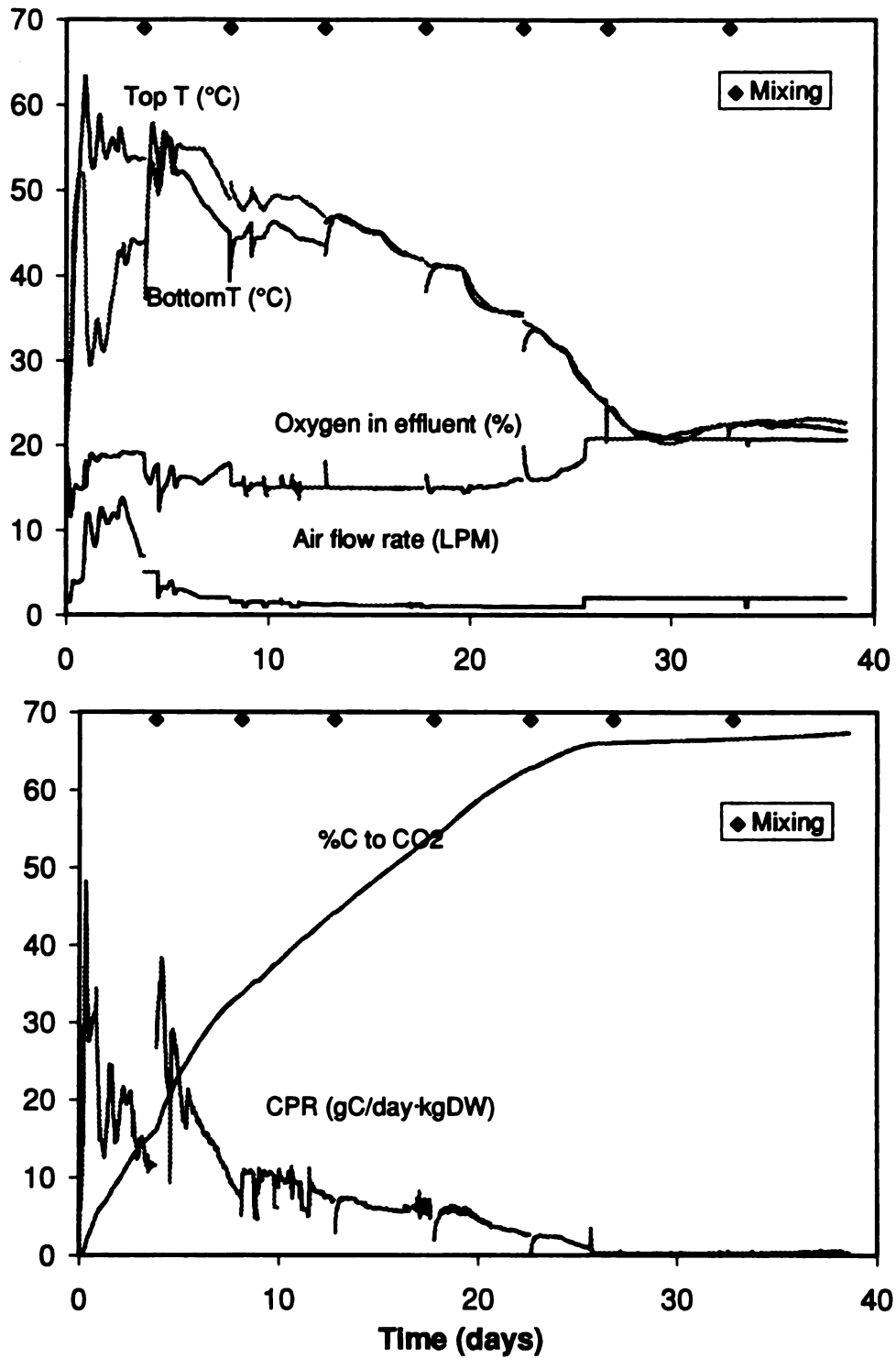


Figure 6-11. Process dynamics for pilot-scale composting of Kraft paper in yard debris mixture.

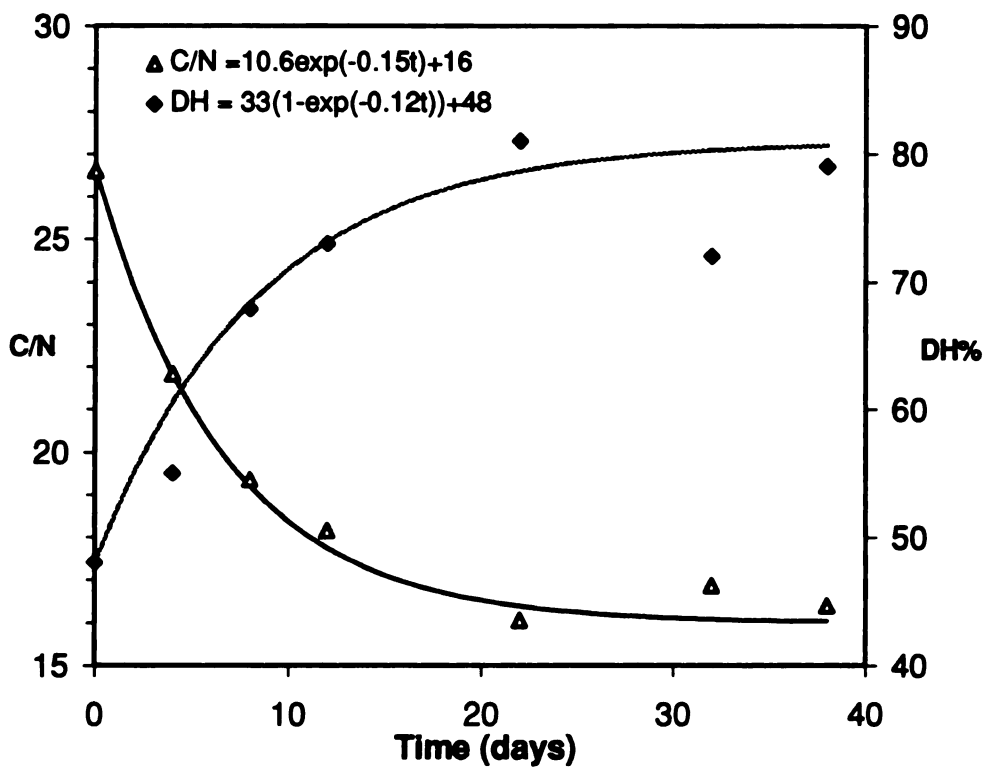
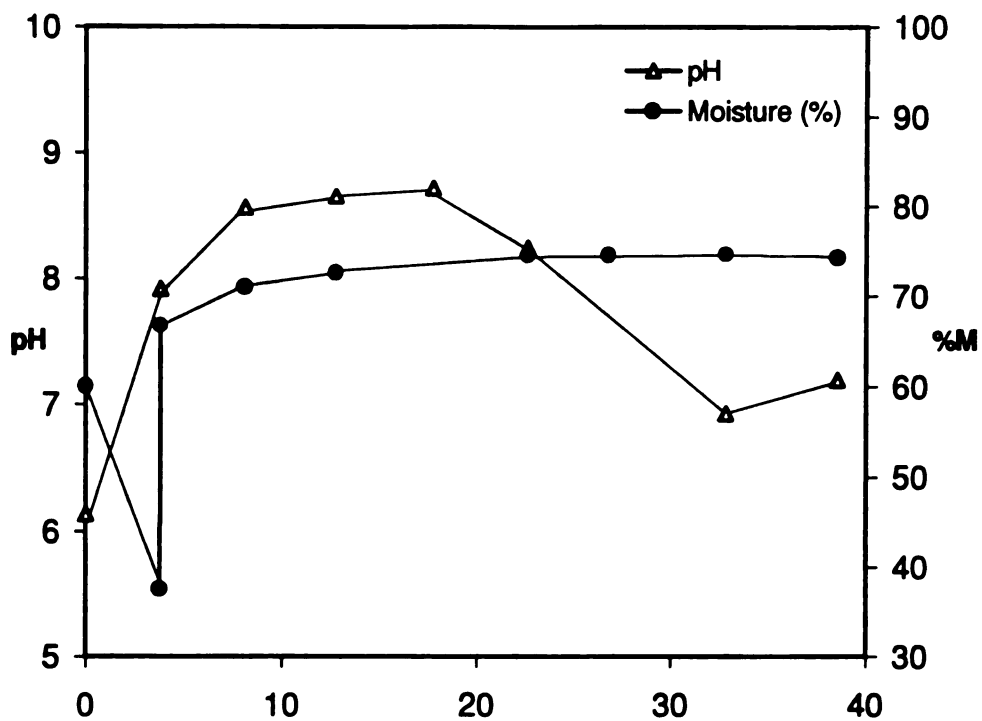


Figure 6-12. Chemical parameters during pilot-scale composting of Kraft paper mixture.

Tracking of chemical parameters provided insight into the transformation of the yard debris mixture into a stabilized compost (Figure 6-12). Initially the yard debris mixture was at pH 6.1 and had risen to pH 7.9 within four days. The low initial pH results from the formation of organic acid intermediates in the yard debris mixture, and the subsequent rise to pH 8.7 is due to the rapid thermophilic growth of microorganisms capable of metabolizing these intermediates. As the composting temperature fell below 40°C the pH lowered to near neutral.

TABLE 6-10. Analysis of Kraft paper/yard waste mixture.

Moisture content(%)	60
pH	6.1
%Carbon	44.6
%Nitrogen	1.68
C/N ratio	26.6

Table 6-11 shows the carbon balance for the composting experiment. Solid phase carbon was measured by CHN elemental analysis and carbon dioxide evolution was calculated using the air flow rate and effluent gas composition. This respirometric calculation of carbon evolved as carbon dioxide was less reliable than the solid phase analysis. Based on the solid phase analysis 51% of the initial carbon was converted to carbon dioxide as opposed to 65% based on respirometry.

The effect of this carbon loss on the carbon to nitrogen ratio is shown in Table 6-12. High temperature and alkalinity during the first half of the experiment provided conditions favorable for the release of nitrogen as ammonia, and total

TABLE 6-11. Carbon balance for Kraft paper/yard waste composting.

Carbon species	Designation	g Carbon
Initial mixture	C_i	2227
Final compost	C_f	1099
Mineralization to CO_2	C_{CO_2}	1397
Carbon balance closure	$(C_f + C_{CO_2})/C_i \times 100$	(112%)

TABLE 6-12. Change in C/N during Kraft/yard waste composting.

	Initial	Final
Dry weight (g)	5000	2701
%Carbon	44.6	40.7
%Nitrogen	1.68	2.41
Total carbon (g)	2227	1099
Total nitrogen (g)	84	65
C/N	26.6	16.9

nitrogen content decreased. Since the total nitrogen content decreased by only 23% while the total carbon content decreased by over 50%, the carbon to nitrogen ratio decreased from 26.6 to 16.9 over the course of the experiment as shown in Figure 6-12.

Fractionation of humic substances provided a means of following the changes in the carbon species present (Ciavatta et al., 1990). As described in Chapter 4, compost organic matter was separated into the alkaline extractable carbon (TE) and the non-extractable carbon, or humin (HU). The portion of the TE fraction that precipitated below pH 2 is called humic acid (HA). Chromatographic fractionation of the pH 2 soluble material on polyvinylpyrrolidone isolated the soluble humified fraction, fulvic acid (FA), from the non-humified (NH) components.

The degree of humification (DH), i.e. the ratio of humified carbon (HA + FA) to total extractable carbon (TE), increased rapidly from 48% at the beginning of composting and converged on 80% at the end of composting (Figure 6-12). The contribution of each extractable carbon fraction to the TE is shown in Figure 6-13. Increasing DH during composting was due to an increase in the relative amount of HA carbon, a stable level of FA carbon, and a decrease in NH carbon. The compost sample collected on day 32 gave a C/N ratio and humic substance profile that was characteristic of a less mature compost than the prevalent trend, and was treated as the result of poor sampling.

Table 6-13 shows the initial and final carbon species distributions both on the basis of carbon species weight and as percentage of the total carbon in the solid phase. There was no net change in the amount of HA during composting. However, the mineralization of HU, NH, and FA to carbon dioxide resulted in a final HA concentration twice that of the initial mixture. This large increase in HA and small decrease in FA relative to the large decrease in NH caused the high DH of the composted material.

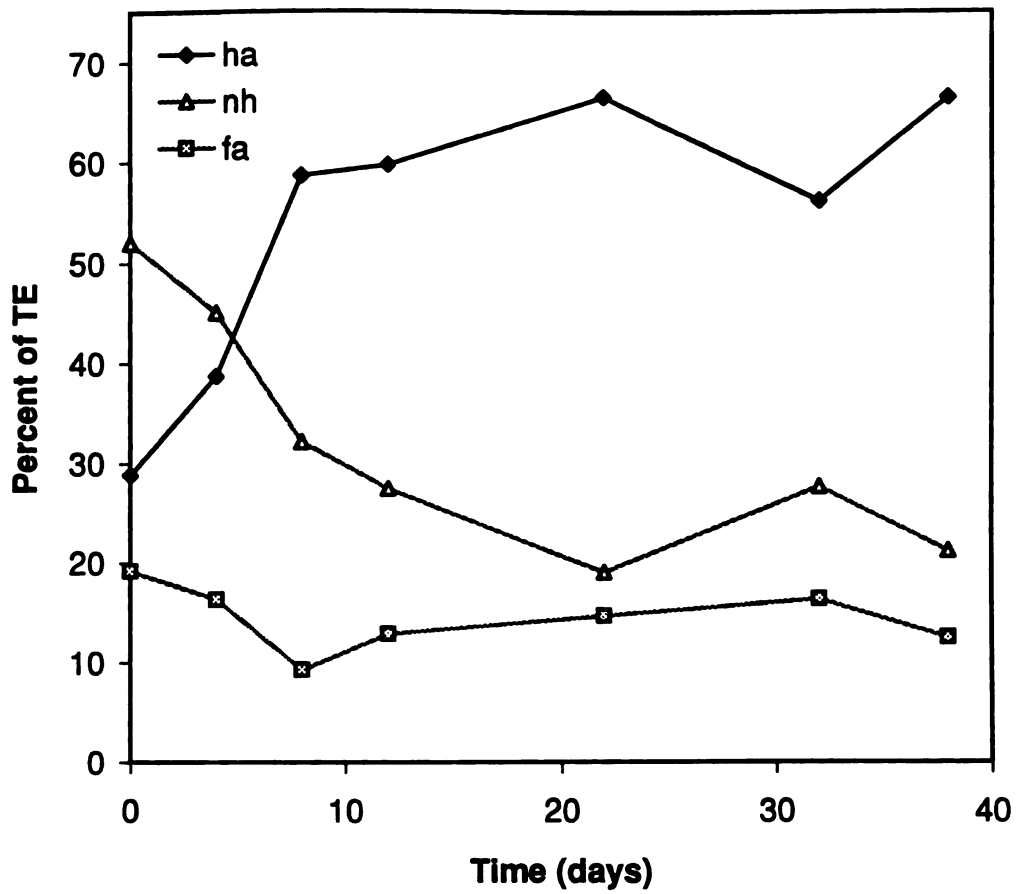


Figure 6-13. Contribution of each extracted fraction to the total extractable carbon.

Kraft paper rapidly disintegrated in the pilot-scale yard debris composting trial. The high moisture content through most of the trial aided in the loss of structural integrity. In addition, the Kraft paper discolored and by day 22 visual distinction of the Kraft paper became difficult. At the end of the 38 day composting trial the compost product was a homogeneous brown-black color with no distinguishable paper residue.

TABLE 6-13. Distribution of carbon in humic fractions.

Species	Initial g C	Final g C	Initial % of solid phase C	Final % of solid phase C
Carbon dioxide	0	1128	0	0
Humins (HU)	1858	943	83.4	85.8
Humic acid (HA)	106	104	4.8	9.4
Fulvic acid (FA)	71	19	3.2	1.8
Non-humified (NH)	192	33	8.6	3.0

6.4 BIODEGRADATION OF POLYLACTIDE FILM

After the composting experiments in Section 6.3 established process dynamics and chemical transformations that typically occur during pilot-scale composting, the final round of experiments were performed to determine the effects of polylactide film on process dynamics and compost product quality. Polylactide molecular weights were measured after two and four weeks, and compared to the values predicted by the model of polylactide hydrolytic degradation.

6.4.1 Experimental Method

The four pilot-scale composting experiments lasted 28 days each, using the mixtures outlined in Table 6-14. Polylactide film, Kraft paper, and polyethylene film, all in 6 x 6 inch sheets, were loaded at 12.2% on a dry weight basis into a mixture of shredded green yard debris and anaerobic digester sludge from the Fairfield WPCF. Table 6-15 gives the initial characteristics of this mixture. Since the mixture consisted primarily of green yard debris, the process control setpoints and PID tuning parameters were set as for the yard debris composting experiment in Section 6.3.3. On days 4, 7, 11, 14, 18, 21, and 25 the composts were mixed by transferring the contents of each pilot vessel into five pails, mixing the contents in the pails, and reloading the vessel in reverse order. The compost pH was measured six times over the course of the experiment. Samples of the compost and sheets of the test materials were removed after two weeks and four weeks for chemical analysis.

TABLE 6-14. Mixtures for pilot-scale composting experiments.

	Compost (kg d.w.)	Test Matl. (kg d.w.)	Total (kg d.w.)	Thickness (mil)
Blank	6.80	-	6.80	-
polyethylene	6.80	0.942	7.74	1.0
40# Kraft paper	6.80	0.942	7.74	5.6
polylactide	6.80	0.942	7.74	2.9

TABLE 6-15. Compost feedstock characteristics

Moisture content	$66 \pm 2\%$
pH	7.3 ± 0.5
Ash content	$19.2 \pm 2.4\%$
Carbon (dry weight basis)	$43.3 \pm 2.1\%$
Nitrogen (dry weight basis)	$1.56 \pm 0.19\%$
C/N ratio	28.1 ± 4.1

6.4.2 Effect of Polylactide on Process Dynamics

The four compost test batches displayed process dynamics resembling those of the polylactide compost mixture shown in Figure 6-14. These mixtures behaved similarly to the sludge-wood chip mixture composting described in Section 6.3.2, but the use of green brush and yard debris material in place of wood chips resulted in less process stability and increased setpoint overshoots. For the first half of the experiment temperature-based process control dominated. Compost temperatures exceeded the 55°C setpoint only briefly during this period, and at these times only in the top portion of the vessels. The bulk of the compost remained within temperature ranges desired for minimizing odor production. Figure 6-15 shows the average compost temperatures of the four mixtures. During the first half of the experiments the average temperatures of the four batches stayed approximately equal. However, toward the end of the experiments the compost containing Kraft paper maintained higher temperatures than the other three batches. The Kraft

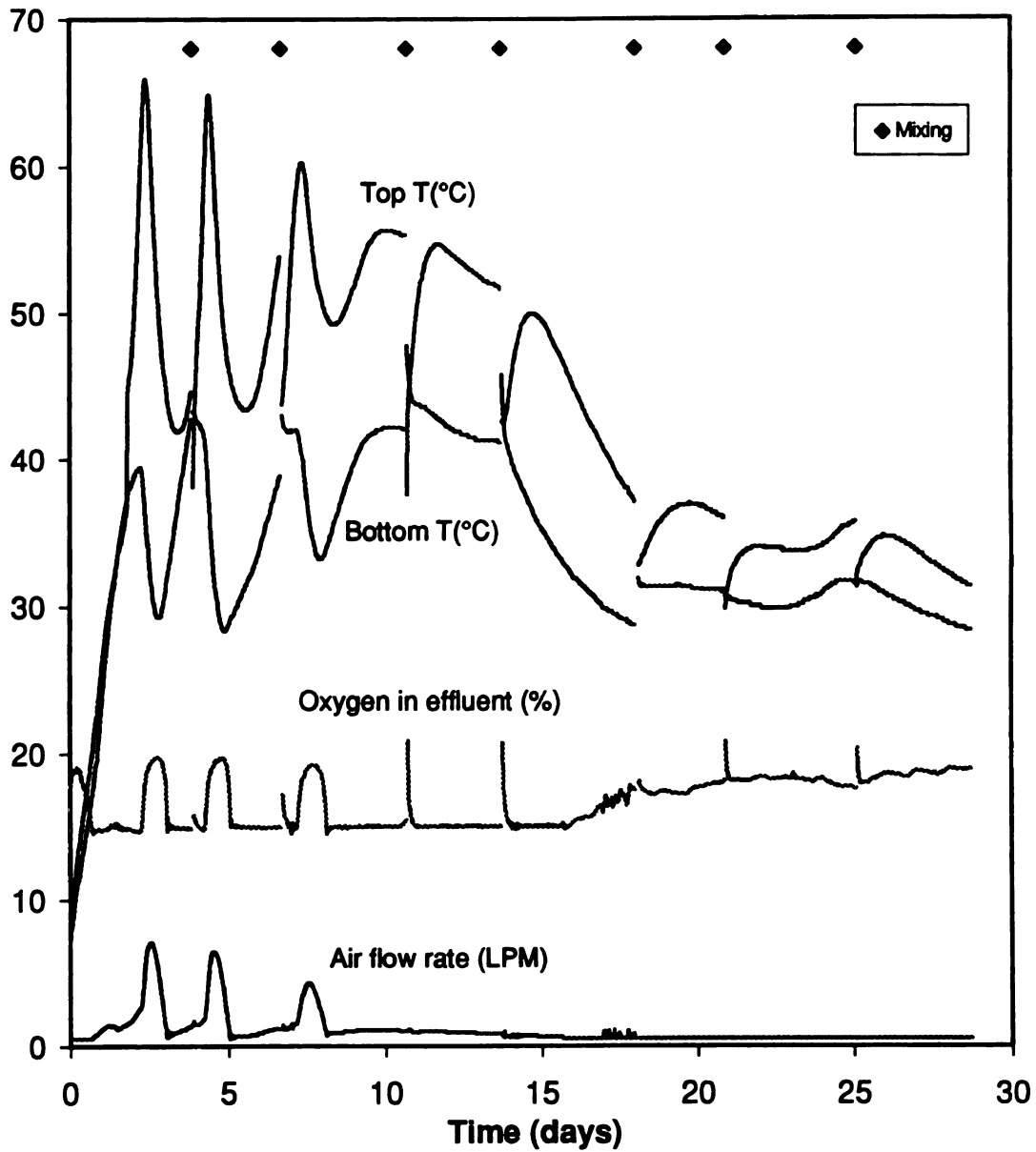


Figure 6-14. Process dynamics for compost mixture containing polylactide film.

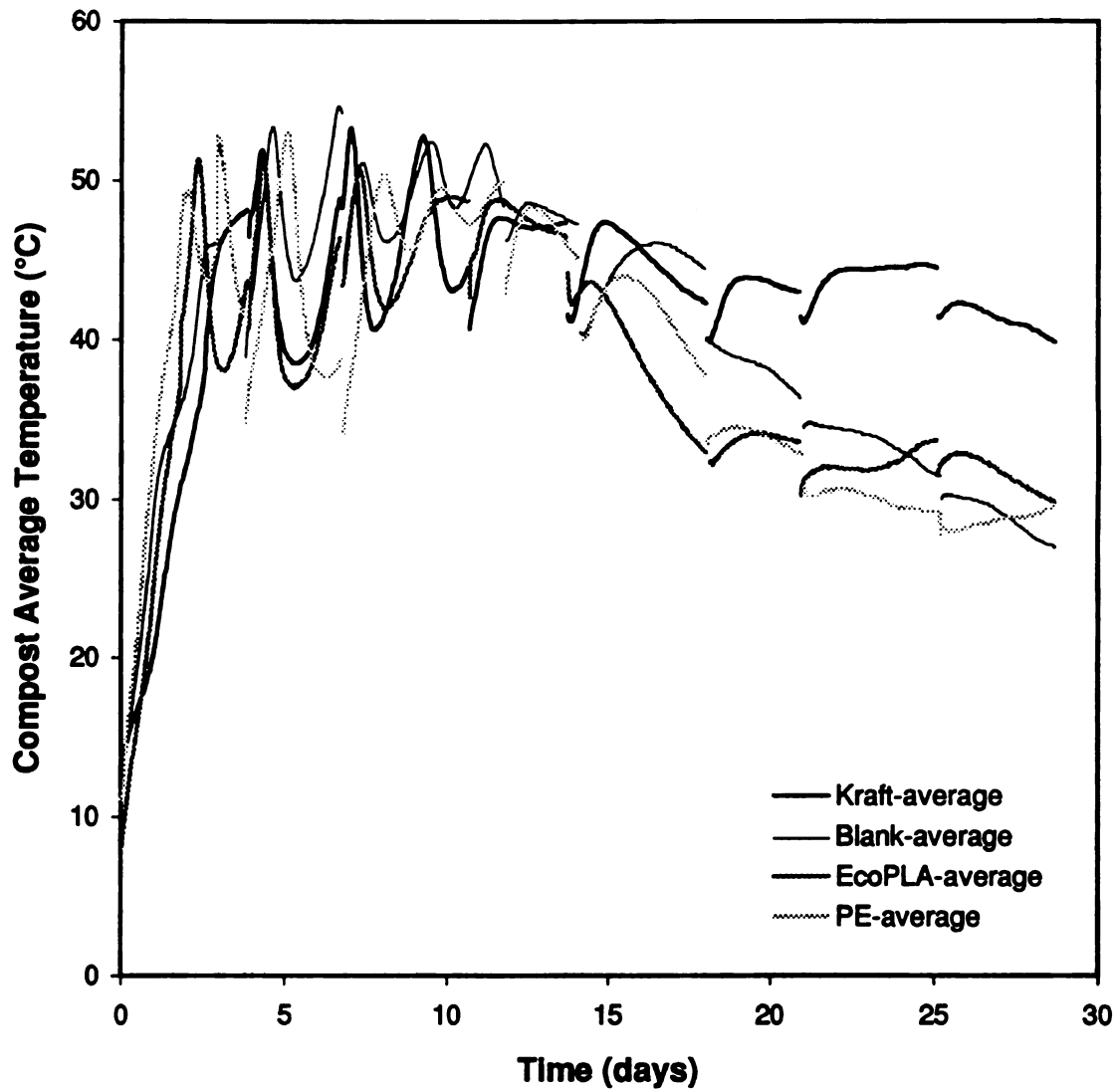


Figure 6-15. Average temperatures in the vessels during pilot-scale composting.

paper added an extra energy source to the compost mixture; addition of polyethylene and polylactide films did not affect the compost temperatures.

Mineralization of the carbon in the mixtures to carbon dioxide followed the trends of the polylactide compost mixture shown in Figure 6-16. The highest rate of carbon dioxide generation coincided with the high temperatures that occurred during the first two weeks of the experiments. Peak rates of carbon dioxide evolution during the first five days exceeded 10 gC/day·kg d.w., but generally remained at levels below 5 gC/day·kg d.w. This carbon dioxide production rate followed the trends of the sludge-woodchip mixture composting described in Section 6.3.2. However, as with the temperature, the green yard debris used in place of wood chips resulted in an oscillatory process (and rate of carbon dioxide production) during the early stages of the experiments.

The cumulative mineralization of the carbon in the mixture to carbon dioxide was calculated on the basis of the compost materials alone, or on the basis of the total carbon in the compost plus the test material. Figure 6-16 shows the percent mineralization to carbon dioxide evolution from the polylactide on these two bases. A comparison of the different rates of mineralization for the four batches is made in Figure 6-17. The percentages shown were calculated based on the assumption that the Kraft paper contributed to the carbon dioxide production and the polyethylene and polylactide films did not. Even with the Kraft paper batch conversion calculated on this basis, the cumulative percentage was greater than for the other batches. Part of this could be because the 12.2% additional Kraft paper mineralized at a rate greater than the compost material itself. However, most of this excess conversion can be attributed to the higher overall microbial activity in

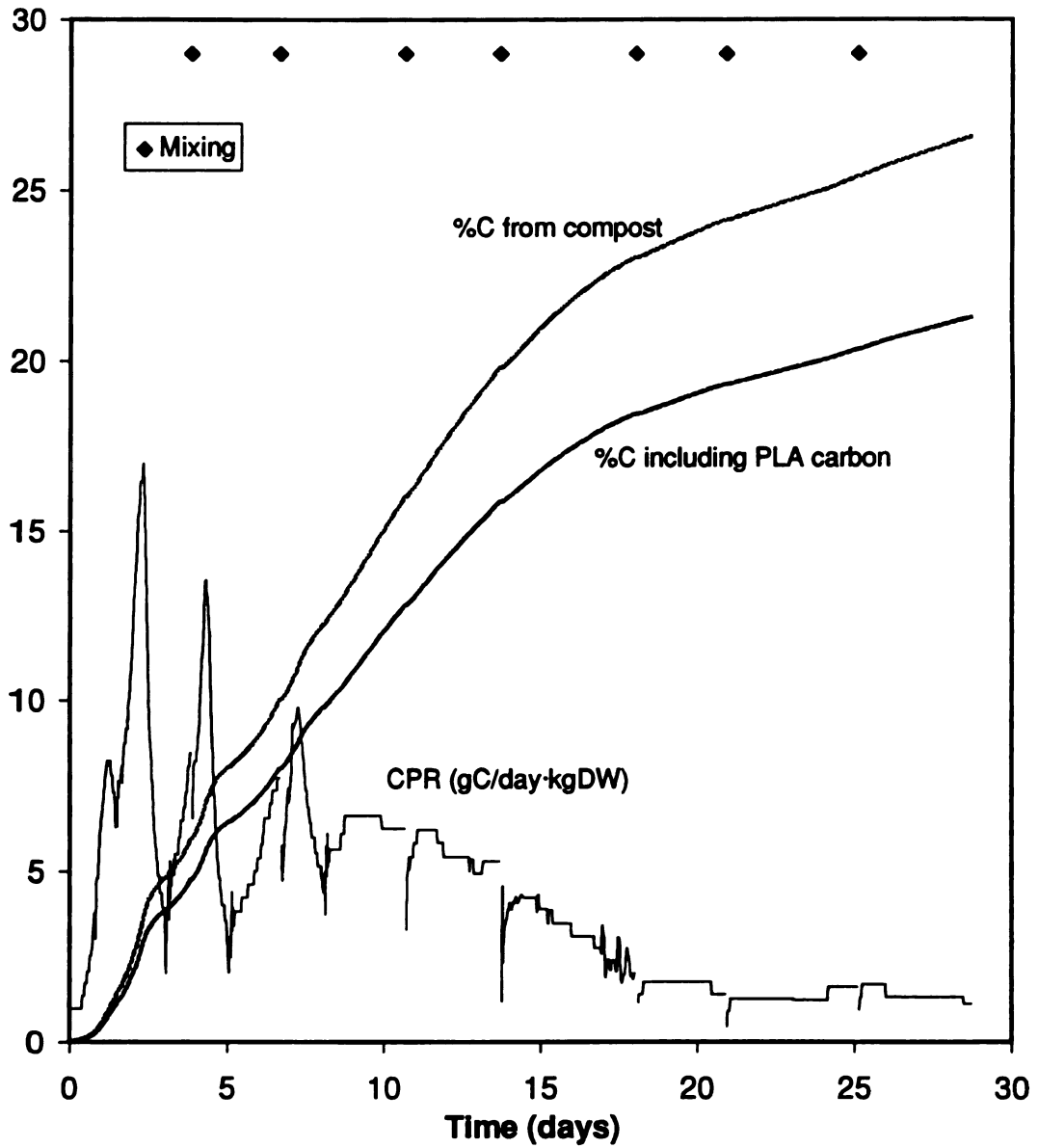


Figure 6-16. Respirometric data for compost mixture containing polylactide film.

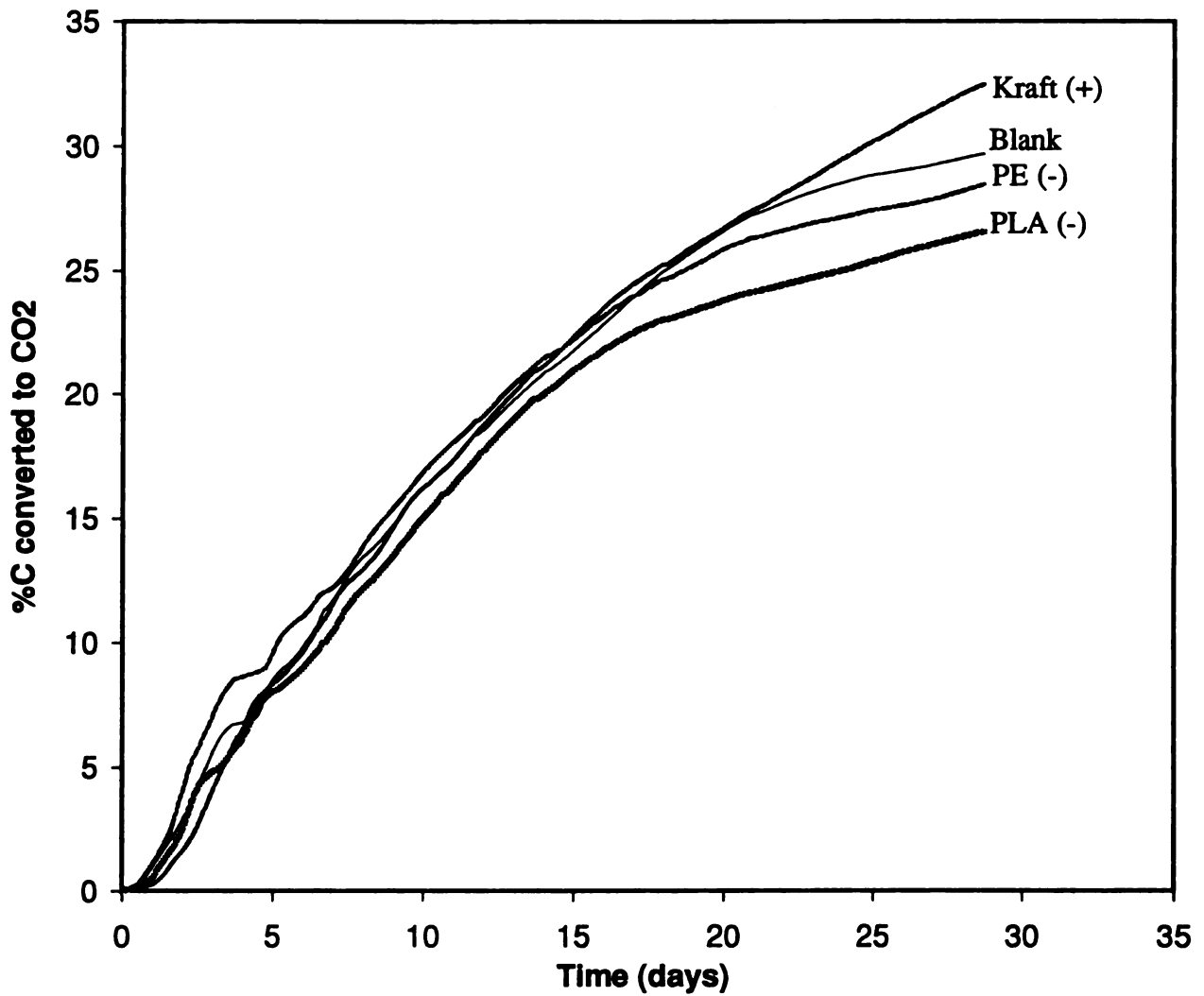


Figure 6-17. Percent mineralization of initial carbon to carbon dioxide during pilot-scale composting.

the mixture, since the excess carbon dioxide generation from the Kraft paper mixture corresponds to the period when this batch maintained a higher temperature.

The addition of polylactide film did not affect the temperature of the compost or have a large impact on the rate of carbon dioxide generation from the compost mixture. The cumulative carbon dioxide production from the mixture containing polylactide film was slightly lower than the production from the blank and polyethylene mixtures. Most of this difference resulted during a period of lower temperature in the polylactide-compost mixture at day 15. The difference could be simply an effect of this lower temperature, or could be the result of microbial activity inhibition by the high concentration (12.2% loading) of polylactide film. Polylactide underwent little reduction of molecular weight, so inhibition is probably not due to diffusion of lactic acid or oligamers into the compost. Without further data to support this explanation, no firm conclusion can be drawn.

The carbon dioxide rate, initial and final compost carbon contents, and total dry weights gave the carbon balances shown in Table 6-16. The first three rows give the total grams of carbon present initially, and show how the initial carbon partitioned between the carbon dioxide and the final product. The next two rows describe the partition as the percentage of initial carbon that ended up in each of the final fractions. For the polyethylene mixture a lower percent of the original carbon was recovered as carbon dioxide and end product, possibly because the separation of the polyethylene film and compost into two phases resulted in the collection of a non-representative sample of compost.

TABLE 6-16. Carbon balances for Pilot-Scale Composting Experiments.

Carbon species (grams)	Blank	PE	Kraft	PLA
Initial mixture (C_i)	2938	3711	3353	3390
Final compost (C_f)	2118	2309	2469	2363
Mineralization (C_{CO_2})	894	858	1108	789
%Initial C as compost	72%	62%	74%	70%
%Initial C as CO_2	30%	23%	33%	23%
Carbon balance closure	(102%)	(85%)	(107%)	(93%)

6.4.3 Effect of Polylactide on Product Quality

Characterization of the four composts after two weeks and four weeks was performed to determine whether the addition of polylactide film at 10% loading affected the quality of the compost product. Measurements of compost moisture content, total weight, pH, carbon to nitrogen ratio, ash content, volatile solids reduction, degree of humification, and cress seed germination index provided a wide range of compost monitoring and product quality parameters. These measurements do not reveal any changes to the compost product quality due to the addition of polylactide film, but do give a record of the chemical environment to which the polylactide was exposed.

Moisture content

The moisture content of the raw compost feedstock started at 66%. Addition of 12.2% dry test materials to three of the batches brought their moisture contents to

63%. Over the course of the 28 day experiments, the moisture contents remained in the range of 63-68%.

Total weight

After two and four weeks the contents of the vessels were removed and weighed. The composts underwent a 21-26% reduction in dry weight of the four week experiments (Figure 6-18a).

Compost pH

The pH of the compost was measured six times during the experiments. At the end of one week all of the composts reached their maximums of pH 8.3 to 8.5. After this the pHs decreased to final values of pH 5.9 to 6.6 (Figure 6-18b). This is nearly identical to the pH during the yard debris composting experiment in Section 6.3.3.

Carbon to nitrogen ratio

Initially the carbon to nitrogen ratios of the composts were 26 to 27. By the second week they were very close to their final values of 17 to 19 (Figure 6-18c). This mirrored the initial and final carbon to nitrogen ratios of the yard debris composting experiment.

Ash content

The ash content increased from 17% initially to 21.5-23.0% over the first two weeks. Each batch also increased during the second half of the experiment, to final values of 23.1-24.6% ash (Figure 6-18d).

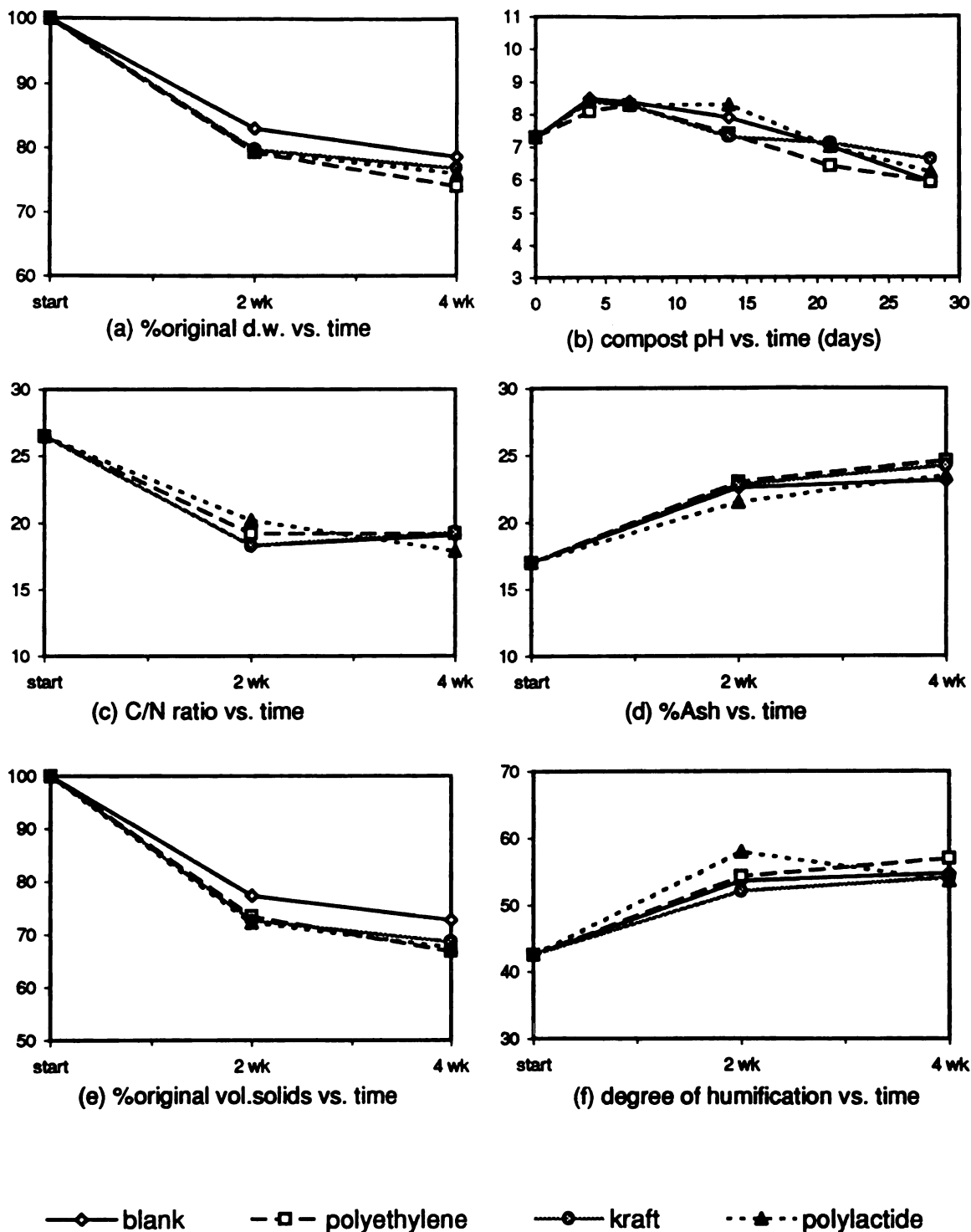


Figure 6-18. Pilot-scale composting product quality parameters.

Volatile solids reduction

The change in mass of volatile solids was calculated for the total dry weights of the composts. By the end of four weeks the total volatile solids of the initial compost mixes had been reduced by 27 to 33% (Figure 6-18e).

Degree of humification

Modest humification of the compost mixes occurred compared to the yard debris humic substance increases seen during yard waste composting in Section 6.3.3. The initial degree of humification of 43% was only slightly lower than the initial degree of humification of the yard debris mixture, but only increased by about 10% to final values of 53.6-57.0%. This is much less than the over 30% increase in degree of humification during the yard debris composting experiments.

Cress bioassay

The results of cress germination and root elongation bioassays of the raw and finished composts are shown in Figure 6-19. Results are shown as the total weight of seeds germinated in full strength compost extract as a percentage of the total weight of seeds germinated in the water control. Fresh composts prevent germination and inhibit root growth due to the presence of transient species, such as organic acids. As composts mature this toxicity decreases. This type of calculation accounts for both the lack of germination due to high concentration toxicity and the inhibition of root growth caused by low concentration toxicity. Error bars show the 95% confidence interval for the ten replicate dishes of ten seeds each. The initial compost strongly inhibited germination and root elongation, giving only 49% of the germination/elongation of water. By the end of four weeks the blank, Kraft paper, polylactide, and polyethylene composts gave 95, 92, 89, and 76%, respectively. The final values show less inhibition than the

fresh compost, but the level of germination of the four batches are not different from each other at the 95% confidence level.

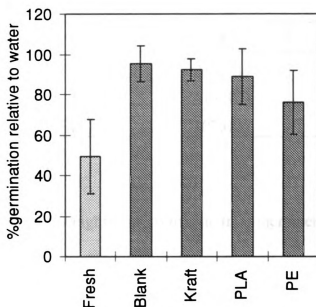


Figure 6-19. Results of germination and root elongation bioassay for fresh (0 day) and finished (28 day) pilot-scale composts. (Error bars show the 95% confidence intervals for n=10 dishes with 10 seeds each)

6.4.4 Pilot-Scale Polylactide Degradation

Samples of polylactide film were recovered from the pilot-scale vessels after two weeks and four weeks of composting, and the molecular weight distributions were determined by GPC. Pieces of film equivalent to approximately two 6 x 6 inch

sheets were removed and air dried at room temperature. Table 6-17 shows the results of the GPC analysis.

TABLE 6-17. GPC analysis of films from pilot-scale composting.

Time (days)	M_n	M_w	M_w/M_n
0	96,000	215,000	2.24
14	55,000	115,500	2.10
28	45,800	107,000	2.33

The decrease in molecular weight over 10 minute time increments was calculated using Equation 3-10:

$$\ln M_n = \ln M_{n,0} - 3.664 \times 10^{18} \cdot \exp\left(\frac{-14543}{T}\right) \cdot t \quad (3-10)$$

and the temperature average of the compost in the pilot-scale vessel during each time increment. Figure 6-20 shows the model's predictions for M_n over the course of the experiment compared to the M_n measured by GPC. Most of the molecular weight reduction occurred during the periods of peak temperature during the first two weeks of the experiment. The molecular weight average reached M_n 55,000 after two weeks and decreased slightly to M_n 45,800 after two more weeks. During the second half of the experiment the compost average temperatures were much lower so very little hydrolysis occurred. With the small reduction in molecular weight, the polydispersity of the polylactide molecular weights remained nearly constant during the experiment.

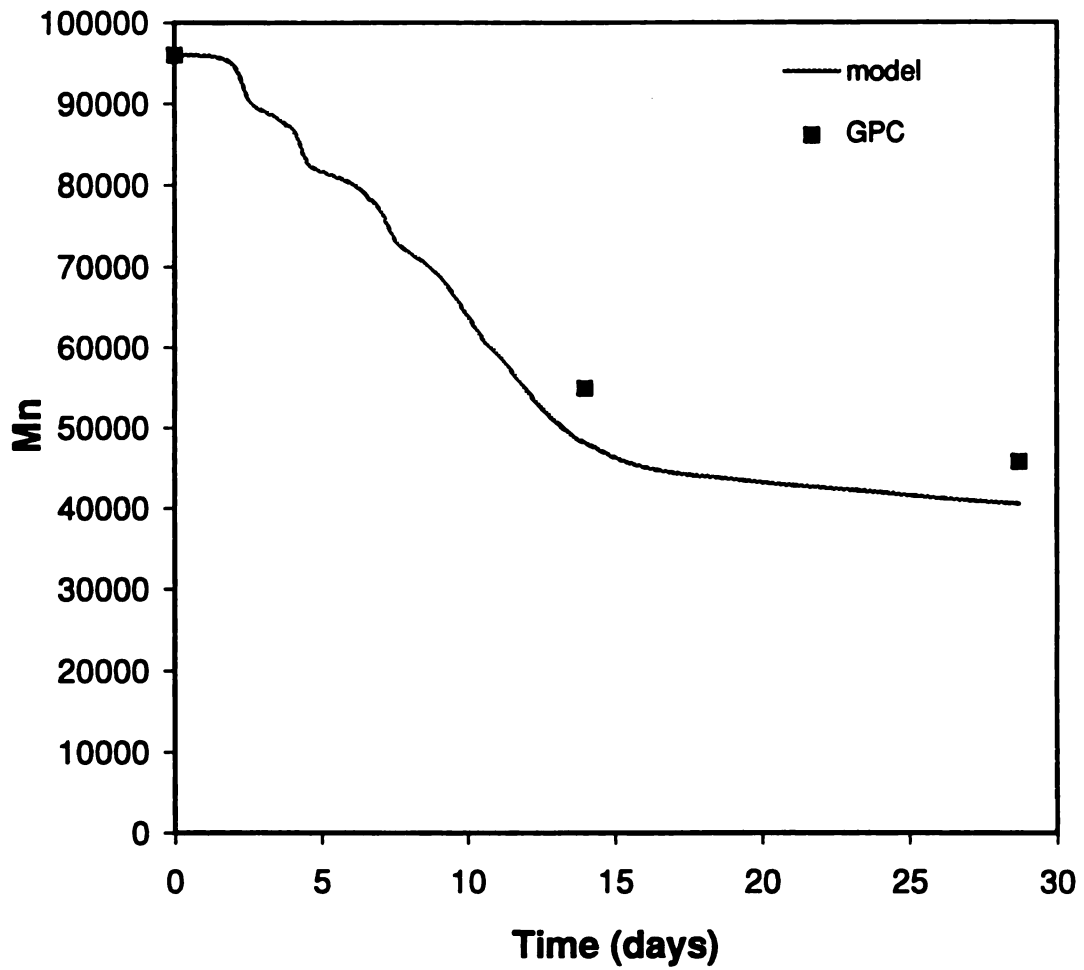


Figure 6-20. Comparison of predicted and measured decrease in M_n during pilot-scale composting.

The photographs in Figure 6-21 show the appearance of the film initially and after two and four weeks. By day three the transparent film was opaque white as a result of increased crystallinity. The film became brittle early in the experiment as the molecular weight decreased, but at the end of composting the sheets of film remained essentially intact.

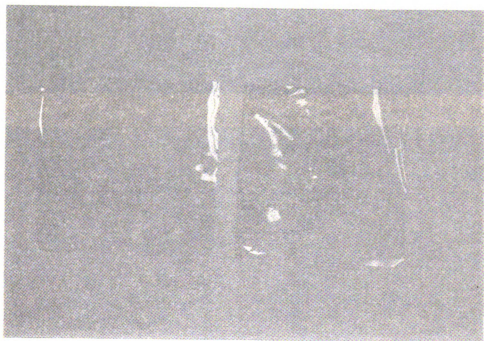


Figure 6-21(a). Photograph of polylactide film prior to pilot-scale composting.

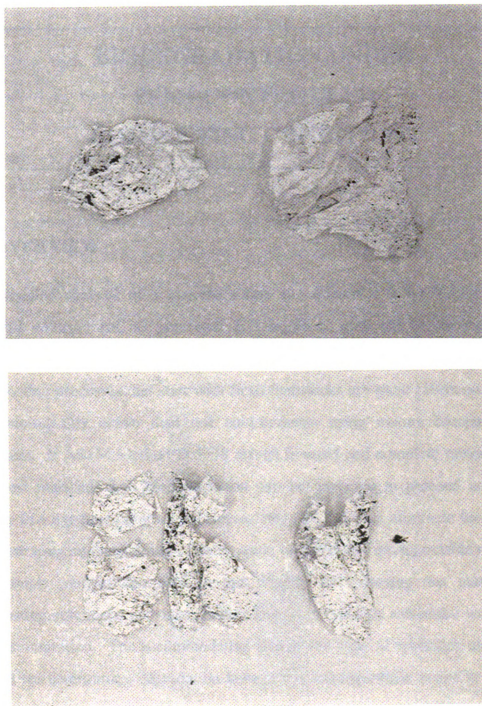


Figure 6-21(b). Photographs of polylactide film after composting two weeks (top) and four weeks (bottom).

CHAPTER 7

BIODEGRADATION UNDER SEMI-CONTROLLED COMPOSTING CONDITIONS

7.1 OVERVIEW

The detailed analysis of a material's fate and effects in a feedback-controlled compost environment, as presented in Chapter 6, may not be necessary after inherent biodegradability has been established using the methods in Chapter 5. Composting processes that start with fresh feedstocks are more biochemically and microbiologically active than test environments using mature compost as an inoculum. If ASTM Method D 5338 results in rapid and complete mineralization of a test material, then biodegradation can be expected to proceed at least as rapidly in a dynamic compost. However, this still does not eliminate the need for demonstrating compostability of items made of inherently biodegradable materials. The simple method described in this chapter for exposing test materials to composting conditions provides another look at polylactide molecular weight loss and disintegration. The accommodating size of this type of apparatus also makes it ideal for determining degradation behavior of biodegradable resins in end-user form.

7.2 TEST APPARATUS AND CONDITIONS

The vessel for the semi-controlled compost exposure consisted of a twenty liter pail fitted with a perforated false floor for air distribution (Figure 7-1). Humidified air entered the vessel at 150 ml/min from the bottom and exited from the top. A synthetic compost prepared from eight substrates (Table 7-1) provided the matrix for exposure. This mixture (1 kg dry weight) had a carbon to nitrogen ratio of 25:1 and a moisture content of 60%, and filled over half of the vessel. Three squares of polylactide film 5 cm x 5 cm were placed in plastic berry baskets with compost, and three baskets were loaded into the center of the vessel. These baskets facilitated the recovery of partially disintegrated film fragments. The entire set-up was subjected to the ASTM D 5338-92 temperature profile.

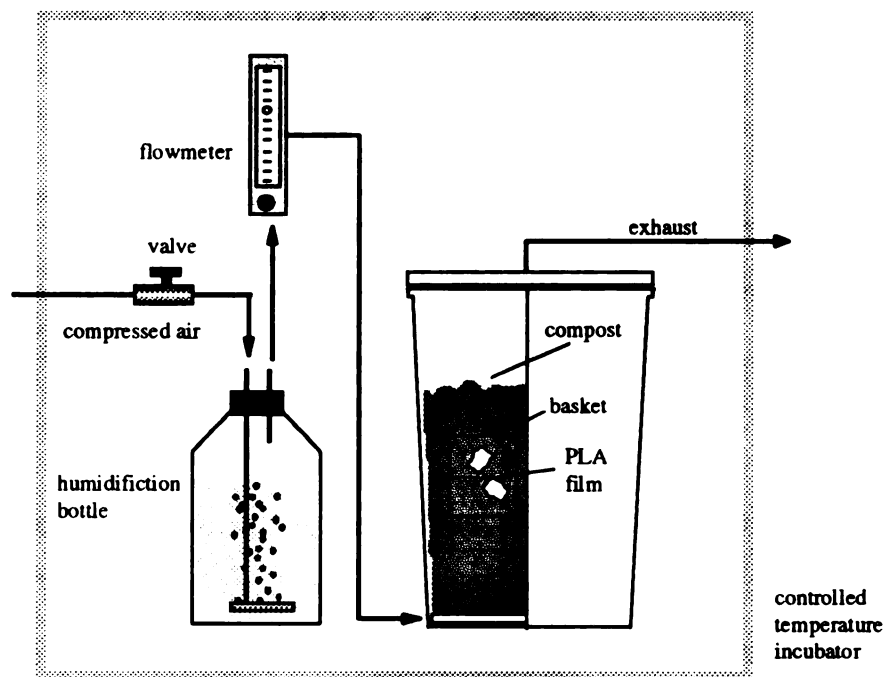


Figure 7-1. Apparatus for semi-controlled composting experiment.

Temperature was measured nine times over the course of the experiment using a handheld thermocouple unit. Carbon dioxide concentration of the exhaust gas was measured by gas chromatography. Every four days the baskets were removed from the vessel, pieces of film were retrieved, the compost pH was measured, and the compost was mixed and returned to the vessel.

TABLE 7-1. Synthetic compost mixture for semi-controlled composting.

FEEDSTOCK	Type	%C	%N	%M	totalC	totalN	g DW	g WW
cypress mulch	C	48.5	0.14	53	728	2	150	319
Kraft paper	C	44.1	0.05	1	441	1	100	101
corn cob grits	C	59.0	0.60	5	885	9	150	158
ground carrots	C,N	42.7	1.06	86	214	5	50	357
shredded leaves	C,N	43.0	1.16	5	645	17	150	158
alfalfa	N	45.0	3.30	5	1125	83	250	263
cat food bits	N	50.6	5.80	32	506	58	100	147
mature compost	inoc.	23.0	2.00	28	115	10	50	69
water								925
TOTALS					4658	184.8	1000	2500

Figure 7-2 shows the processing conditions of the semi-controlled composting experiment. The compost self-heated above the temperature of the incubator; this behavior is the reason for referring to the conditions as semi-controlled. Compost carbon dioxide evolution reached a peak during the mesophilic warm-up period and another peak after one week. During these peaks of activity the carbon

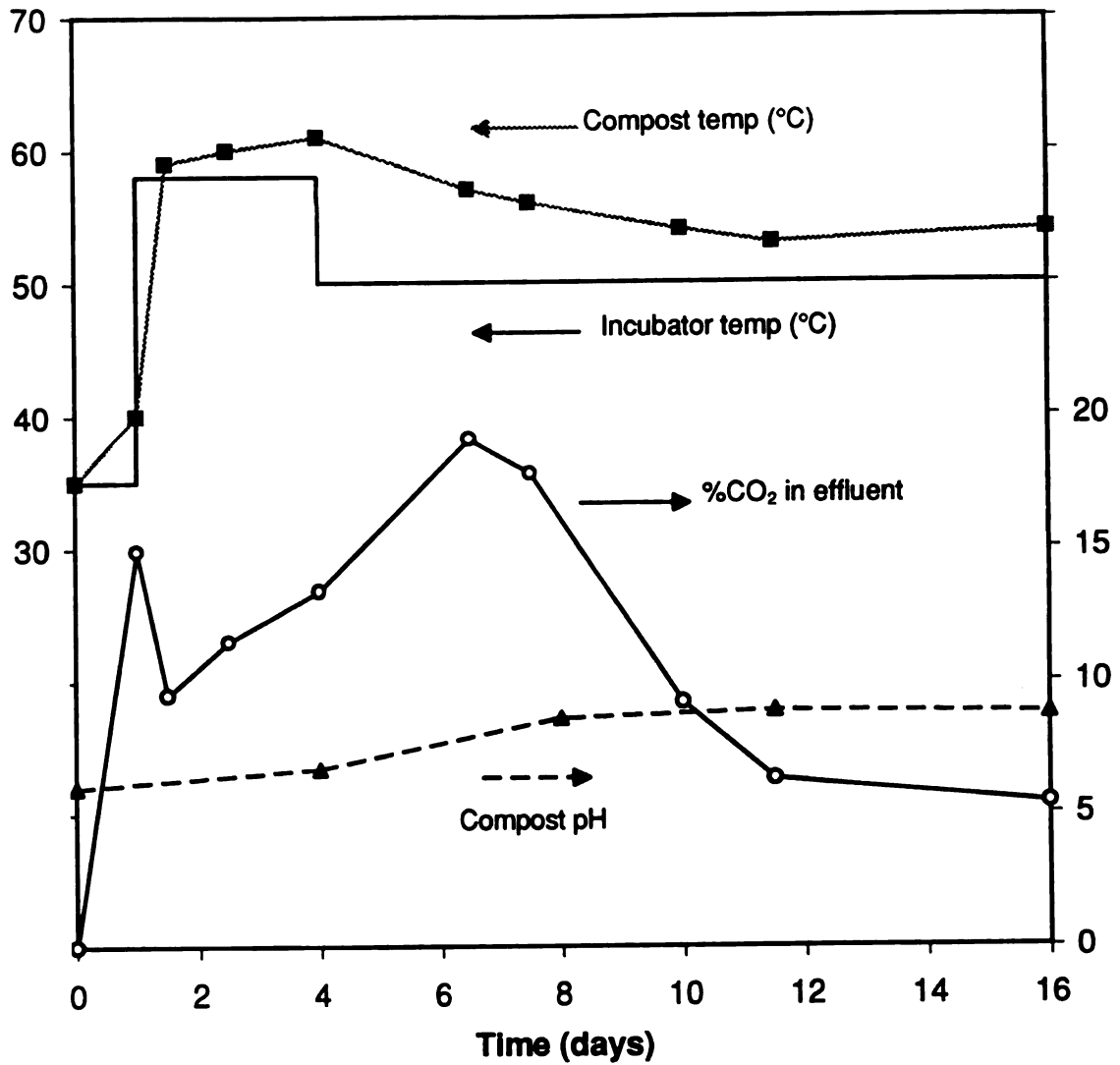


Figure 7-2. Processing conditions for semi-controlled composting exposure of polylactide film.

dioxide concentrations exceeded 15%. The compost pH increased from an initial value of pH 6.0 to a final value of pH 8.8.

7.3 POLYLACTIDE DEGRADATION

Samples of polylactide film were recovered after 4, 8, and 12 days of composting. On day 16 no distinguishable fragments of film could be found. The molecular weight reduction of the polylactide again followed the kinetic model for polylactide degradation (Figure 7-3). By day 12 the number average molecular weight had decreased below M_n 5000 and the polydispersity index had fallen to M_w/M_n 1.40 as shown in Table 7-2. Due to the higher temperatures, polylactide degradation proceeded more rapidly than in either the externally controlled or feedback-controlled composting experiments.

TABLE 7-2. GPC analysis of films from semi-controlled composting.

Time (days)	M_n	M_w	M_w/M_n
0	96,000	215,000	2.24
4	28,700	58,000	2.03
8	10,400	19,000	1.86
12	4,800	6,700	1.40

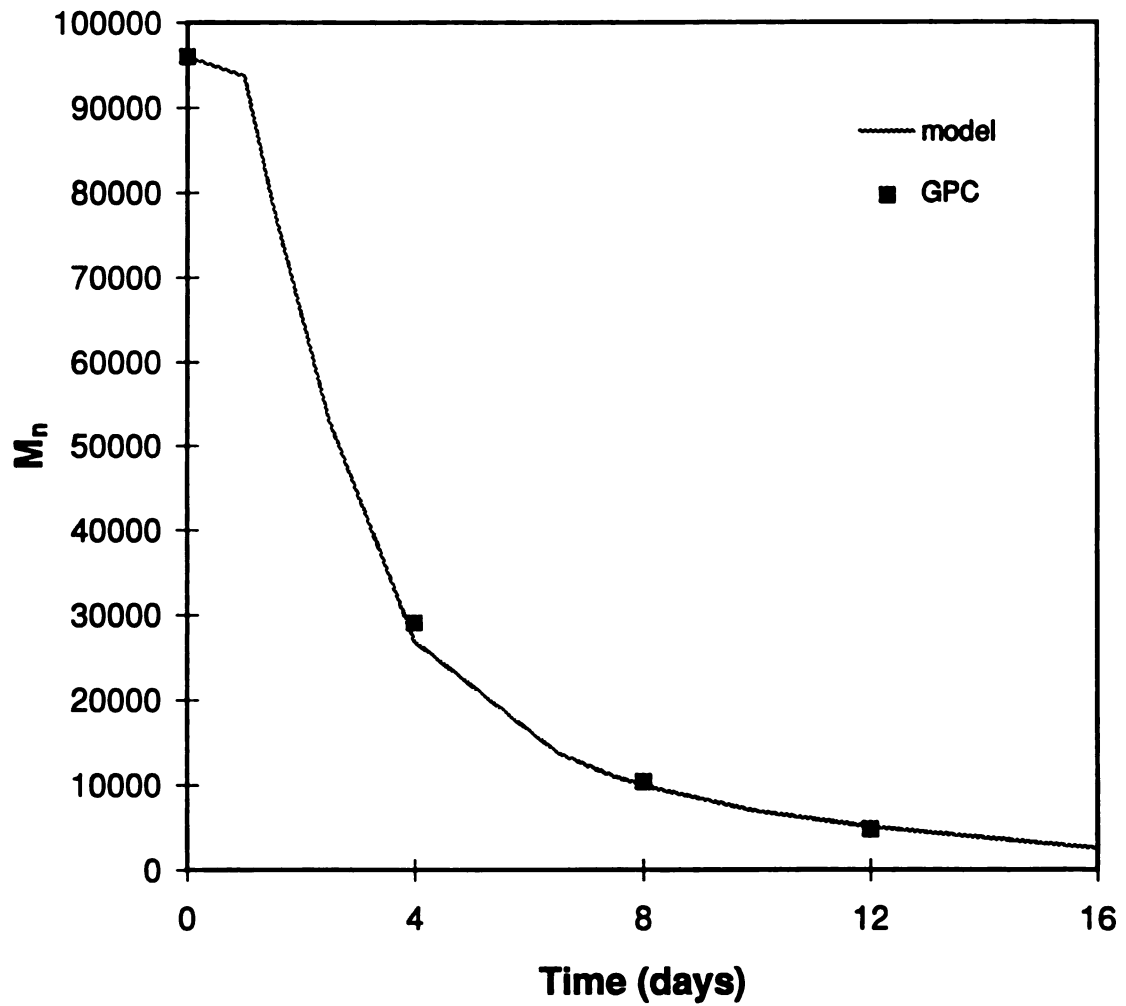


Figure 7-3. Comparison of predicted and measured decrease in M_n during semi-controlled composting.

CHAPTER 8

CONCLUSIONS AND RECOMMENDATIONS

8.1 CONCLUSIONS

Composting is increasingly being recognized as a cost-effective and environmentally sound method for managing certain solid waste streams. Unlike other methods of recycling, composting does not require segregation of individual material types. Any mix of compostable materials can be collected and processed simultaneously.

The thesis provided an evaluation of the potential of polylactide as a compostable replacement for current plastic packaging. The following conclusions can be made:

- Polylactide and other biodegradable plastics can replace current non-biodegradable plastics in certain applications to result in completely compostable waste streams. For a material to be compostable it must not end up in the reject fractions, must be completely biodegradable, and must not be detrimental to compost product quality or processing.
- A new respirometric biodegradability testing apparatus allows accurate and reliable measurement of carbon dioxide evolution from biodegradable materials under externally controlled composting conditions as per ASTM Method D 5338.

- Upon exposure to the ASTM D 5338 conditions, the molecular weight average of polylactide film rapidly decreases by non-enzymatic hydrolysis. Microbial utilization begins when the molecular weight average approaches M_n 10,000 and continues at a rate that is nearly first order with respect to temperature. The ASTM D 5338 temperature profile results in 85% conversion of polylactide carbon to carbon dioxide after 70 days. The majority of the biodegradation occurs before day 28, when the temperature is decreased from 50°C to 35°C.
- The pilot-scale composting system using PID feedback control provides conditions similar to those found in full-scale forced aeration composting processes. Tight control at temperature and oxygen concentration setpoints requires linear and stationary process dynamics. Even though biologically active composts display non-ideal temperature dynamics, control is possible with only brief periods of temperature setpoint overshoot.
- As substrate carbon is mineralized to carbon dioxide, the carbon to nitrogen ratio of the compost decreases, the ash content increases, the degree of humification increases, and the phytotoxicity decreases. Feedstock transformation into compost proceeds rapidly during the initial stages of composting when the temperatures are high. As feedstock materials stabilize, the temperature drops and chemical and biochemical character of the compost changes slowly.
- Under forced aeration a temperature gradient is established in the compost that ranges from the cooling air temperature to the temperature control setpoint. Since the average compost temperature is low the rate of polylactide molecular

weight reduction is slow. Polylactide film exposed to the pilot-scale temperatures decreases in average molecular weight from M_n 96,000 to M_n 48,600 after four weeks of composting. Most of this molecular weight decrease occurs during the first two weeks, when the temperature is higher. Since the polylactide film does not degrade under these conditions, its presence does not affect compost process dynamics or product quality.

- The semi-controlled composting apparatus provides a simple method for exposing biodegradable materials to a dynamic matrix of synthetic compost. The compostability of larger items in their end-user form can be testing in this apparatus after their inherent biodegradability has been established.
- The semi-controlled compost maintains temperatures higher than the externally controlled or feedback-controlled composts. Polylactide film exposed by this method degrades rapidly. After only twelve days of exposure the molecular weight average drops to M_n 4,800 and after sixteen days fragments of polylactide film are indistinguishable in the compost.
- A first-order model of polylactide molecular weight reduction exists which was developed based on the kinetics of polylactide degradation when implanted into animal tissues. Some data on polylactide degradation is available for temperatures out of the physiological range. The rate constant as a function of temperature can be developed by applying Arrhenius kinetics to this molecular weight reduction data. The resulting rate constant expression:

$$\ln M_n = \ln M_{n,o} - 3.664 \times 10^{18} \cdot \exp\left(\frac{-14543}{T}\right) \cdot t \quad (3-10)$$

can then be applied in the model to predict the degree of polylactide degradation during a composting exposure with time-variant temperature. Molecular weight reductions measured by GPC confirm that the temperature dependent model is applicable to polylactide degradation in compost.

- The molecular weight reductions predicted by the kinetic model and measured by GPC, and the rate of carbon dioxide evolution give evidence for the biodegradation mechanism of polylactide during composting. Carbon dioxide evolution from the polylactide ensues only after the average molecular weight has been dramatically reduced. This reveals that utilization by compost microorganisms occurs after non-enzymatic degradation of polylactide produces low molecular weight oligamers that are able to diffuse out of the polymer bulk.

8.2 RECOMMENDATIONS FOR FURTHER WORK

Based on this research, a strategy for evaluating compostability of biodegradable materials can be recommended. Knowledge of chemical and enzymatic degradation mechanisms for a particular material can aid in the design of biodegradability and compostability experiments. Inherent biodegradability under composting conditions can be determined using standard sized pellets, powders, or films in the new test apparatus for ASTM D 5338. If a material reaches 100% biodegradation in a reasonable time, this is evidence that the material and its degradation products are not strongly inhibiting microbial activity in the compost inoculum. For some materials, ASTM D 5338 biodegradability may be rapid but not reach 100%. The process dynamics of pilot-scale composting may reveal

inhibition effects from such materials. The semi-controlled exposure method described in Chapter 7 can replace the pilot-scale system as a method for exposing large items to a dynamic compost. However, certain attributes of the pilot-scale system that translate to full-scale processes, particularly the temperature gradients, are not present in the semi-controlled exposure method.

As described in Section 3.2.1, there may be an increase in the slope of the degradation rate constant vs. temperature for polylactide at the glass transition temperature. During most of the polylactide exposures in this research the temperature remained near or below T_g . Exposures of polylactide to compost at constant temperatures near and above T_g could be used to generate a separate temperature dependent rate expression for temperatures above T_g . This modification would result in dependable predictions of degradation behavior at higher temperatures.

The kinetics of polylactide degradation make temperature the most critical parameter for achieving rapid degradation, as long as other process characteristics are in their typical ranges. However, odor management is the primary problem of most composting facilities, and compost researchers have determined that aeration and low temperatures minimize odor generation. As compost facilities successfully control odor production by temperature control the potential for polylactide degradation is reduced, as in the pilot-scale experiments of Section 6.4. New process control strategies that maintain an even temperature profile could benefit composting by ensuring low odor formation potential and rapid degradation of polylactide and other substrates. Composting facilities tuned to

provide favorable conditions for both processing and biodegradation will allow widespread use of biodegradable materials in a rational approach to solid waste management.

LIST OF REFERENCES

LIST OF REFERENCES

- American Society of Testing and Materials, ASTM D 425-88 Standard Test Method for Centrifuge Moisture Equivalent of Soils, *Annual Book of ASTM Standards*, Vol. 04.08, 1988.
- American Society of Testing and Materials, ASTM D 5209-91 Standard Test Method for Determining the Aerobic Biodegradation of Plastic Materials in the Presence of Municipal Sewage Sludge, *Annual Book of ASTM Standards*, 1991.
- American Society of Testing and Materials, ASTM D 5338-92 Standard Test Method for Determining Aerobic Biodegradation of Plastic Materials Under Controlled Composting Conditions, *Annual Book of ASTM Standards*, 1992.
- Carroll, B.A., Caunt, P., and G. Cunliffe, *J. IWEM*, 7:175-181, 1993.
- Ciavatta, C., Govi, M., Vittori Antisari, L., and P. Sequi, *J. Chromatog*, 509:141-146, 1990.
- Cohen, G.H., and G.A. Coon, *Trans. ASME*, 75:827-839, 1953.
- Craig, P.J., Williams, J.A., Davis, K.W., Magoun, A.D., Levy, J.A., Bogdansky, S., and J.P. Jones, *Surg. Gynecol. Obstet.*, 141:1-10, 1975.
- Curran, M.A., *Environ. Sci. Technol.*, 27(3):430-436, 1993.
- Cutright, D.E., Beasley, J.D., and B. Perez, *Oral Surg.*, 32:165-173, 1971.
- David, J., *Master's Thesis*, Dept. of Chemical Engineering, Michigan State University, 1994.
- Dijkstra, P.J., Eeninck, M.J.D., and J. Feijen in *Degradable Materials: Prospects, Issues, and Opportunities*, CRC Press, 1990.

- Dreinhofer, L.H., *IEEE Control Systems Mag.*, 56-60, April 1988.
- Fava, J.A. et al., Soc. Environ. Toxicol. Chem. Smuggler's Notch workshop, 1990.
- Flaig, W. in *Humic Substances and Their Role in the Environment*, F. H. Frimmel and R. F. Christman, Eds., Wiley, Chichester, p 75-92 (1988).
- Flaig, W., Beutelspacher, H., and E. Rietz, in *Soil Components Vol 1*, J.E. Gieseking Ed., Springer-Verlag, New York, p 1-211 (1975).
- Finger, S.M., Hatch, R.T., and T. M. Regan, *Biotech. Bioeng.*, 17:1193-1218, 1976.
- Fordyce, A.P., Rawlings, J.B., and T.F. Edgar, in *Computer Control of Fermentation Processes*, Ed. by D.R. Omstead, 165-220, CRC Press, 1990.
- Gruber, P.R., Hall, E.S., Kolstad, J.J., Iwen, M.L., Benson, R.D., Borchardt, R.L. *U.S. Patent Number 5,274,073*, Dec. 1993.
- Hamelers, H.V.M., in *Science and Engineering of Composting: Design, Environmental, Microbiological, and Utilization Aspects*, H. A. J. Hoitink and H. M. Keener, Ed., p. 36-58, 1993.
- Hayes, M.H.B., MacCarthy, P., Malcolm, R.L., and R.S. Swift, Ed., *Humic Substances II, In Search of Structure*, p. 6-7, 1989.
- Holland, S.I., Tighe, B.J., and P.G. Gould, *J. Control Rel.*, 4:144-180, 1986.
- Iannotti, D.A., Pang, T., Toth, B.L., Elwell, D.L., Keener, H.M., and H.A.J. Hoitink, *Compost Sci. & Util.*, 1(3):52-65, 1993.
- Jeris, J.S., and R.W. Regan, *Compost Science*, 8-15, March-April 1973.
- Kulkarni, R.K., Pani, K.C., Neuman, C., and F. Leonard, *Arch. Surg.*, 93:839-843, 1966.
- Li, S.M., Garreau, H., Vert, M., *J. Materials Sci.:Materials in Medicine*, 1:123-130, 1990a.
- Li, S.M., Garreau, H., Vert, M., *J. Materials Sci.:Materials in Medicine*, 1:131-139, 1990b.

- Luyben, W.L., *Process Modelling, Simulation, and Control for Chemical Engineers, 2nd Ed.*, McGraw-Hill, 1990.
- MacGregor, S.T., Miller, F.C., Psarianos, K.M., and M.S. Finstein, *Appl. Environ. Microbiol.*, 41(6), p 1321-1330, 1981.
- Mason, N.S., Miles, C.S., and R.E. Sparks, *Polymer Science and Technology*, American Chemical Society, 279-291, 1980.
- McKinley, V.L., and J.R. Vestal, *Appl. Environ. Microbiol.*, 47(5):933-941, 1984.
- Narayan, R., *Kunststoffe*, 79(10):1022-1027, 1989.
- Narayan, R., *INDA Nonwoven Res.*, 3:1, 1991.
- Narayan, R., *ACS Symp. Ser. 476*, 1-10, 1992.
- Narayan, R. in *Science and Engineering of Composting: Design, Environmental, Microbiological, and Utilization Aspects*, H. A. J. Hoitink and H. M. Keener, Ed., p. 339-362, 1993a.
- Narayan, R. in *Opportunities for Innovation: Biotechnology*, U.S. Dept. of Commerce NIST GCR 93-633, R.M. Busche, Ed., p. 135-150, 1993b.
- Ozeki, E., and H. Ohara, *Third International Workshop on Biodegradable Plastics and Polymers*, Osaka, 1993.
- Pitt, C.G., Chasalow, F.I., Hibionada, Y.M., Klimas, D.M, and A. Schindler, *J. Appl. Polym. Sci.*, 26:3779, 1981.
- Pitt, C.G., in *Biodegradable Polymers and Plastics*, ed. M. Vert, J. Feijen, A. Albertsson, G. Scott, and E. Chiellini, Royal Society of Chemistry, 1992.
- Reed, A.M., and D.K. Gilding, *Polymer*, 22:487-498, 1980.
- Seborg, D.E., Edgar, T.F., and D.A. Mellichamp, *Process Dynamics and Control*, Wiley Publ., 1989.
- Schindler, A., Jeffcoat, R., Kimmel, G.L., Pitt, C.G., Wall, M.E., and R. Zweidinger, *Contemp. Top. Polym. Sci.*, 2:251-286, 1977.
- Sikora, L.J., and M.A. Sowers, *J. Environ.Qual.* 14(3):434-439, 1985.

- Sinclair, R.G., *Environ. Sci. Technol.*, 7:955, 1973.
- Snook, J.B., and R. Narayan, in *Waste Management and Recycling International 1994*, M.A. Johnson and Y.Samiullah, Ed., Sterling Publ. Ltd., London, 40-43, 1994.
- Spinu, M., *U.S. Patent Number 5,270,400* Dec. 1993.
- Stentiford, E.I., Taylor, P.I., Leton, T.G., and D.D. Mara, *Wat. Pollut. Control*, 23-32, 1985.
- Strom, P.F., *Appl. Environ. Microbiol.*, 50(4):899-905, 1985.
- Suler, D.J., and Finstein, M.S., *Appl. Environ. Microbiol.*, 33(2):345-350, 1977.
- United States Federal Trade Commission, *Guides for the Use of Environmental Marketing Claims*, July, 1992.
- Vestal, J.R., and D.C. White, *BioScience*, 39(8):535-541, 1989.
- Wedel, A.W. and C.R. Daubert, *J. Ferm. Qual. Control*, 13:45-64, 1994.
- Williams, D.F., *Eng. Med.*, 10(1):5-7, 1981.
- Wilson, J.A., in *Measurement and Control in Bioprocessing*, Ed. by K.G. Carr-Brion, Elsevier, London, p 1-35, 1991.
- Yolles, S., *Acadamy of Pharm. Sci.*, San Francisco, 1971.
- Zeigler, J.G. and N.B. Nichols, *Trans. ASME*, 64:759-768, 1942.
- Zhu, K.J., Hendren, R.W., Jensen, K., and C.G. Pitt, *Macromolecules*, 24:1736, 1991.